DTU Fotonik
Department of Photonics Engineering

DTU

The Quantum Zeno Effect Applied to Quantum Dots

Authors:
Charles Christensen (s113046)
Torkil Petersen (s113059)

Supervisor:
Prof. Jesper Mørk, DTU Fotonik

Assistant supervisor:
Dara McCutcheon, DTU Fotonik

Physics Project, 34029
Technical University of Denmark
May 15, 2015

Abstract

In this thesis we investigate the quantum Zeno effect (QZE). We try to clarify the confusion around the definition of the QZE. We find that its physical appearance shall not be regarded as caused by frequent collapses of a system due to measurements, but rather as a general effect obtained whenever a system is dominated by strong disturbances. Many different manifestations of the QZE will be studied both analytically and numerically – including a simplified version of the experiment of Itano et al. [1]. This will be done using the Lindblad formalism and a more rigorous approach based on derivation of the Born-Markov master equations from first principles.

Preface

This project is submitted as part of a mandatory course in the Physics and Nanotechnology Bachelor of Science in Engineering from the Technical University of Denmark (DTU). The project has been over the duration of one semester and awards 15 ECTS points.

Acknowledgements

We would like to thank our assistant supervisor Dara McCutcheon, Postdoc at Department of Photonics Engineering, and our project supervisor Jesper Mørk, Professor and Group Leader for Nanophotonics Theory and Signal Processing at Department of Photonics Engineering.

Contents

1 Introduction **1**
- 1.1 Quantum dots . . . 1
- 1.2 Quantum computers . . . 2
- 1.3 The history of QZE . . . 3

2 Basic quantum mechanics **4**
- 2.1 Quantum state . . . 4
- 2.2 Evolution of closed systems . . . 4
  - 2.2.1 Evolution with density operator . . . 5
- 2.3 Composite systems . . . 6
- 2.4 Measurement . . . 6
  - 2.4.1 Von Neumann projections . . . 6
  - 2.4.2 Decoherence . . . 7
- 2.5 Open systems . . . 7
  - 2.5.1 Born-Markov master equation . . . 8
    - 2.5.1.1 Approximation . . . 8
  - 2.5.2 Correlation functions . . . 9

3 The Quantum Zeno Effect **11**
- 3.1 How to read this thesis . . . 12
- 3.2 QZE: Projective measurements . . . 12
- 3.3 The measurement problem w.r.t. the QZE . . . 14

4 General analysis of QZE **15**
- 4.1 Two-level system . . . 15
  - 4.1.1 Lindblad master equation . . . 16
  - 4.1.2 Equations of motion in a two-level system . . . 16
  - 4.1.3 Population number in two-level system . . . 17
  - 4.1.4 Analytical solutions . . . 17
  - 4.1.5 Solutions in two-level system . . . 20
    - 4.1.5.1 Bloch sphere . . . 22
- 4.2 QZE by projective measurements . . . 24
  - 4.2.1 QZE by projective measurements: theoretical aspect . . . 25
  - 4.2.2 QZE by projective measurements with time dependent dissipation . . . 26
- 4.3 QZE by strong dephasing . . . 28
- 4.4 Three-level system . . . 29
- 4.5 Qutrit system . . . 29
  - 4.5.1 Description of a three-level system . . . 29
  - 4.5.2 QZE in three-level systems . . . 31

5 Master equation from first principles **34**
- 5.1 Spontaneous emission with driving . . . 34

5.2 Pure dephasing with driving . . . 39
5.2.1 QZE: pure dephasing with strong 'continuous coupling' . . . 40
5.3 Three level system: spontaneous emission with driving . . . 41
5.4 Three level system: multiple Rabi oscillations . . . 44
5.5 Justification of Lindblad formalism . . . 46
5.5.1 Spontaneous emission for three-level QD . . . 46
5.6 Non-Markovian master equation . . . 47

6 Further analysis of QZE **50**
6.1 Numerical solutions for dephasing master equation . . . 50
6.2 Numerical solutions for spontaneous emission master equation . . . 51
6.2.1 Two-level system . . . 51
6.2.2 Three-level system . . . 52

7 Overview and discussion **53**
7.1 QZE: projective measurements . . . 53
7.2 QZE: strong 'continuous coupling' . . . 53

8 Conclusion **55**

References **56**

A Appendix **58**
A.1 Analytical solutions to Lindblad master equations . . . 58
A.1.1 Spontaneous emission . . . 58
A.1.2 Pure dephasing . . . 59
A.2 Numerical solution to two-level systems with time-dependent dissipation . . . 59
A.3 Time dependent spontaneous emission rate . . . 61
A.4 Time dependent dephasing rate . . . 61
A.5 Complete master equation solved in Mathematica . . . 62

Chapter 1

Introduction

The quantum Zeno Effect (QZE, henceforth) is a phenomenon usually understood as a 'damping' effect that slows down or eventually freezes the evolution of a quantum system due to frequent measurements performed on it, thereby (hindering the transition out of the initial state) preventing its decay. The phenomenon has been marked by a lot of controversy and confusion ever since it became popularized by George Sudarshan and Baidyanath Misra in 1977 [2]. The controversy originates form the physical manifestation of the QZE, since it seems to require the collapse of the quantum state, which is a concept not universally agreed on in the scientific community. Nowadays the QZE is however pictured in a much broader context by most physicists. Its physical manifestation is reformulated as an effect that appears whenever a strong disturbance or perturbation dominates the dynamics of a quantum system.

The primary goal of this thesis is to clarify the confusion that is around the definition of the QZE, and describe it as being a more general effect that physically appears whenever a system is dominated by strong disturbances, while it theoretically also can be understood through the collapse of the wave function – even though this conjecture never has been experimentally proven. We will start off by studying the QZE in quantum dots influenced by frequent measurements - describing the general QZE definition. Thereafter we will consider quantum dots influenced by different types of environments, which lead to both spontaneous emission and pure dephasing of the quantum dot. This will be done using the theoretical well-established Lindlad master equation and also through a more rigorous approach based on a derivation of the Born-Markov master equation from first principles.

1.1 Quantum dots

Quantum dots have been extensively studied in recent years because of their potential for technological applications. Briefly stated a quantum dot (QD) is a portion of matter whose excitons are confined in all three spatial dimensions. This means that an electron that is in the interior of a QD will experience a potential barrier in all directions [3]. The dimensions of QDs usually range from 1 nm to 20 nm. They can be fabricated from many different kinds of semiconductor materials and in various geometrical shapes (cubes, spheres and cones for instance). All these opportunities can be utilized to achieve certain desirable properties of the QD – for example, by varying the size appropriately a QD can be produced with a very specific band gap making them ideal for optical applications, where a certain wavelength of light is desired. In fact for laser applications QDs have such potential that a whole field of research on quantum dot lasers have emerged.

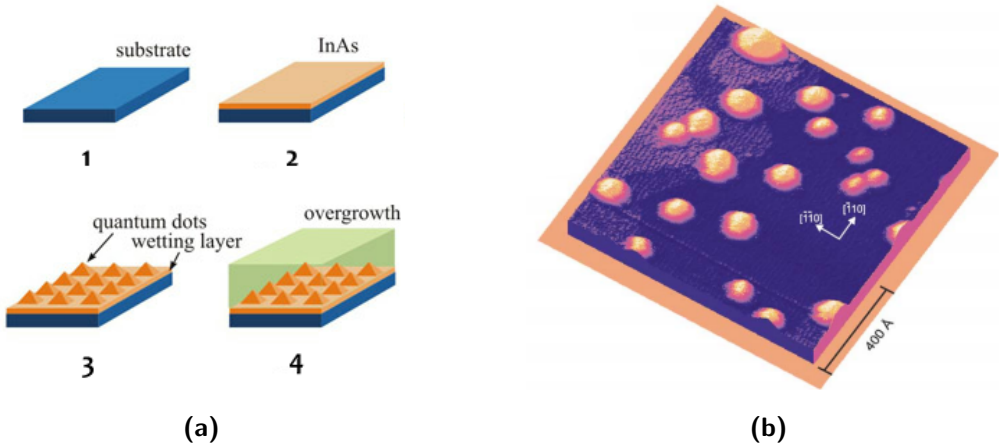

Figure 1.1: (a) Schematically depiction of the four steps in the process of QDs formation in Stranski–Krastanow regime. (b) 3-D STM (scanning Tunnel Microscope) image of InAs QDs on GaAs [4].

The fabrication of QDs have gone through various phases since its initial discovery in the late 70's and early 80's, including lithographic processes that create two-dimensional structures that could then be etched down to isolate the dot [5]. However a newer method that is usually the one used for lasers is to grow self-assembling dots by growing a layer of semiconductor material unto a wetting layer. The growth of quantum dots is based on a mismatch of lattice- and surface energy parameters that causes strain in material, which then pulls together resulting in "islands" of quantum dots. This is also known as Stranski-Krastanov growth, see figure 1.1a. The main limitations of growing quantum dots this way are the cost of fabrication and the lack of control over positioning of individual dots, however significant efforts has been made to enable control of the dot size [6] [7]. Self-assembled dots are typically between 5 and 50 nm in size. By carefully choosing the semiconductor material, there is a high degree of control over the band gap and therefore the operational frequency of quantum dot laser.

QDs are sometimes called artificial atoms, because they exhibit behavior very similar to that of atoms. Hence, QDs are a platform that are relatively representative of general quantum mechanical behavior, while they are also very likely to be incorporated in various future technologies; e.g. quantum computing gates [8] for which the QZE may be essential (see sec. 1.2). Due to this we have chosen to base our calculations on QD systems exclusively. As such we will tend to use parameters in our calculations that are appropriate for typical QDs.

1.2 Quantum computers

Quantum computers are expected to rely heavily on the undisturbed evolution of quantum coherences. Hence, to perform a quantum computation it is required that decoherence (see sec. 2.4.2) is managed such that coherent states are preserved. However, there has yet to be found a reliable way to avoid decoherence. Isolating the system of qubits in a quantum computer, while stile being able to handle instructions etc., seems to be a difficult task [9] – especially when adding more qubits to the system in order to increase computation power.

It may be possible that the QZE, in one the manifestations investigated in this thesis, can be used to manage decoherence in quantum computers.

1.3 The history of QZE

The QZE has a history that dates back to the early 1930s, when von Neumann first encountered and understood the central aspects of QZE [10]. He proved that a quantum state $|\phi\rangle$ can evolve into any other quantum state $|\psi\rangle$ by appropriate measurements and if these states coincide they could yield the effect known today as QZE. However, his conclusions were forgotten for over 30 years, when Beskow and Nilsson in an article [11] describing a measurement experiment, discussed the possibility that frequent position measurements could hinder the decay of an unstable particle. This intriguing idea drew a lot of attention that among other things lead to a mathematical perspective on the effect by Friedman in 1972 [12]. The effect became known as the QZE, when G. Sudarshan in collaboration with B. Misra in 1977 cast the problem into a more rigorous mathematical framework and associated the effect with the philosopher Zeno of Elea. Ever since this article, the QZE has been receiving constant attention by the scientific community that has explored many different aspects of the phenomenon.

The QZE was genuinely considered a paradox until 1988 when the theorist Cook [13] claimed that the QZE could be tested experimentally on oscillating systems, which eventually led to the first experiment done on the QZE performed by Itano et al. in 1989 [1]. This experiment among others lead to a huge debate concerning the interpretation of the experimental results, since many suggested that it proved the so-called reduction-postulate[1], which is not a universally accepted postulate among the different interpretations of quantum mechanics, e.g. the ensemble interpretation. The controversy of the experimental results has since been debated by a number of authors [14][15], who emphasize that the measurement processes in the experiments hinge upon unitary dynamics of the system with no explicit use of projection operators and non-unitary dynamics.

[1] The reduction postulate states that measurements causes a collapse (reduction) of the wave function.

Chapter 2

Basic quantum mechanics

2.1 Quantum state

The foundation of the mathematical description of quantum mechanics revolves around postulates that are experimentally established. The first essential postulate concerns the description of the quantum systems. It states that all quantum systems have an associated Hilbert space, which is a vector space containing all physical states of the system. The quantum state is a vector in the Hilbert space that completely describes the state of the system and is therefore usually called the state vector. The most simple case is a state vector that describes a two-level system, which potentially could be a two-level quantum dot, with one excited and a ground state. The Hilbert space for this system is two dimensional and the general description of the state vector in "bra-ket" notation, is given by:

$$|\Psi\rangle = a\,|g\rangle + b\,|e\rangle\,, \tag{2.1}$$

where the ground state $|g\rangle$ and the excited state $|e\rangle$ are orthogonal basis vectors of the Hilbert space and the coefficients a and b are arbitrary constants. The normalization condition is $\langle\Psi|\Psi\rangle = 1$, where $\langle\Psi| = (|\Psi\rangle)^\dagger$. This condition is the same as requiring $|a|^2 + |b|^2 = 1$, so that $|\Psi\rangle$ has unit length. $|a|^2$ and $|b|^2$ represent the probability of measuring the eigenvalue of respectively $|a\rangle$ or $|b\rangle$ with respect to a given observable. The state vector given above is called a pure state. More generally a quantum state for a system can either be pure or mixed, but the mixed description, can only be represented through the density operator, which will be thoroughly discussed in the following.

2.2 Evolution of closed systems

The general description of a closed system is that the system can be completely be described in terms of the time-dependent Hamiltonian, even though the system is not completely isolated from environmental influence. Such systems could for example be the evolution of particles subjected to time varying electric or magnetic fields. The evolution of the state $|\psi(t)\rangle$ of the system is postulated to be described by the Schrödinger equation:

$$i\frac{d\,|\Psi\rangle}{dt} = H(t)\,|\Psi\rangle \tag{2.2}$$

where the operator $H(t)$ is the time-dependent Hamiltonian of the system, which is a Hermitian operator. It has the formal solution given by:

$$|\Psi(t)\rangle = U(t,t_0)\,|\Psi(t_0)\rangle = e^{-i\int_{t_0}^{t} H(s)ds}\,|\Psi(t_0)\rangle \tag{2.3}$$

with $U(t, t_0)$ being the unitary time evolution operator. This is an important feature of the closed system: the time evolution is always unitary. The same goes for totally isolated systems, where the Hamiltonian is not influenced by some external environment and therefore is time independent, $H(t) = H$. An example of an isolated system is an atom in free space, and the unitary operator governing the evolution state reduces into the simpler form:

$$U(t, t_0) = e^{-iH(t-t_0)} \tag{2.4}$$

2.2.1 Evolution with density operator

Alternatively the Schrödinger equation can be represented through the density operator $\rho(t)$, instead of the pure state $|\psi(t)\rangle$. The density operator with $\{p_n\}$ being the probabilities and $\{|\Psi_n(t)\rangle\}$ an ensemble of states, is given by:

$$\rho(t) = \sum_n p_n \left|\Psi_n(t)\right\rangle \left\langle\Psi_n(t)\right| \tag{2.5}$$

Only if $p_n = 1$ for some n and every other $p_n = 0$, then the density operator $\rho(t)$ is said to be in a pure state, since we have complete knowledge about the system, meaning that we know exactly which state the system is in. If any other p_n is different from zero the state is said to be mixed, since we then only have partial knowledge of which state the system is in. This representation of the state of the system therefore reaches way beyond the state representation (2.1), since the density operator implicitly describes both the mixed and the pure states. The Schrödinger equation with respect to the density operator is given by:

$$\frac{d\rho(t)}{dt} = -i\left[H(t), \rho(t)\right] \tag{2.6}$$

This equation is generally known as the Liouville Neumann equation and for closed system the solution to it is unitary:

$$\rho(t) = U(t, t_0)\rho(t_0)U^\dagger(t, t_0) \tag{2.7}$$

Where $\rho(t_0)$ is the initial density operator.

Before going any further we state a couple of properties of the density operator:

- $\mathrm{Tr}(\rho) = 1$
- $\rho = \rho^\dagger$
- For pure states: $\rho^2 = \rho \Rightarrow \mathrm{Tr}\left(\rho^2\right) = \mathrm{Tr}\left(\rho\right) = 1$
- For mixed states: $\mathrm{Tr}\left(\rho^2\right) < \mathrm{Tr}\left(\rho\right) = 1$
- The expectation value of a random operator A, is the weighted average value of its observable. It can be derived from the density operator:

$$\langle A\rangle = \mathrm{Tr}\left(A\rho\right) \tag{2.8}$$

2.3 Composite systems

A composite system is one involving two or more noninteracting subsystems, which act in different Hilbert spaces. The state space of such system is postulated to be constructed as the tensor product of the different state spaces of the subsystems. If for example the first system is in state $|\psi\rangle_A$ and the second in state $|\phi\rangle_B$, the state of the composite system is given by $|\psi\rangle_A \otimes |\phi\rangle_B$. In this notation an operator relating exclusively to component 1 is denoted $A_i^{(1)} = A_i \otimes I$, and one relating exclusively to component 2 is denoted as $B_j^{(2)} = I \otimes B_j$. The shorthand notation of the composite system is: $|\psi\rangle_A \otimes |\phi\rangle_B = |\psi\rangle\,|\phi\rangle$. In considering noninteracting subsystems like this, it is possible to only look at the dynamics of one subsystem by tracing out the unwanted subsystems. This procedure is called partial trace, and is given by: $\rho_A = \mathrm{Tr}_B\,(\rho_{\mathrm{total}})$.

2.4 Measurement

Measurements are described by measurement operators defined by the measurement basis. If $|a\rangle$ is a vector in the measurement basis with the eigenvalue λ_a with respect to a given observable, its associated measurement operator is $M_a = |a\rangle\langle a|$. This operator is also known as a projector, because finding the expectation value of this operator corresponds to projecting the state, $|\psi\rangle$ or ρ, onto $|a\rangle$, whereby we find the magnitude of this component in the state. This magnitude is the probability that a measurement will have λ_a as an outcome. Thus,

$$p(\lambda_a) = \langle\psi|\, M_a\, |\psi\rangle \quad \textbf{or} \quad p(\lambda_a) = \mathrm{Tr}(M_a\rho), \tag{2.9}$$

where the expectation value to the right is based on the density operator description of a state.

Depending on the interpretation that is adopted the idea of one particular outcome of a single measurement may not be meaningful[1], but in any case (2.9) describes the ratio of λ_a in a number of repeated measurements on the same system.

Whether the system changes as a direct consequence of having performed a measurement is debated; several interpretations (e.g. the Copenhagen interpretation) support this idea[16], called the observer effect, while other interpretations (e.g. the ensemble interpretation) are against this. In the Copenhagen interpretation it is assumed that the observer effect results in a wave function collapse – this assumption is known as the von Neumann projection postulate or the reduction postulate, which is discussed further in the following.

2.4.1 Von Neumann projections

Von Neumann's projection postulate states that the act of measurement leads to a non-unitary change of the state and hence is in complete contrast to the unitary dynamics of quantum mechanics predicted by the Schrödinger equation. This change is described as either a strong or weak von Neumann projection[17].

- **The strong von Neumann projection** describes the wave function collapse as a projection of the state into a single one of its basis vectors. Let an observable have eigenvalues a_i with corresponding eigenvectors $|a_i\rangle$, and assume the outcome of a

[1] E.g. the ensemble interpretation in which the wave function does not apply to a single experiment, i.e. a single measurement, but rather an ensemble.

measurement yields a_n, then the state vector $|\psi\rangle$ undergoes the following discontinuous evolution

$$|\psi\rangle = \sum_i c_i |a_i\rangle \rightarrow |a_n\rangle . \tag{2.10}$$

- **The weak von Neumann projection** regards all the possible measurement outcomes and collapses the state into a mixed state of the corresponding eigenvectors, namely

$$|\psi\rangle = \sum_i c_i |a_i\rangle \rightarrow \rho = \sum_i |c_i|^2 |a_i\rangle \langle a_i| , \tag{2.11}$$

  where the density operator ρ is required to describe the non-pure state.

In this thesis we will tend to use both kinds of projections, when considering wave function collapses.

2.4.2 Decoherence

Decoherence is a description of loss of phase difference between the states of the system, i.e. dephasing, due to the entanglement between a system and its environment. It does not generate actual wave function collapse, but provides an explanation for the transition of the system to a mixture of states corresponding to those states observers perceive[18].

Decoherence can be thought of as the loss of information from a system into the environment. Hence, when considered alone the system's dynamics are non-unitary, but the combined system plus environment evolves in a unitary fashion.

Loss of coherence in a state means that the quantum superposition of components is destroyed, and thus decoherence can be used to explain thought experiments like Schrödinger's cat or Wigner's friend [19]. At the same time decoherence poses a challenge for quantum computers due to the reasons discussed in the sec. 1.2.

2.5 Open systems

An open system is characterized as a system influenced by some external environment. The dynamics of such systems are fundamentally different from the deterministic dynamics of closed systems. Open systems are stochastic in nature, which comes from the fact that the state does not only evolve according to its own internal dynamics, but is affected by the dynamics of the environment. The interaction of the system with the environment introduces decoherence, which makes the state of the system more mixed.

Because of the state mixing of an open system, it is necessary to characterize it through the density operator instead of the state vector, since it describes both the mixed and pure states. Furthermore, the environmental influence on the system means that the evolution of the system is generally not unitary, which makes it a difficult task to solve the dynamics of the Hamiltonian. The state dynamics becomes extremely dependent on the system and on the environmental influence under consideration. Its necessary to derive a so-called master equation representing the dynamics of the reduced density operator, given by the partial trace over the environment: $\rho_s(t) = \mathrm{Tr}_e(\rho(t))$, which leaves us with the dynamics of the system. The reason why this reduced density operator represents the dynamics of the system, is because the system and environment are considered distinguishable, such that the full Hilbert space is given by the tensor product: $\mathcal{H} = \mathcal{H}_S \otimes \mathcal{H}_E$. This means that the reduced density operator describes everything about the system and nothing about the environment, because it gets traced out.

2.5.1 Born-Markov master equation

Everything discussed so far can now be put together to derive a master equation describing the dynamics of an system influenced by some external environment. More specifically we are going to derive the so-called weak-coupling Born-Markov master equation, which describes the time-evolution of the system operator when weak dissapative and decohering effects of the environment is being considered. The primary approximation for this master equation is thus that the environmental interaction with the system is weak. The Born-Markov master equation is one of the best candidates describing the intrinsic spontaneous emission and pure dephasing of an open system, which we are going to use later in this thesis.

First we need to write out the full Hamiltonian that we are considering:

$$H = H_S + H_E + H_I \tag{2.12}$$

where the first and second term is the Hamiltonian for respectively the system and the environment, and the last term is an interaction Hamiltonian that describes the coupling between the system and the environment and their degrees of freedom. One crucial part of the derivation of the master equation is the use of the interaction picture. This picture removes the contribution of the system-environment Hamiltonian ($H_S + H_E$) by a unitary transformation on the density operator and the interaction Hamiltonian H_I. This is done because generally the evolution of H_S and H_E is simple to solve, but the evolution of the interaction Hamiltonian H_I is complicated and needs to be approximated. More explicitly, the interaction Hamiltonian becomes:

$$\tilde{H}_I = e^{i(H_S+H_E)(t-t_0)} H_I e^{-i(H_S+H_E)(t-t_0)} \tag{2.13}$$

The tilde represents operators that are transformed into the interaction picture. The assumption is that the system and environment combined, define the total system and is therefore closed. This means, according to the general description of closed systems that within the interaction picture, the density operator of the total system satisfies:

$$\frac{\partial \tilde{\rho}(t)}{\partial t} = -i \left[\tilde{H}_I(t), \tilde{\rho}(t) \right] \tag{2.14}$$

with the formal solution:

$$\tilde{\rho}(t) = \tilde{\rho}(t_0) - i \int_{t_0}^{t} \left[\tilde{H}_I(s), \tilde{\rho}(s) \right] ds \tag{2.15}$$

If this solution is substituted back into (2.14) and the trace is taken over the environment, we then get:

$$\frac{\partial \tilde{\rho_S}(t)}{\partial t} = -i \mathrm{Tr}_E \left(\left[\tilde{H}_I(t), \rho(0) \right] \right) - \int_0^t \mathrm{Tr}_E \left(\left[\tilde{H}_I(t), \left[\tilde{H}_I(s), \tilde{\rho}(s) \right] \right] \right) ds \tag{2.16}$$

where we have set t_0 equal to zero. We have now derived an equation that describes the dynamics of the reduced density operator $\rho_S(t)$, which we would like to calculate. The equation is put into a convenient form that let us make some appropriate approximations in order to simplify the equation.

2.5.1.1 Approximation

- Born approximation: We assume that the total density operator can be factorized into its system and environment components at all times:

$$\tilde{\rho}(t) \approx \tilde{\rho_S}(t) \otimes \rho_E$$

where it is assumed that the environmental density operator ρ_E is time-independent. The foundation of this approximation relies on the weak coupling strength between the system and environment, so that their corresponding density operators do not become substantially entangled. The approximation therefore relies on systems that do not influence the environment, which thus stay practically unaffected and static. After this approximation the master equation takes the form:

$$\frac{\partial \tilde{\rho_S}(t)}{\partial t} = -\int_0^t \mathrm{Tr}_E \left[\tilde{H_I}(t), \left[\tilde{H_I}(s), \tilde{\rho_S}(s) \otimes \rho_E\right]\right] ds$$

where we have set $\mathrm{Tr}_E \left[\tilde{H_I}(t), \rho(0)\right] = 0$, since this can be ensured by absorbing it into the system Hamiltonian H_S.

- Markov Approximation: The complexity of the master equation is further reduced by bringing the equation into a time local form, such that the dynamics of the system density operator $\tilde{\rho_S}$ only depends on its present state and not past history through the integration over $\tilde{\rho_S}(s)$. The approximations in the Markov approximation are as follows:
  - $\tilde{\rho_S}(s)$ gets replaced with $\tilde{\rho_S}(t)$, thereby making it independent on its past history since its not longer part of the integral. The validity of this approximation is justified, if the environment memory time, which is the time over which the environment remembers the past system states, is short in comparison to the system evolution time. This approximation is in close relation to the Born approximation, since it assumes that the environment is practically unaffected by the system.
  - The substitution of $s \to t - \tau$ is made, so that the limit of the integral can go to infinity - justified by the large timescale difference between the environment memory time and the system evolution time.

  With these approximations the master equation becomes:

$$\frac{\partial \tilde{\rho_S}(t)}{\partial t} = -\int_0^\infty \mathrm{Tr}_E \left[\tilde{H_I}(t), \left[\tilde{H_I}(t-\tau), \tilde{\rho_S}(t) \otimes \rho_E\right]\right] d\tau \tag{2.17}$$

These approximations have hereby provided the Born-Markov master equation in the interaction picture, which can describe the evolution of an open system influenced by weak coupling to the environment.

2.5.2 Correlation functions

We are now going to put the Born-Markov master equation into a more convenient and notorious form that gives us more insight of its nature. In doing this, we define the interaction Hamiltonian H_I having the general form:

$$H_I = \sum_\alpha \hat{A}_\alpha \otimes \hat{B}_\alpha \tag{2.18}$$

where $\hat{A}_\alpha$ and $\hat{B}_\alpha$ are respectively system and environmental operators. In the interaction picture this Hamiltonian has the form:

$$\begin{aligned} \tilde{H_I}(t) &= \sum_\alpha A_\alpha(t) \otimes B_\alpha(t) \\ &= \sum_\alpha e^{iH_S t} A_\alpha e^{-iH_S t} \otimes e^{iH_E t} B_\alpha e^{-iH_E t} \end{aligned} \tag{2.19}$$

If we now expand the commutators of (2.17):

$$\frac{\partial\tilde{\rho_S}(t)}{\partial t} = \int_0^\infty \mathrm{Tr}_E \Big(\Big[\tilde{H_I}(t-\tau)\tilde{\rho}(t)\rho_E\tilde{H_I}(t) - \tilde{H_I}(t)\tilde{H_I}(t-\tau)\tilde{\rho}(t)\rho_E\Big] + \tilde{H_I}(t)\tilde{\rho_S}(t)\rho_E\tilde{H_I}(t-\tau) - \tilde{\rho_S}(t)\rho_E\tilde{H_I}(t-\tau)\tilde{H_I}(t)\Big)\, d\tau \tag{2.20}$$

and insert the definition of $\tilde{H_I}(t)$ into this equation, where $\tilde{H}(t-\tau)$ and $\tilde{H}(t)$ will be separated by summing over respectively β and α. This gives the following expression for the dynamics of the density operator:

$$\begin{aligned}\frac{\tilde{\rho_S}(t)}{dt} &= \sum_{\alpha\beta}\int_0^\infty \mathrm{Tr}_E\left(A_\beta(t-\tau)\tilde{\rho_S}(t)A_\alpha(t)\otimes B_\beta(t-\tau)\rho_E B_\alpha(t) - A_\alpha(t)A_\beta\tilde{\rho_S}(t)\otimes B_\alpha(t)B_\beta\rho_E\right.\\ &\qquad \left. - A_\alpha B_\alpha\tilde{\rho_S}(t)\otimes\rho_E B_\alpha(t)B_\beta(t-\tau) + \tilde{\rho_S}(t)A_\beta(t-\tau)A_\alpha(t)\rho_E B_\beta(t-\tau)B_\alpha(t)\right)d\tau\\ &= -\sum_{\alpha\beta}\int_0^\infty \left([A_\alpha(t), A_\beta(t-\tau)\tilde{\rho_S}(t)]\,\mathrm{Tr}_E\left(B_\alpha(t)B_\beta(t-\tau)\rho_E\right)\right.\\ &\qquad \left. + [\tilde{\rho_S}(t)A_\beta(t-\tau), A_\alpha]\,\mathrm{Tr}_E\left(B_\beta(t-\tau)B_\alpha(t)\rho_E\right)\right)d\tau\end{aligned} \tag{2.21}$$

Here we have also used cyclic invariance of the trace, which led to: $\mathrm{Tr}_E\left(B_\alpha(t)B_\beta(t-\tau)\rho_E\right) = \mathrm{Tr}_E\left(B_\beta(t-\tau)\rho_E B_\alpha(t)\right)$ and $\mathrm{Tr}_E\left(B_\beta(t-\tau)B_\alpha(t)\rho_E\right) = \mathrm{Tr}_E\left(B_\alpha(t)\rho_E B_\beta(t-\tau)\right)$. These factors are correlation functions of the environment. Since the Born-Markov approximation assumes that the environment is in a stationary state, such that $\frac{\partial\rho_E}{\partial t} = -i\left[H_E,\rho_E\right] = 0$, means that the correlation functions become:

$$\begin{aligned}\mathrm{Tr}_E\left(B_\alpha(t)B_\beta(t-\tau)\rho_E\right) &= \mathrm{Tr}_E\left(e^{iH_Et}B_\alpha e^{-iH_Et}e^{iH_E(t-\tau)}B_\beta e^{-iH_E(t-\tau)}\rho_E\right)\\ &= \mathrm{Tr}_E\left(e^{iH_E\tau}B_\alpha e^{-iH_E\tau}B_\beta\rho_E\right)\\ &= \langle B_\alpha(\tau)B_\beta(0)\rangle_E = C_{\alpha\beta}(\tau)\end{aligned} \tag{2.22}$$

And for the other one we get $\mathrm{Tr}_E\left(B_\beta(t-\tau)B_\alpha(t)\rho_E\right) = C_{\beta\alpha}(-\tau)$. These correlation functions are functions that define the correlation of the operators B_α and B_β at two different points in time. In this context they justify the Markov-approximation, since the infinity-limit of the integration is dealt with because the correlation functions die off fast. Inserting these correlation functions into (2.21) and transforming (2.21) back into the Schrödinger picture using: $\frac{\partial\rho_S}{\partial t} = -i\left[H_S,\rho_S(t)\right] + e^{-iH_St}\left(\frac{\partial\tilde{\rho_S}(t)}{\partial t}\right)e^{iH_St}$, we get the master equation in the Schrödinger picture:

$$\frac{\tilde{\rho_S}(t)}{dt} = -i\left[H_S,\rho_S(t)\right] - \sum_{\alpha\beta}\int_0^\infty \left([A_\alpha, A_\beta(-\tau)\rho_S(t)]\,C_{\alpha\beta}(\tau) + [\rho_S(t)A_\beta(-\tau), A_\alpha]\,C_{\beta\alpha}(-\tau)\right)d\tau \tag{2.23}$$

The first term on the right-hand-side represents the closed system and generates unitary evolution of time for the system H_S, while the remaining terms represent the environmental influence on the system, and generates therefore non-unitary evolution. This is the equation that will be of great use in this thesis.

Chapter 3

The Quantum Zeno Effect

Formulating the QZE as a phenomenon that hinders the evolution of a quantum system by the use of frequent measurements links to the work done by Sudarshan and Misra [2]. This formulation is often referred to as the genuine QZE [20], which will be a descriptive term repeatedly used in the thesis. By most physicists the genuine QZE is considered a physical impossibility, because the requirement of "freezing" the state in its initial state, is only obtained in the limit of infinitely frequent measurements [21]. The formulation is also based on von Neumann measurements, which means that it in addition hinges upon the notion of collapse of the wave function; a concept in quantum theory only accepted by a few of its interpretations and furthermore constitutes the crux of the 'measurement problem' of quantum theory. For many theorists the genuine QZE is therefore just a mathematical construct, and physically it should not even be possible to slow down the evolution of the quantum state in this manner [22]. The theoretical scientist Pascazio, who is well-endowed in this field, has explicitly stated that the QZE "cannot be ascribed to the 'collapse' of the wave function"[15]. Albeit its controversy, it has not been experimentally proven or disproven and maybe never will be. If it would be, it would certainly put many of the interpretations of quantum theory in danger.

The formulation of the QZE has however changed over the years and is now not only defined by the previous conjecture, but covers a much broader context. The experimentally verified manifestations of the QZE, e.g. [1], can be understood as a consequence of how the dynamics of quantum systems gets modified by complex interactions with the external macroscopic environment. It turns out according to the article [15] that practically any interaction that greatly disturbs the considered system can provoke a QZE. Considering this statement, the QZE as a phenomenon reaches far beyond the context formulated by its original definition; whenever a strong perturbation provokes the dynamics of the system. It has to be emphasized that this description of the QZE has been widely known, and has appeared in literature on quantum theory many times in different contexts.

The external apparatus performing the measurement on the system therefore needs not be a von Neumann measurement, which yields the collapse of the wave function. To obtain the QZE it is sufficient to indirectly "measure" the system with e.g. unitary "continuous coupling"[23]. This is physically equivalent to influencing the system with a driving oscillating electric field (a laser), which induces Rabi-oscillation[1] of the system [15]. Likewise, it is possible to obtain the QZE by influencing a system with laser-pulses; corresponding mathematically to so-called unitary kicks [24], which in essence are instantaneous unitary

[1] Oscillation between two levels of a system, is known as Rabi-oscillation

processes that in comparison to von Neumann measurements, do not leave a collapsed state [21].

3.1 How to read this thesis

We start out by outlining the theory behind the controversial genuine form of the QZE based on von Neumann (projection) measurements - or rather the 'collapse' of the wave function. Afterwards we are going to discuss the 'measurement problem' in QZE context, followed by an extensive analysis of the QZE in QDs by projective measurements. The QZE will then by analysed in QDs influenced by 'continuous coupling' and different types of external environments that lead to spontaneous emission or pure dephasing of the QD. In this thesis we are not going to consider unitary kicks.

Also note that we use the following terminology:

- Dissipation is used if it is clear whether is refers to spontaneous emission or dephasing.
- 'Continuous coupling' and driving are used interchangeably and gives for Rabi oscillations induced by external fields.
- The terms coupling strength and Rabi frequency refer to the same quantity, Ω.
- Projective measurements and von Neumann measurements both refer to measurements where wave function collapse is assumed.
- Later when we derive new master equations they will be referred to as rigorous or complete master equations, whereas the master equation obtained through the Lindblad formalism is referred to as the Lindblad master equation.

3.2 QZE: Projective measurements

In classical statistical mechanics, the model for the decay of any system is an exponential function of time. However, while the decay of quantum systems is similar, there are some unavoidable deviations from the classical model at certain timescales. The quantum evolution, governed by the Schrödinger equation, will at short timescales be modelled by a quadratic function of time.

This can be shown by considering the decay of an unstable quantum state, prepared in an initial state $|\psi(t_0)\rangle$; a normalized vector in the Hilbert space $\mathcal{H}$. Because the considered system is closed, the time evolution of the system is unitary and evolves in time according to the Schrödinger equation (2.2). As previously stated, the state will therefore evolve under the unitary operator $U(t)$; $|\phi(t)\rangle = U(t)\,|\phi(t_0)\rangle = e^{-iHt}\,|\phi(t_0)\rangle$. The survival probability, P(t), i.e., the probability that the system retains its initial state at time t, will be given by:

$$P(t) = |A(t)|^2, \quad \text{with} \quad A(t) = \langle\phi(t_0)|\, e^{-iHt}\,|\phi(t_0)\rangle \tag{3.1}$$

Where $A(t)$ is called the survival amplitude. From this expression one can easily show that the decay of any quantum system is not exponential. A Taylor expansion of the survival probability is:

$$P(t) \approx 1 - \langle H\rangle\, t^2 + \langle H\rangle^2\, t^2 + .. = 1 - \left\langle (H - \langle H\rangle)^2 \right\rangle t^2 + ... = 1 - \frac{t^2}{\tau_z^2} + ... \tag{3.2}$$

Where τ_z is the 'Zeno time' and the averages are taken over the initial state $|\phi(t_0)\rangle$. If these averages are finite, it therefore follows that the survival probability is quadratic rather than exponential for short times.

By a straightforward calculation done in [22] it can also be shown that the survival amplitude can be written as the Fourier transform of the energy spectral function $\eta(E)$ for the state $|\phi(t_0)\rangle$, given by:

$$A(t) = \int_0^\infty e^{-iE_n t}\eta(E)dE, \quad where \quad \eta(E) = \sum_n |\langle E_n|\phi(t_0)\rangle|^2\delta(E-E_n) \tag{3.3}$$

The only way the survival probability will be a exponential function of time, is if the survival amplitude also is a exponential function of time. Since the Fourier transform relation between ηE and $A(t)$ is a one to one correspondence, it follows that this can only be the case, if the spectral function $\eta(E)$ has the form of a Lorentzian distribution[22]. The expectation values $\langle H^n\rangle = \int E^n\eta(E)dE$ in (3.2), will not be convergent at their infinite upper limit with this spectral function. The survival probability can therefore never be exponential at this timescale.

Now we will introduce the strong von Neumann (projective) measurements that will lead to the manifestation of the QZE. Let us suppose that the unstable system is measured N times at the time intervals $\tau = T/N$. Since τ is very small, the survival probability of the system will be given by (3.2). If the system is found in its initial state every time it is measured, the wave function collapses and the state of the system is projected back onto its initial state $|\phi(t_0)\rangle$[2]. The probability of survival in state $|\phi(t_0)\rangle$ at the end of the sequence of N independent measurements, will therefore be the product of the probabilities for surviving each of the short intervals, and thus we get:

$$P(T) = [P(T/N)]^N = \left[1 - \left(\frac{T}{N\tau_z}\right)^2\right]^N \sim e^{-(\frac{T}{N\tau_z})^2} \underbrace{\longrightarrow}_{N\to\infty} 1 \tag{3.4}$$

For large N the evolution of the system is slowed down and in the limit of infinite measurements, i.e., when $N \to \infty$, the probability that the state will not decay goes to 1. The system therefore never changes its state if it is "continuously" measured - it is frozen in its initial state. This is the QZE in its most general form.

This derivation of the QZE shows that the system is forced to remain in its initial state. However, it has to be stressed that this formulation of the QZE is restrictive, since it does not take into account incomplete measurements. By 'incomplete' measurements is meant that the projection operator is multi-dimensional rather than one-dimensional as in this case - which happens if e.g. the measurement apparatus has insufficient resolution. If we were to consider the case of frequent measurements by a multi-dimensional projection operator - firmly derived by Misra and Sudarshan [2] - the QZE would necessarily not freeze everything, but would rather constrain the evolution of the initial state into the subspace defined by the 'measurement'. The evolution of the state within the projected "Zeno subspace" is usually called "quantum Zeno dynamics", but is not a topic of our concern - it should just not be overlooked.

[2]The system can also be found in its orthogonal state $|\phi(0)\rangle^\perp$, with quadratic probability 1-P(τ)=$(\frac{\tau}{\tau_z})^2$, but since $\tau = O(1/N)$, such an event becomes increasingly unlikely as N increases.

3.3 The measurement problem w.r.t. the QZE

The problem of what happens in the aftermath of a measurement is what constitutes the 'measurement problem'. Some interpretations of quantum mechanics depend on the collapse to explain the connection between the Schrödinger equation and measurement outcomes, but they generally fail to explain exactly how and why the collapse occurs.

However there are alternative theories on the measurement process based on decoherence, which avoid the issues involved with the measurement problem by assuming that collapse does not occur. We will briefly discuss an argument of one such theory [14] and what it means for the QZE.

We consider a dynamical variable R belonging to an object we want to measure with a given apparatus, prepared in an initial state $|\alpha_0\rangle$. If the initial state of the object is a coherent superposition of the eigenvectors $|r\rangle$ of R, then the state of the complete system starts in the uncorrelated state: $|\Psi(t_i)\rangle = \sum_r c_r |r\rangle \otimes |\alpha_0\rangle$. After some time with unitary evolution the initial state will evolve into the final state – the premeasurement state:

$$|\Psi(t_f)\rangle = \sum_r c_r |r\rangle \otimes |\alpha_r\rangle . \tag{3.5}$$

The density operator $\rho(t_f) = |\Psi(t_f)\rangle \langle\Psi(t_f)|$ evidently describes a pure state. But if we were now to make measurements on the object alone, we are neglecting the apparatus and thus tracing it out of the complete state. Hence, the measured state will be a partial state $\rho^{(o)}(t_f) = \mathrm{Tr}_a(\rho(t_f))$. If we make it more concrete we might assume that the premeasurement state is given by $|\Psi(t)\rangle = c_e |e\rangle \otimes |\alpha_e\rangle + c_g |g\rangle \otimes |\alpha_g\rangle$. Then the density operator becomes

$$\begin{aligned} \rho(t_f) = |c_e|^2 |e\rangle \langle e| \otimes |\alpha_e\rangle \langle\alpha_e| + c_e c_g^* |e\rangle \langle g| \otimes |\alpha_e\rangle \langle\alpha_g| \\ + c_g c_e^* |g\rangle \langle e| \otimes |\alpha_g\rangle \langle\alpha_e| + |c_g|^2 |g\rangle \langle g| \otimes |\alpha_g\rangle \langle\alpha_g| . \end{aligned} \tag{3.6}$$

If we trace out the apparatus assuming the apparatus states are mutually orthogonal, then it will describe an incoherent mixture

$$p^{(o)}(t_f) = |c_e|^2 |e\rangle \langle e| + |c_g|^2 |g\rangle \langle g| . \tag{3.7}$$

Hence, we see that the partial state may be incoherent, but the complete system remains pure and coherent. The apparent loss of coherence in the system, when considering measurement outcomes therefore do not necessarily require the notion of wave function collapse.

The argument illustrates that collapse need not be essential to the theory of quantum. The genuine QZE relies strictly on the validity of von Neumann projections and if wave function collapse is not real this manifestation of QZE should not be real either. And indeed some authors finds QZE objectionable because of this. For instance Ballentine states in his book on quantum mechanics [22]: "Like the old saying 'A watched pot never boils', we have been led to the conclusion that a continuously observed system never changes its state! This conclusion is, of course, false".

While the formulation of the QZE has changed to cover a much broader range of phenomena that do not require the notion of collapse – whenever a strong perturbation provokes the dynamics of the system [28] - this particular manifestation represents a physical distinction between the interpretations. As stated earlier, if experimental evidence were to support this manifestation it should be possible to objectively falsify a number of interpretations.

Chapter 4

General analysis of QZE

The aim of this chapter is to analyze the requirements for obtaining the QZE in two- and three level QDs influenced by various disturbances from the external environment. The dynamics of the QD is both going to be considered in open and closed quantum systems. In the closed systems the QDs are only going to be influenced by time varying electric fields – i.e. 'continuous coupling' – while in the open systems the effects of spontaneous emission and pure dephasing are going to be introduced to the dynamics of the QDs. We start off by considering two-level QDs.

4.1 Two-level system

In a two-level system states are described in a two-dimensional Hilbert space by two linearly independent basis vectors – we will call them $|g\rangle$ (ground state) and $|e\rangle$ (excited state). The density operator is a 2x2 matrix, and can thus be expressed as a linear combination of four linearly independent matrices such as I, σ_x, σ_y and σ_z. From this we write:

$$\rho(t) = \frac{1}{2}(I + \alpha \cdot \sigma) = \frac{1}{2}\begin{pmatrix} 1+\alpha_z(t) & \alpha_x(t) - i\alpha_y(t) \\ \alpha_x(t) + i\alpha_y(t) & 1-\alpha_z(t) \end{pmatrix} \tag{4.1}$$

The factor $\frac{1}{2}$ has been chosen such that $\mathrm{Tr}(\rho) = 1$. The vector $\sigma = (\sigma_x, \sigma_y, \sigma_z)$ contains the Pauli spin matrices.

Bloch sphere

From the definition of (4.1) and the relation $\mathrm{Tr}(\sigma_i\sigma_j) = 2\partial_{i,j}$ it follows that

$$\langle\sigma_i\rangle = \alpha_i(t) \tag{4.2}$$

and thus $\alpha = (\alpha_x(t), \alpha_y(t), \alpha_z(t))^T$ is a vector of the expectation values of the Pauli spin matrices. It is known as the Bloch vector, which spans what is called the Bloch sphere.

It can easily be shown that the eigenvalues of ρ are $\frac{1}{2}(1 + |\alpha|)$ and $\frac{1}{2}(1 - |\alpha|)$. Since eigenvalues of state operators cannot be negative, this implies that the length of the Bloch vector must be restricted to the range $0 \leq |\alpha| \leq 1$. It can be shown that for pure states the requirement $\mathrm{Tr}\left(\rho^2\right) = 1$ only holds when the length of the Bloch vector is $|\alpha| = 1$, whereas for mixed states the condition is $|\alpha| < 1$. The state is totally mixed when $|\alpha| = 0$, where it is said to be described as a classical superposition. All the points on the surface of

the sphere therefore correspond to pure states of the system, while points on the interior correspond to mixed states. From this it is clear that the Bloch sphere can give a visual insight into the states of the system and also how they evolve.

4.1.1 Lindblad master equation

If we consider a QD undergoing spontaneous emission or pure dephasing, we can use what is called the Lindblad formalism. The Lindblad formalism is a weak-coupling Markovian master equation that can describe the time-evolution of the system operator, when weak dissipative and decohering effects of the environment is being considered. The density operator obeys the equations of motion:

$$\textbf{(spon. emission)} \qquad \frac{d\rho}{dt} = -i\left[H_{S'}, \rho\right] + \Gamma L(\sigma)\rho \tag{4.3}$$

$$\textbf{(pure dephasing)} \qquad \frac{d\rho}{dt} = -i\left[H_{S'}, \rho\right] + \gamma L\left(\sigma_z\right)\rho. \tag{4.4}$$

where $\sigma = |g\rangle\langle e|$, $\sigma_z = |e\rangle\langle e| - |g\rangle\langle g|$ and $H_{S'}$ is the system Hamiltonian in its rotational frame.

The first term describes the unitary and coherent evolution of the system, while the second term is the influence or the coupling to the environment, and generates dissipative non-unitary dynamics of the system. This second term is therefore called the dissipator of the system, and is given by:

$$\mathcal{L}(A)\rho = A\rho A^\dagger - \frac{1}{2}(A^\dagger A\rho + \rho A^\dagger A) = A\rho A^\dagger - \frac{1}{2}\left\{A^\dagger A, \rho\right\} \tag{4.5}$$

The above Lindblad master equations meet all the requirements that any master equation has to meet; it is trace-preserving and has completely positive dynamics.

The equations (4.3) and (4.4) are derived using the general expression (2.23) – more on this in chapter 5.

4.1.2 Equations of motion in a two-level system

For the rest of this chapter we now consider a system Hamiltonian with driving, i.e.

$$H_{S'} = \frac{\Omega}{2}\left(|e\rangle\langle g| + |g\rangle\langle e|\right). \tag{4.6}$$

From (4.2) it follows that

$$\langle\sigma_i\rangle' = \mathrm{Tr}\left[\sigma_i \partial_t \rho(t)\right]. \tag{4.7}$$

We use this relation to find the following two sets of differential equations

Hence, for both cases, we have a system of equations in which $\langle\sigma_y\rangle$ and $\langle\sigma_z\rangle$ are coupled, and $\langle\sigma_x\rangle$ is not only decoupled, but becomes a simple exponential function.

Spontaneous emission	Pure dephasing
$\langle\sigma_x\rangle' = -\frac{1}{2}\Gamma\langle\sigma_x\rangle$ (4.8)	$\langle\sigma_x\rangle' = -2\gamma\langle\sigma_x\rangle$ (4.11)
$\langle\sigma_y\rangle' = -\frac{1}{2}\Gamma\langle\sigma_y\rangle - \Omega\langle\sigma_z\rangle$ (4.9)	$\langle\sigma_y\rangle' = -2\gamma\langle\sigma_y\rangle - \Omega\langle\sigma_z\rangle$ (4.12)
$\langle\sigma_z\rangle' = \Omega\langle\sigma_y\rangle - \Gamma[\langle\sigma_z\rangle + 1]$. (4.10)	$\langle\sigma_z\rangle' = \Omega\langle\sigma_y\rangle$. (4.13)

Table 4.1: Equations of motion for two-level system for the cases of spontaneous emission and pure dephasing.

4.1.3 Population number in two-level system

In the succeeding sections we will tend to calculate the population number given the Bloch vector solution to the equations of motion.

Below we derive a simple relation for the population number of the $|e\rangle$ level

$$\begin{aligned}\langle|e\rangle\langle e|\rangle &= \left\langle \begin{bmatrix} 1 & 0 \\ 0 & 0 \end{bmatrix} \right\rangle \\ &= \left\langle \frac{1}{2}[\mathbf{I} + \sigma_z] \right\rangle \\ &= \frac{1}{2}[1 + \langle\sigma_z\rangle]. \end{aligned} \tag{4.14}$$

And since $\langle|e\rangle\langle e|\rangle + \langle|g\rangle\langle g|\rangle = 1$, we also find

$$\langle|g\rangle\langle g|\rangle = \frac{1}{2}[1 - \langle\sigma_z\rangle]. \tag{4.15}$$

4.1.4 Analytical solutions

From the two systems of equations in table 4.1, the system for spontaneous emission is inhomogeneous, while the system for pure dephasing is homogeneous. This calls for two different methods of solving the systems, but we will first show a general method that can be used to approximate solutions to both the homogeneous and inhomogeneous equation by a series expansion, while also addressing the steady state solutions.

Series expansion

The first-order differential system of equations of table 4.1 can be written in the matrix form

$$\dot{\alpha}(t) = M\alpha(t) + b \tag{4.16}$$

in which $\alpha(t)$ is the Bloch vector, M is the coefficient matrix and b is a constant vector term.

In order to solve this equation we define the following quantity

$$\Delta\alpha(t) = \alpha(t) - \alpha(\infty), \tag{4.17}$$

where $\alpha(\infty)$ is the (steady state) Bloch vector at $t = \infty$ – for which we assume all transients have passed completely such that $\dot{\alpha}(\infty) = 0$. Using this along with the definition (4.17),

we find the following relation

$$\begin{aligned} &\dot{\alpha}(t) = 0 \\ \Leftrightarrow\ &M\alpha(\infty) + b = 0 \\ \Leftrightarrow\ &\boxed{\alpha(\infty) = -M^{-1}b}. \end{aligned} \tag{4.18}$$

We are now able to write

$$\begin{aligned} \Delta\dot{\alpha}(t) = \dot{\alpha}(t) &= M\alpha(t) + b \\ &= M\Delta\alpha(t) + M\alpha(\infty) + b \\ &= M\Delta\alpha(t) + M(-M^{-1}b) + b \\ &= M\Delta\alpha(t). \end{aligned} \tag{4.19}$$

This equation, $\Delta\dot{\alpha}(t) = M\Delta\alpha(t)$, has the simple solution

$$\Delta\alpha(t) = e^{Mt}\Delta\alpha(0), \tag{4.20}$$

where the exponential function of Mt is defined according to the usual exponential function of an operator

$$e^A = \sum_{n=0}^{\infty} \frac{A^n}{n!} = \mathbf{I} + A + \frac{AA}{2!} + \frac{AAA}{3!} + ... \tag{4.21}$$

in which $\mathbf{I}$ is the identity matrix.

From (4.20) it follows that

$$\alpha(t) = e^{Mt}\Delta\alpha(0) + \alpha(\infty) \Leftrightarrow \boxed{\alpha(t) = e^{Mt}\left[\alpha(0) + M^{-1}b\right] - M^{-1}b}. \tag{4.22}$$

Spontaneous emission

To find the complete solution for spontaneous emission we again write up the system of equations as

$$\dot{\alpha}(t) = M\alpha(t) + b, \tag{4.23}$$

where (from table. 4.1)

$$M = \begin{pmatrix} -\frac{\Gamma}{2} & 0 & 0 \\ 0 & -\frac{\Gamma}{2} & -\Omega \\ 0 & \Omega & -\Gamma \end{pmatrix}, \quad b = \begin{pmatrix} 0 \\ 0 \\ -\Gamma \end{pmatrix}. \tag{4.24}$$

The solution can be found by first finding the complete solution α_{hom} to the corresponding homogeneous equation $\dot{\alpha}(t) = M\alpha(t)$, and then adding a particular solution α_{par} such that

$$\alpha_{\text{complete}} = \alpha_{\text{hom}} + \alpha_{\text{par}}. \tag{4.25}$$

The complete solution is given by[25]

$$\alpha(t) = \sum_{i=1}^{3} c_i e^{\lambda_i t}\mathbf{v}_i, \tag{4.26}$$

in which λ_i are the eigenvalues to M, and $\mathbf{v}_i$ are the normalized eigenvectors – see app. A.1.1 eq. (A.1) and (A.2) for the computed eigenvalues and eigenvectors.

The constants c_i are found using the initial values. For the usual case where the systems starts off in the excited state, i.e. $(\alpha_1(0), \alpha_2(0), \alpha_3(0)) = (0, 0, 1)$, we have computed and listed these constants – see app. A.1.1, eq. (A.6).

We now find the particular solution. This is done by assuming that the guess function

$$\alpha_g = \mathbf{c}t + \mathbf{d} \tag{4.27}$$

is a solution. Hence, by inserting in the matrix form of the differential equation

$$\dot{\alpha_g}(t) = \mathbf{c} = M(\mathbf{c}t + \mathbf{d}) + \mathbf{b} \tag{4.28}$$

$$\Leftrightarrow t(M\mathbf{c}) + (\mathbf{d} - \mathbf{c} + \mathbf{b}) = 0. \tag{4.29}$$

Due to linear independence we require that

$$M\mathbf{c} = 0 \quad \text{and} \quad \mathbf{d} - \mathbf{c} + \mathbf{b} = 0. \tag{4.30}$$

Solving these two equations yield

$$\mathbf{c} = \mathbf{0}, \quad \mathbf{d} = \left(0, \frac{2\Gamma\Omega}{\Gamma^2 + 2\Omega^2}, -\frac{\Gamma^2}{\Gamma^2 + 2\Omega^2}\right)^{\mathbf{T}}. \tag{4.31}$$

The particular solution is therefore

$$\alpha_{\text{par}} = \mathbf{d}, \tag{4.32}$$

and consequently the complete solution is

$$\alpha_{\text{complete}} = \left(0, \frac{2\Gamma\Omega}{\Gamma^2 + 2\Omega^2}, -\frac{\Gamma^2}{\Gamma^2 + 2\Omega^2}\right)^{\mathbf{T}} + \sum_{i=1}^{3} c_i e^{\lambda_i t}\mathbf{v}_i. \tag{4.33}$$

Pure dephasing

From table 4.1 the pure dephasing system of equations can be written as

$$\dot{\alpha}(t) = M\alpha(t), \tag{4.34}$$

where

$$M = \begin{pmatrix} -2\gamma & 0 & 0 \\ 0 & -2\gamma & -\Omega \\ 0 & \Omega & 0 \end{pmatrix}. \tag{4.35}$$

This equation has the complete solution[25]

$$\alpha(t) = \sum_{i=1}^{3} c_i e^{\lambda_i t}\mathbf{v}_i. \tag{4.36}$$

The eigenvalues and eigenvectors are listed in app. A.1.1 in eq. (A.9) and (A.10).

The constants are found from the initial values. Again, for the case $(\alpha_1(0), \alpha_2(0), \alpha_3(0)) = (0, 0, 1)$, i.e. the system starts off in the excited state, we have computed and listed these constants – see app. A.1.2, eq. (A.13).

Combining all the computed values and reducing we obtain

$$\alpha_{\text{complete}}(t) = \left(0, \frac{\left(\epsilon^2 - \gamma^2\right)\left(e^{2t\epsilon} - 1\right)e^{-t(\gamma+\epsilon)}}{2\Omega\epsilon}, \frac{e^{-t(\gamma+\epsilon)}\left(\gamma\left(e^{2t\epsilon} - 1\right) + \epsilon\left(e^{2t\epsilon} + 1\right)\right)}{2\epsilon}\right)^{\mathbf{T}}, \tag{4.37}$$

where we have defined $\epsilon = \sqrt{\gamma^2 - \Omega^2}$.

4.1.5 Solutions in two-level system

In the following we will present and discuss results. We will tend to use values that are realistic for QDs, but we may sometimes refrain from this for illustrative purposes.

The systems we will be considering are depicted in fig. 4.1.

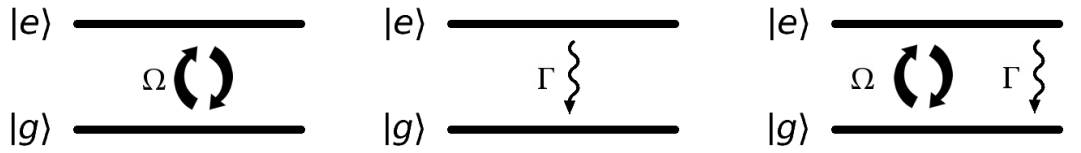

(a) Only Rabi oscillations. **(b)** Only dissipation. **(c)** Driving and dissipation.

Figure 4.1: Diagrams of the systems we will consider in this chapter. Note that the downward arrow labelled Γ represents both spontaneous emission and dephasing, even though the semantic behind the downward arrow is most appropriate for emission.

Solution to spontaneous emission Lindblad master equation

We consider the basic behavior of two-level systems with spontaneous emission and driving. We use the analytical solution (4.33).

Firstly, we look at systems where the driving is dominant. We expect unitary evolution if the dissipation vanishes, $\Gamma \to 0$, meaning that we will maintain a pure state over time with a length of the Bloch vector equal to 1. In figure 4.2 we see this. For weak, but non-zero, dissipation the Rabi oscillations are present for a relatively long time as seen on figure 4.3, until a steady state eventually settles in.

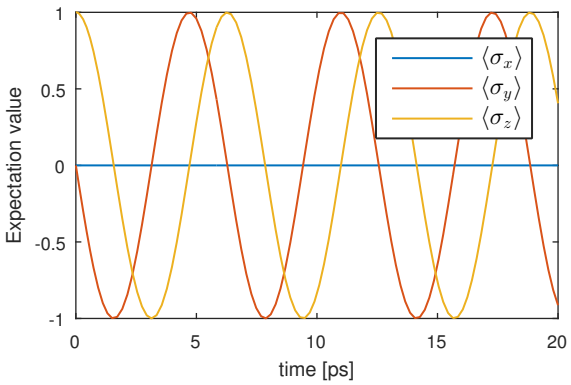

Figure 4.2: Solution with driving strength $\Omega = 1\,\mathrm{ps}^{-1}$ and no dissipation, $\Gamma = 0\,\mathrm{ps}^{-1}$, corresponding to the unitary evolution of a closed system. The Rabi oscillations continue indefinitely.

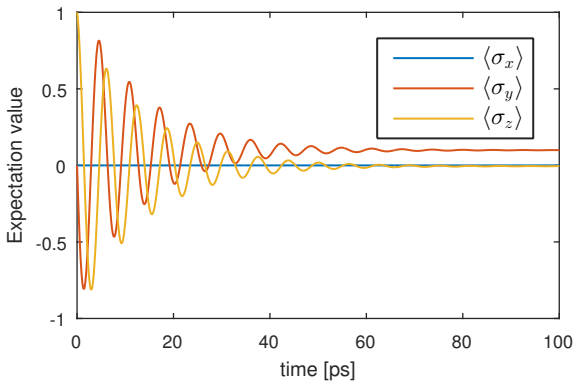

Figure 4.3: Solution with driving stength $\Omega = 1\,\mathrm{ps}^{-1}$ and weak dissipation $\Gamma = 0.1\,\mathrm{ps}^{-1}$. It takes a considerable amount of time to reach the steady state due to the weak dissipation.

In figure 4.4 the driving and dissipation are comparable. This results in Rabi oscillations being present, but only for a short time, after which the components of the Bloch vector reaches steady state. The steady state value for $\langle\sigma_z\rangle$ is displaced downwards, but only slightly. On figure 4.5 however, with strong dissipation, the steady state value goes all the way down to -1, corresponding to a full transition from the excited state to the ground state.

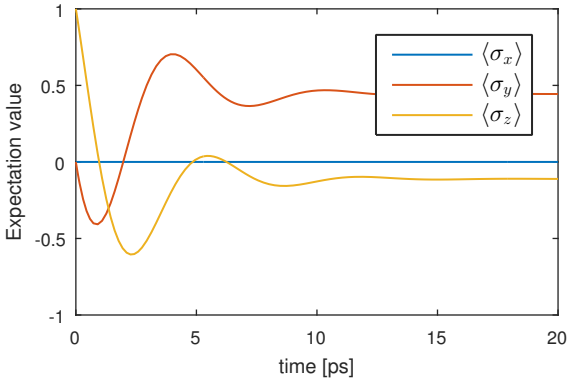

Figure 4.4: Solution with comparable magnitude of driving strength and dissipation rate; $\Omega = 1\,\mathrm{ps}^{-1}$ and $\Gamma = 0.5\,\mathrm{ps}^{-1}$. The steady state is displaced down towards -1, corresponding to a higher population of the $|g\rangle$ state, due to the spontaneous emission. This was not visible on figure 4.3, because the rate was too weak.

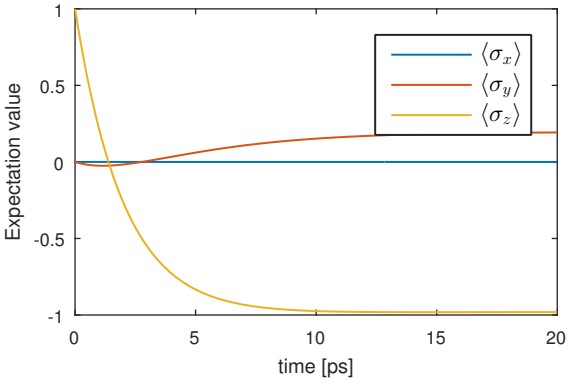

Figure 4.5: Solution with dominating dissipation; $\Gamma = 0.5\,\mathrm{ps}^{-1}$ and $\Omega = 0.05\,\mathrm{ps}^{-1}$. In this regime Rabi oscillations do not appear and the steady state settles in quickly. The steady state value for $\langle\sigma_z\rangle$ goes down to about -1, corresponding to the ground state being populated.

Solution to pure dephasing Lindblad master equation

We now study the basic behavior of systems subjected to pure dephasing and driving. We use the analytical solution (4.37).

Figure 4.6 shows the solution for a system with weak dissipation. Due to the weak dissipation the steady state takes some time to settle in, whereas on figure 4.7, in which the driving strength and dissipation rate are comparable, the steady state is already present at 10 ps.

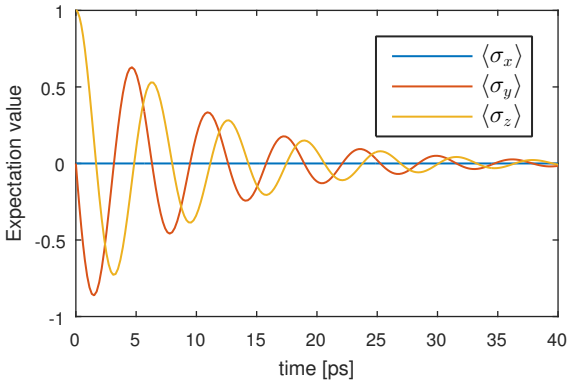

Figure 4.6: Solution with low dissipation; $\omega = 1\,\mathrm{ps}^{-1}$ and $\gamma = 0.1\,\mathrm{ps}^{-1}$.

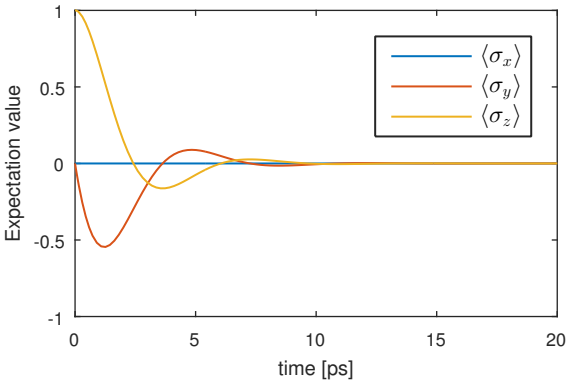

Figure 4.7: Solution with comparable magnitude of driving strength and dissipation rate; $\omega = 1\,\mathrm{ps}^{-1}$ and $\gamma = 0.5\,\mathrm{ps}^{-1}$.

On figure 4.8 we have plotted the solution for a system with strong dissipation and weak driving. As can be seen this results in the steady state being at about 400 ps, which is much more than the 10 ps on figure 4.7, even though these two solutions are based on the same dissipation rate, $\gamma = 0.5\,\mathrm{ps}^{-1}$. This indicates that the driving strength is important to the steady state time. The tendency towards long steady state times is shown even more clearly on figure 4.9, where the dissipation rate has been increased by a factor of 20 compared to the two other figures. We will investigate this in more detail later.

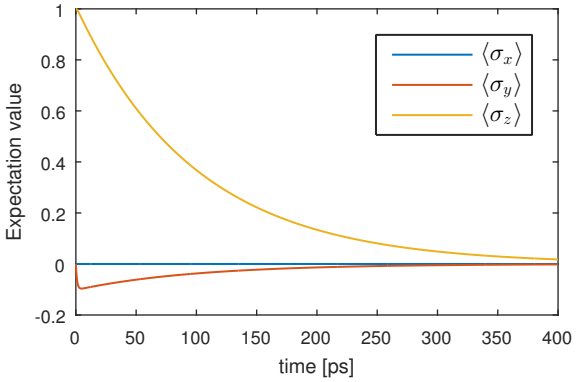

Figure 4.8: Solution with strong dissipation and weak driving strength; $\omega = 0.1\,\mathrm{ps}^{-1}$ and $\gamma = 0.5\,\mathrm{ps}^{-1}$. Note that the time interval had to be increased significantly to encompass the steady state.

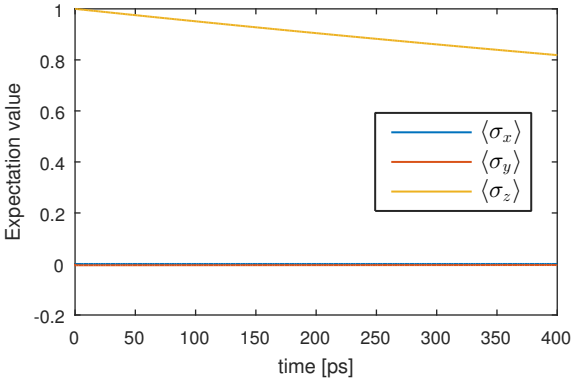

Figure 4.9: Solution with very strong dissipation rate, $\gamma = 10\,\mathrm{ps}^{-1}$ and weak driving $\omega = 0.1\,\mathrm{ps}^{-1}$. The very uneven relationship between the driving and the dephasing rate yields a very slow decay. This is explained later.

4.1.5.1 Bloch sphere

The above plots are all based on the initial state being $|e\rangle$, and thus are not completely representative for the overall behavior of the systems. To represent the solution more generally, we choose to plot the Bloch sphere, whereby we take all possible initial state vectors into consideration and visualize their evolution as a whole.

For this purpose we use the initial state

$$|\psi\rangle = \cos\left(\frac{\theta}{2}\right)|0\rangle + e^{i\phi}\sin\left(\frac{\theta}{2}\right)|1\rangle\,, \quad \theta \in [0,\pi], \quad \phi \in [0,2\pi]. \tag{4.38}$$

By letting θ and ϕ run through their respective intervals, the whole surface of pure states on the Bloch sphere is spanned.

Doing this and then tracking the time evolution for each individual initial state, we can plot the surface at discrete times. This has been done for both the dephasing and spontaneous emission Lindblad master equation, see figure 4.10 and 4.11 respectively.

The first figure 4.10 shows the dynamics of a system undergoing spontaneous emission while being influenced by a relatively weak drive with coupling strength $\Omega = 0.5\,\mathrm{ps}^{-1}$. Since the drive is relatively weak, the system is seen to evolve into a state that on average is more in the ground state than in the excited state. This is true, since the Bloch sphere continuously approaches a state where $\langle\sigma_z\rangle \approx -1$, which is equivalent to the ground state. The bloch sphere also reveals that the system continuously evolves into being a more mixed state, because the sphere shrinks as time goes on. The sphere will however never evolve into a single point, formed when $\langle\sigma_z\rangle = -1$, because the system is being driven. This can be seen on the figure showing the bloch sphere after $t = 6$ ps where the system has approximately reached its steady state. Since spontaneous emission is not a phenomenon that greatly affects the coherence of the system, the $\langle\sigma_x\rangle$ and $\langle\sigma_y\rangle$ are not wiped out right away, but decrease slowly.

The figure 4.11 shows the dynamics of a system undergoing pure dephasing while being influenced by a weak drive with coupling strength $\Omega = 0.4\,\mathrm{ps}^{-1}$. The Bloch sphere almost instantly evolves into a tilted line, reducing $\langle\sigma_x\rangle$ and $\langle\sigma_y\rangle$ to almost zero. This is expected since pure dephasing destroys the coherence of the pure state, which is equivalent to reducing $\langle\sigma_x\rangle$ and $\langle\sigma_y\rangle$ - see (4.1). The Bloch sphere is seen to continuously evolve into a more mixed state, and at the steady state limit it will eventually reach a single point

at $\langle\sigma\rangle = (0,0,0)^T$. This means that the system with time will evolve into a fully mixed state, which is expected.

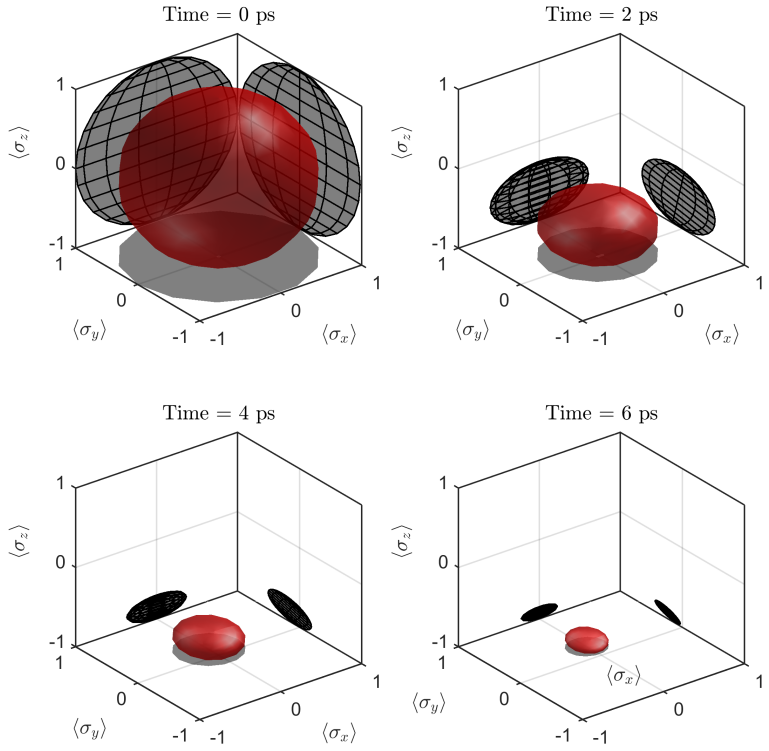

Figure 4.10: Bloch spheres for a two-level system with spontaneous emission and driving using $\Gamma = 0.1\,\mathrm{ps}^{-1}$ and $\Omega = 0.5\,\mathrm{ps}^{-1}$. Ω gives rise to the skewness of the surface.

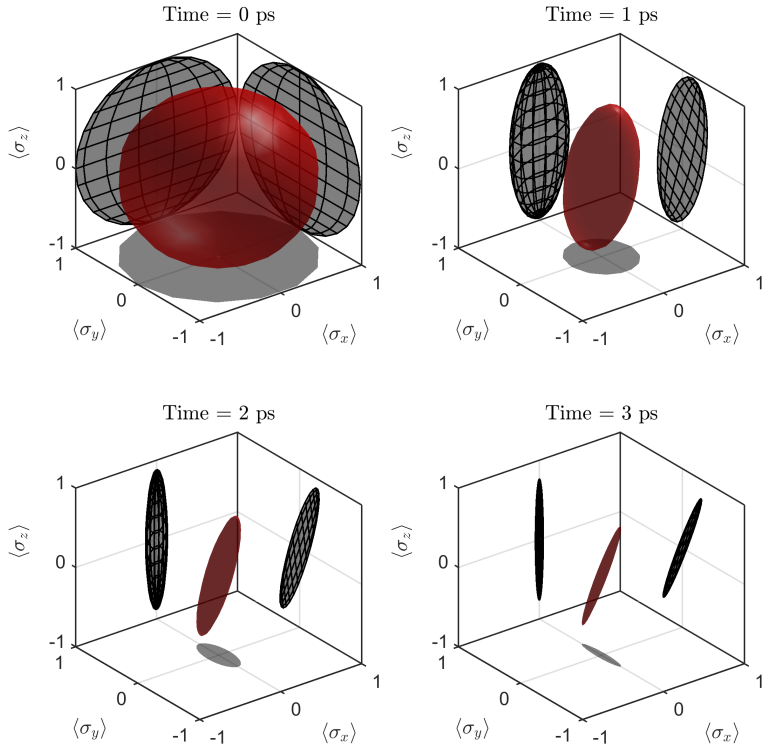

Figure 4.11: Bloch spheres for a two-level system with dephasing and driving using $\gamma = 0.5\,\mathrm{ps}^{-1}$ and $\Omega = 0.4\,\mathrm{ps}^{-1}$. Ω gives rise to the skewness of the surface.

4.2 QZE by projective measurements

In this section we will assume the von Neuman projection postulate and use it in our calculations. We assume that we are able to make any number of measurements on our system, and each measurement entails wave function collapse modelled either as a strong or weak von Neumann projection.

The strong von Neumann projections are probabilistic in nature (the state collapses onto a random basis vector). We can simulate strong von Neumann projections using random numbers, and then we could average over the different outcome sequences to obtain a distribution. A possible outcome sequence has been illustrated in figure 4.12.

Averaging over repeated strong von Neumann projections is equivalent to using weak von Neumann projections from the start. This has been done one a system with spontaneous emission and no driving – see fig. 4.16.

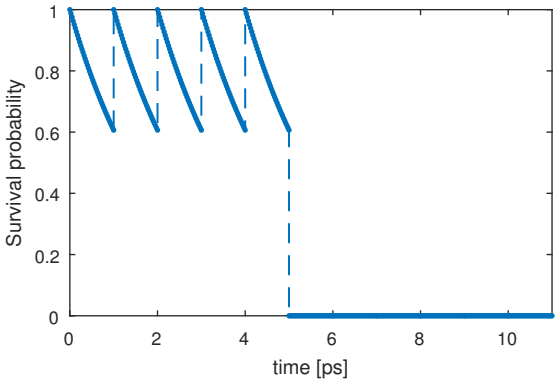

Figure 4.12: Survival probability for $|e\rangle$ during several measurements in a system with spontaneous emission rate $\Gamma = 0.5\,\mathrm{ps}^{-1}$ and no driving. The specific course of outcomes represents a single outcome sequence, which constitutes a member of the complete outcome ensemble.

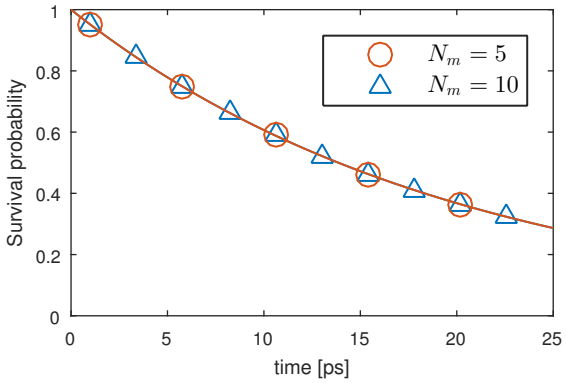

Figure 4.13: Average survival probability for $|e\rangle$ during 5 and 10 measurements, respectively, in a system with spontaneous emission rate $\Gamma = 0.5\,\mathrm{ps}^{-1}$ and no driving. The increased number of measurements has no effect in this case.

From the figure 4.13 we see that even assuming the von Neumann projection postulate the collapses have no effect. This is expected due to the constant dissipation rate Γ – as we will see in sec. 4.2.1 the survival probability is given by $P_e(t) = P_e(0)^N e^{-\Gamma t}$ for Γ being constant, which is consistent with figure 4.13.

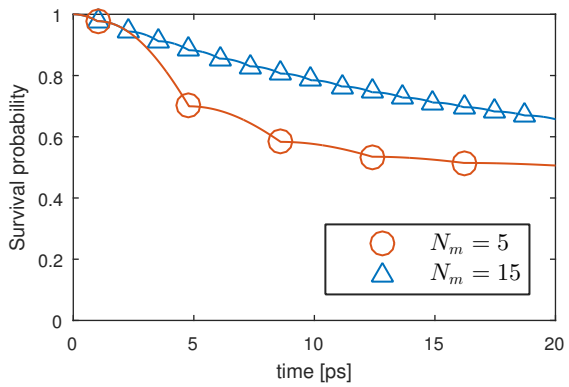

Figure 4.14: Survival probability for $|e\rangle$ during 5 and 25 measurements, respectively, in a system with driving $\Omega = 0.3\,\mathrm{ps}^{-1}$ and no dissipation. This shows the QZE by von Neumann measurements for the somewhat trivial case of a system that only has with unitary evolution.

However, if we make measurements on a system that only has unitary evolution, i.e. driving and no dissipation, we are able to obtain confined dynamics – see figure 4.14. This is consistent with the analysis in sec. 3.2.

4.2.1 QZE by projective measurements: theoretical aspect

We will now theoretically investigate a two-level QD undergoing spontaneous emission and no driving. The system Hamiltonian is given by $H_S = \frac{\Omega_x}{2} = 0$, which is equivalent to physically turning off the driving Ω in the system. The Lindblad master equation hence only consists of the dissipator term, which represents the spontaneous emission of the QD. By looking at the evolution of the survival probability of the excited state we may then study the occurrence of QZE:

$$\begin{aligned}
\frac{dP_e(t)}{dt} &= \mathrm{Tr}\left(|e\rangle\langle e|\frac{d\rho_S}{dt}\right) \\
&= \mathrm{Tr}\left(|e\rangle\langle e|\,\Gamma\left(\sigma\rho_S\sigma^\dagger - \frac{1}{2}\left\{\sigma^\dagger\sigma, \rho_S\right\}\right)\right) \\
&= \mathrm{Tr}\left(|e\rangle\langle e|\,\Gamma\left(|g\rangle\langle e|\,\rho_S\,|e\rangle\langle g| - \frac{1}{2}\left\{|e\rangle\langle e|, \rho_S\right\}\right)\right) \\
&= -\frac{1}{2}\Gamma\mathrm{Tr}\left(|e\rangle\langle e|\,\rho_S + |e\rangle\langle e|\,\rho_S\,|e\rangle\langle e|\right) \\
&= -\Gamma P_e(t).
\end{aligned} \tag{4.39}$$

The survival probability of the excited state is then given by the solution to this equation: $P_e(t) = P_e(0)e^{-\Gamma t}$. The evolution of the survival probability is therefore a exponential function of time, which ultimately means that the system never can generate a QZE; even with projective measurements. If we suppose that the unstable system is measured/observed N times at the time intervals $\tau = T/N$ and that the system is found in its initial state at every measurement, the probability of survival will be given by the product of the probabilities for each interval:

$$P_e(T) = [P(T/N)]^N = \left[P_e(0)e^{-\Gamma\frac{T}{N}}\right]^N = P_e(0)^N e^{-\Gamma T} \tag{4.40}$$

Which shows that the dependence on the measurements for this probability is not changing the fact that the system will eventually decay.

4.2.2 QZE by projective measurements with time dependent dissipation

As seen in the previous section frequent measurements had no effect on the survival probability, because the dissipation rate was taken to be constant. This is because $\partial_t P_e(t) = -\Gamma P_e(t)$, eq. (4.39). But if Γ is instead taken to be a function of time, $\Gamma(t)$, that starts from zero, the time derivative will also be zero, and then if we keep projecting it back to zero by doing frequent measurements, the derivative will on average get closer to zero.

We demonstrate this for a system with spontaneous emission and driving using a realistic model for $\Gamma(t)$, which is derived later in sec: 5.6,

$$\Gamma(t) = 2\int_0^\infty \frac{\sin\big(t(\omega_l-\omega)\big)}{\omega_l-\omega} J(\omega)\,d\omega\,, \quad J(\omega) = \eta\omega^3 e^{-\omega/\omega_c}. \tag{4.41}$$

Changing Γ to be a function of time renders the analytical solution (4.33) inapplicable, and we must resort to numerical solvers [1]. We have implemented this time dependent function for $\Gamma(t)$ – it has been plotted on figure 4.15. The associated solution to the two-level system with spontaneous emission and driving is shown on figure 4.16, where the higher number of measurements lead to a higher survival probability as expected, and thus demonstrates the confined dynamics of the QZE for $N_m \to \infty$. See app. A.2 for the code.

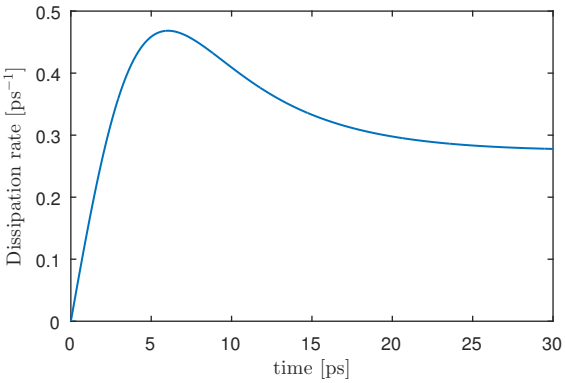

Figure 4.15: Dissipation rate, $\Gamma(t)$, computed from (4.41). We have used $\omega_l = 0.1\,\mathrm{ps}^{-1}$, $\omega_c = 0.1\,\mathrm{ps}^{-1}$, $\eta = 121\,\mathrm{ps}^2$. These values may not be realistic in QD systems, but they have been chosen for illustrative purposes, and such that $\Gamma(t)$ peaks at approximately the same value as the constant Γ value used in figure 4.13.

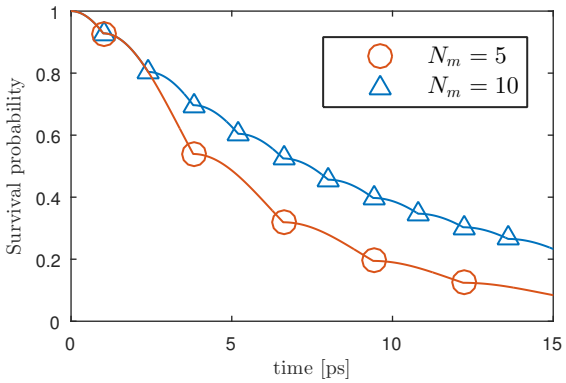

Figure 4.16: Average survival probability for $|e\rangle$ during 5 and 10 measurements, respectively, in a system with spontaneous emission and driving. The used model for $\Gamma(t)$ is described and shown in figure 4.15, and we have used $\Omega = 0.1\,\mathrm{ps}^{-1}$. The increased number of measurements induces an increased survival probability.

We now want to show that the QZE can also be obtained by von Neumann measurements in a system with dephasing and driving.

We use a realistic model for $\gamma(t)$, which is derived later in sec: 5.6,

$$\gamma(t) = 2\int_0^\infty \frac{\sin\big(t(\Omega-\omega)\big)}{\Omega-\omega} J(\omega)N(\omega)\,d\omega\,, \quad J(\omega) = \alpha\omega^3 e^{-\omega^2/\omega_c^2}, \tag{4.42}$$

where $N(\omega)$ is the Bose-Einstein occupation number given by

$$N(\omega) = \frac{1}{1+e^{\omega\hbar/k_BT}}. \tag{4.43}$$

[1] Mathematica and MATLAB has been used for this purpose with the functions `NDSolve` and `ode45`, respectively.

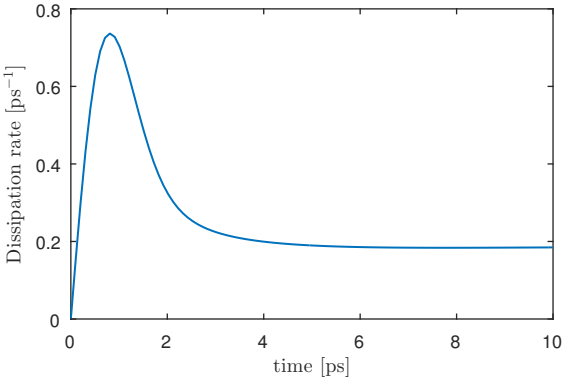

Figure 4.17: Dissipation rate, $\gamma(t)$, computed from (4.42). We have used $\Omega = 0.4\,\mathrm{ps}^{-1}$, $T = 50\,\mathrm{K}$, $\alpha = 121\,\mathrm{ps}^2$ and $\omega_c = 2.2\,\mathrm{ps}^{-1}$. These values are realistic for QD systems [26].

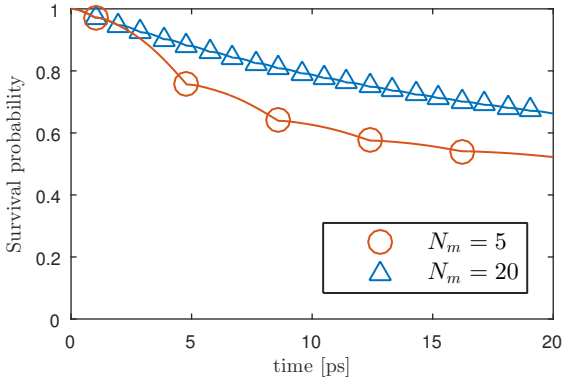

Figure 4.18: Average survival probability for $|e\rangle$ during 5 and 20 measurements, respectively, in a system with dephasing and driving. The used model for $\gamma(t)$ is described and shown in figure 4.17, and we have used $\Omega = 0.4\,\mathrm{ps}^{-1}$. Again, we see that an increased number of measurements induces an increased survival probability.

We conclude that if von Neumann measurements are performed on a system, the QZE can be obtained as long as the dissipation is time dependent as long.

Effect of spontaneous emission rate

A rather obvious parameter that we may also adjust in order to increase the survival probability in a system with spontaneous emission and driving, is the spontaneous emission rate itself.

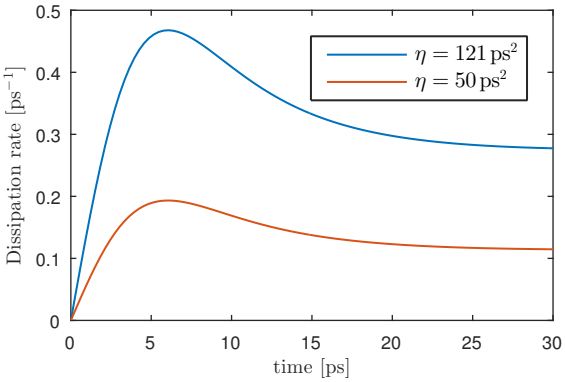

Figure 4.19: Dissipation rate, $\Gamma(t)$, computed from (4.41). We have used $\omega_l = 0.1\,\mathrm{ps}^{-1}$, $\omega_c = 0.1\,\mathrm{ps}^{-1}$, and $\eta = 121\,\mathrm{ps}^2$ or $\eta = 50\,\mathrm{ps}^2$. Since η scales $\Gamma(t)$, so it is useful for showing differences between a strong and weak dissipation.

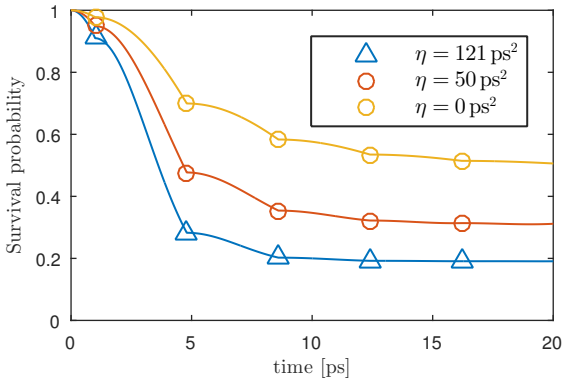

Figure 4.20: Survival probability of $|e\rangle$ in a system with dissipation, where the rate is scaled by η, and driving; $\Omega = 0.3\,\mathrm{ps}^{-1}$. Lowering the dissipation rate increases the survival probability, but only to a certain extent, which is outlined by the $\eta = 0$ curve.

On figure 4.19 we see the spontaneous emission rate for two different values of the parameter η, which scales $\Gamma(t)$ linearly through the relationship in (4.41). The value $\eta = 121\,\mathrm{ps}^2$ is the one that was used previously in figure 4.20. Based on the time-dependent rates shown on figure 4.19, we have plotted the survival probability of $|e\rangle$ during 5 measurements in a system with spontaneous emission and driving, see figure 4.20. On this figure we have also plotted the survival probability for $\eta = 0$ for reference – this corresponds to unitary evolution, no dissipation, and should simply generate a Rabi oscillation as on

figure 4.2; however the projective measurements interrupts the oscillations, which reduces the amplitude, and thus projective measurements act similarly to dissipation.

From figure 4.20 we see that a higher survival probability can be obtained by lowering the dissipation rate, which is not that surprising, but the survival probability can never go beyond the $\eta = 0$ line, because the survival probability is also affected by the driving. The only way to obtain QZE in this system is therefore to increase the number of measurements.

4.3 QZE by strong dephasing

In this section we show that the Zeno effect occurs when the dephasing rate γ is high. We assume that the system initially starts off in the state $|e\rangle$. Applying dephasing and driving the system is expected to approach a maximally mixed state with population number of 0.5 for both $|e\rangle$ and $|g\rangle$. This behaviour cannot be avoided, but it can be stalled.

From (4.37) we see that

$$\langle\sigma_z\rangle = \alpha_3(t) = \frac{e^{-t\left(\sqrt{\gamma^2-\Omega^2}+\gamma\right)}\left(\sqrt{\gamma^2-\Omega^2}\left(e^{2t\sqrt{\gamma^2-\Omega^2}}+1\right)+\gamma\left(e^{2t\sqrt{\gamma^2-\Omega^2}}-1\right)\right)}{2\sqrt{\gamma^2-\Omega^2}}. \tag{4.44}$$

For strong dephasing, or weak driving, i.e. $\gamma \gg \Omega$, we can use the approximation $1 + \Omega^2/\gamma^2 \to 1$. Inserting this into (4.44) evaluates to

$$\langle\sigma_z\rangle\,|_{(1+\Omega^2/\gamma^2\to 1)} = 1 \Leftrightarrow \langle|e\rangle\langle e|\rangle = 1. \tag{4.45}$$

Using the parameter $\epsilon = \sqrt{1-\Omega^2/\gamma^2}$, and absorbing γ into the time variable t in (4.44), $T = t\gamma$, we have plotted the expression (4.44) in fig. 4.21. The figure shows that the population number of $|e\rangle$ on a fixed time interval approaches 1 as expected.

For any non-zero value of Ω^2/γ^2 the behavior $\langle\sigma_z\rangle \to 0$ is still intact for high enough times, but in the limit $1 + \Omega^2/\gamma^2 \to 1$ we have $\langle\sigma_z\rangle = 1$ regardless of t.

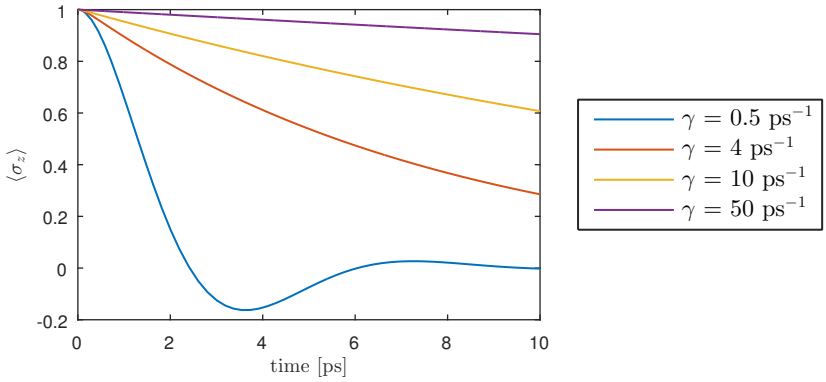

Figure 4.21: Time evolution of $\langle\sigma_z\rangle$ in a system with pure dephasing and driving, where $\Omega = 1\text{ps}^{-1}$. For any finite value of γ, we still have $\langle\sigma_z\rangle \to 1$ for $t \to \infty$, but as indicated on the plot, $\langle\sigma_z\rangle$ approaches 1 on a fixed time interval, and then so does the population number of $|e\rangle$, as $1 + \Omega^2/\gamma^2$ approaches 1. From the figure we see that stronger dephasing – or equivalently; weaker driving – leads to the Zeno effect.

4.4 Three-level system

4.5 Qutrit system

We shall now consider the more advanced case of a three-level system. New features arise when an additional level is coupled with previously the considered two-level system. We find that this will allow for new manifestations of the QZE. The added level is called the pump level, $|p\rangle$, such that we now have $|p\rangle$, $|e\rangle$ and $|g\rangle$ described by the basis vectors $(1,0,0)$, $(0,1,0)$ and $(0,0,1)$, respectively.

The systems that are considered in this chapter are shown in figure 4.22.

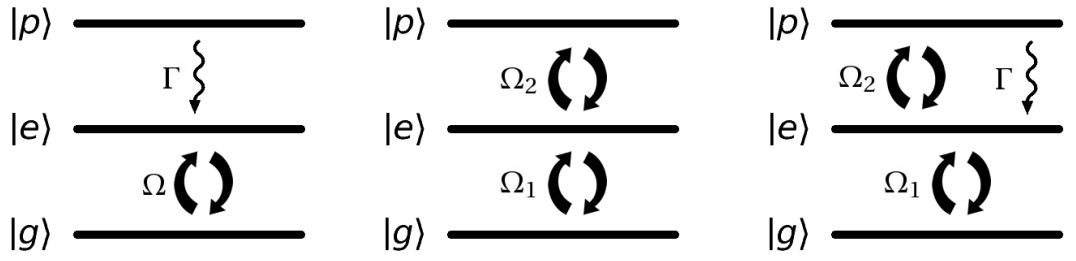

(a) Dissipation and driving. **(b)** Only driving. **(c)** Dissipation and double driving.

Figure 4.22: Diagrams of the three-level systems we will consider in this thesis. Note that the downward arrow labeled Γ represents both spontaneous emission and dephasing, even though the semantic behind the downward error is most appropriate for emission.

4.5.1 Description of a three-level system

Using the Lindblad formalism as for the two-level system, we can construct a master equation

$$\frac{d\rho}{dt} = -i\left[\hat{H_{S'}}, \rho\right] + \Gamma L\left(M\right)\rho, \tag{4.46}$$

where M is an operator that specifies either spontaneous emission or pure dephasing between two states.

Again we must solve the master equation based on the expectation values of a complete set of matrices in a three-level system. Such a complete set is given by the Gell-Mann matrices,

$$\lambda_1 = \begin{pmatrix} 0 & 1 & 0 \\ 1 & 0 & 0 \\ 0 & 0 & 0 \end{pmatrix},\ \lambda_2 = \begin{pmatrix} 0 & -i & 0 \\ i & 0 & 0 \\ 0 & 0 & 0 \end{pmatrix},\ \lambda_3 = \begin{pmatrix} 1 & 0 & 0 \\ 0 & -1 & 0 \\ 0 & 0 & 0 \end{pmatrix} \tag{4.47}$$

$$\lambda_4 = \begin{pmatrix} 0 & 0 & 1 \\ 0 & 0 & 0 \\ 1 & 0 & 0 \end{pmatrix},\ \lambda_5 = \begin{pmatrix} 0 & 0 & -i \\ 0 & 0 & 0 \\ i & 0 & 0 \end{pmatrix},\ \lambda_6 = \begin{pmatrix} 0 & 0 & 0 \\ 0 & 0 & 1 \\ 0 & 1 & 0 \end{pmatrix} \tag{4.48}$$

$$\lambda_7 = \begin{pmatrix} 0 & 0 & 0 \\ 0 & 0 & -i \\ 0 & i & 0 \end{pmatrix},\ \lambda_8 = \frac{1}{\sqrt{3}}\begin{pmatrix} 1 & 0 & 0 \\ 0 & 1 & 0 \\ 0 & 0 & -2 \end{pmatrix}. \tag{4.49}$$

From these linearly independent matrices we define the density operator as [27]

$$p(t) = \frac{1}{3}\left(I + \sqrt{3}\sum_{i=1}^{8}\lambda_i\alpha_i(t)\right). \tag{4.50}$$

Unlike the Pauli matrices, the Gell-Mann matrices do not lead to the simple relationship $\langle\lambda_i\rangle = \alpha_i(t)$, but instead

$$\begin{aligned}\langle\lambda_i\rangle = \mathrm{Tr}(\lambda_i p(t)) &= \mathrm{Tr}\left[\lambda_i \frac{1}{3}\left(I + \sqrt{3}\sum_{n=1}^{8}\lambda_n\alpha_n(t)\right)\right] \\ &= \mathrm{Tr}\left(\lambda_i\frac{1}{3}I\right) + \mathrm{Tr}\left(\frac{1}{3}\sqrt{3}\sum_{n=1}^{\infty}\lambda_i\lambda_n\alpha_n(t)\right) \\ &= 0 + \frac{1}{\sqrt{3}}\sum_{n=1}^{\infty}\mathrm{Tr}\left(\lambda_i\lambda_n\alpha_n(t)\right) = \frac{2}{\sqrt{3}}\alpha_i(t). \end{aligned} \tag{4.51}$$

Here we have used the traceless property of the Gell-Mann matrices along with the relation $\mathrm{Tr}(\lambda_i\lambda_j) = 2\delta_{i,j}$. The vector of the α values is the three-level Bloch vector, which is analogous to the two-level Bloch vector. It follows from (4.51) that

$$\langle\lambda_i\rangle' = \mathrm{Tr}\left(\lambda_i\partial_t p(t)\right) = \frac{2}{\sqrt{3}}\alpha_i'(t). \tag{4.52}$$

This relation can be used to construct a system of 8 coupled equations of motion, which can in principle be solved analytically by using (4.22), but in practice we use the numerical solvers mentioned earlier.

Population number

The population number in a given level $|\psi\rangle$ is given by $\mathrm{Tr}(|\psi\rangle\langle\psi| p)$. From the definition of the density operator (4.50) we find that

$$p(t) = \begin{bmatrix} \frac{1}{3}\left(\sqrt{3}\left(\alpha_3(t) + \frac{\alpha_8(t)}{\sqrt{3}}\right) + 1\right) & \frac{\alpha_1(t) - i\alpha_2(t)}{\sqrt{3}} & \frac{\alpha_4(t) - i\alpha_5(t)}{\sqrt{3}} \\ \frac{\alpha_1(t) + i\alpha_2(t)}{\sqrt{3}} & \frac{1}{3}\left(\sqrt{3}\left(\frac{\alpha_8(t)}{\sqrt{3}} - \alpha_3(t)\right) + 1\right) & \frac{\alpha_6(t) - i\alpha_7(t)}{\sqrt{3}} \\ \frac{\alpha_4(t) + i\alpha_5(t)}{\sqrt{3}} & \frac{\alpha_6(t) + i\alpha_7(t)}{\sqrt{3}} & \frac{1}{3}\left(1 - 2\alpha_8(t)\right) \end{bmatrix}, \tag{4.53}$$

and thus for the population number in the excited state $|e\rangle$ we have

$$\mathrm{Tr}(|e\rangle\langle e| p) = \frac{1}{3}\left(\alpha_8(t) - \sqrt{3}\alpha_3(t) + 1\right). \tag{4.54}$$

4.5.2 QZE in three-level systems

Of the systems shown in figure 4.22 we will at present consider 4.22b and 4.22c. The system 4.22a will be considered thoroughly later in the thesis.

For both the considered three-level systems we use a system Hamiltonian, analogous to that of the two-level system, given by

$$\hat{H}_{S'} = \frac{\Omega_{eg}}{2}\big(\,|e\rangle\langle g| + |g\rangle\langle e|\,\big) + \frac{\Omega_{pe}}{2}\big(\,|p\rangle\langle e| + |e\rangle\langle p|\,\big). \tag{4.55}$$

Firstly, we try to set $\Omega_{pe} = \Omega_{eg}$, which leads to completely balanced population numbers as seen in figure 4.23. By making the driving in the pe-subsystem strong relative to Ω_{eg}, we suppress the population number of $|g\rangle$ – this is shown on figure 4.24.

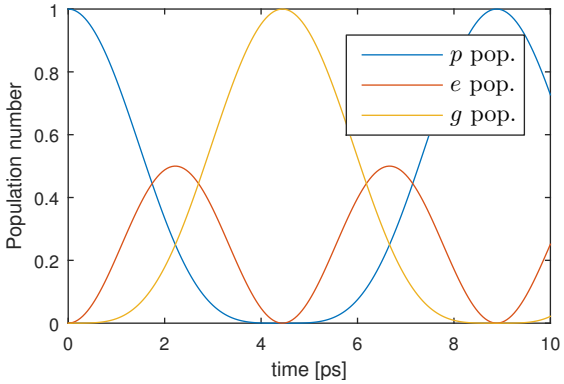

Figure 4.23: Population number for three-level system with continuous coupling where $\Omega_{pe} = 1\,\mathrm{ps}^{-1}, \Omega_{eg} = 1\,\mathrm{ps}^{-1}$ and $\Gamma = 0$. The amplitude of the $P(e)$ oscillation is only half that of the $P(p)$ and $P(g)$ oscillations due to $|e\rangle$ being coupled both to $|p\rangle$ and $|g\rangle$.

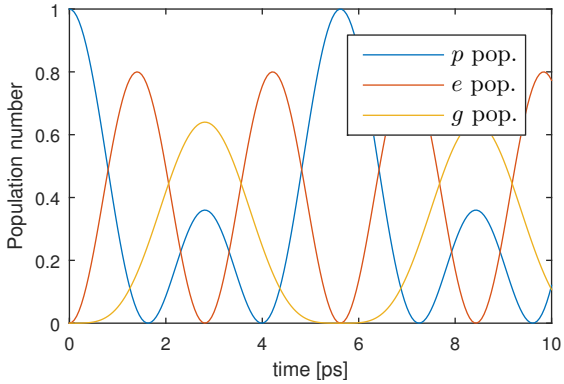

Figure 4.24: Population number for three-level system with continuous coupling where $\Omega_{eg} = 1\,\mathrm{ps}^{-1}, \Omega_{pe} = 2\,\mathrm{ps}^{-1}$ and $\Gamma = 0$. The stronger driving between the p and e level results in a smaller amplitude of $P(g)$, whereas the $P(e)$ amplitude increases.

Now, if we do the opposite by making the driving strong in the eg-subsystem relative to Ω_{pe}, we get the converse effect; the population number of $|p\rangle$ becomes "isolated" in a sense – see figure 4.25 and figure 4.26, where it is even more clear. This is a well-known feature of continuous coupling in a three-level system [21] and is often referred to as a manifestation of the QZE. This is also explained in sec. 5.3 by electromagnetically induced transparency.

It can argued that this manifestation of the QZE is not that relevant, because the confined dynamics is obtained in a system that has no dissipation at all. If we introduce just the slightest dissipation in the system, the scheme will not work. This has been shown on figure 4.27, where we show the population number of $|p\rangle$ for different dissipation rates. Even for a small dissipation rate the QZE fails to be obtained, and this is regardless of how large Ω_{eg} is. This is due to the dissipation being completely independent on the driving, which is not the case if the system is modelled more realistically – we shall see this later. For now though, the only counteraction to dissipation in this system is by performing von Neumann measurements; this has been shown on figure 4.28.

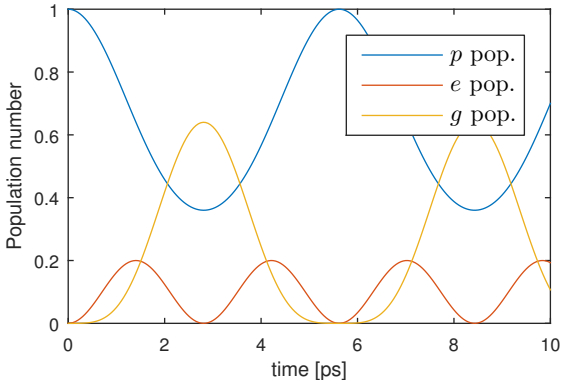

Figure 4.25: Population number for three-level system with continuous coupling where $\Omega_{pe} = 1\,\mathrm{ps}^{-1}, \Omega_{eg} = 1.5\,\mathrm{ps}^{-1}$ and $\Gamma = \gamma = 0$. Compared to fig. 4.23 we see that due to $\Omega_{eg} > \Omega_{pe}$ the population number of p starts to increase.

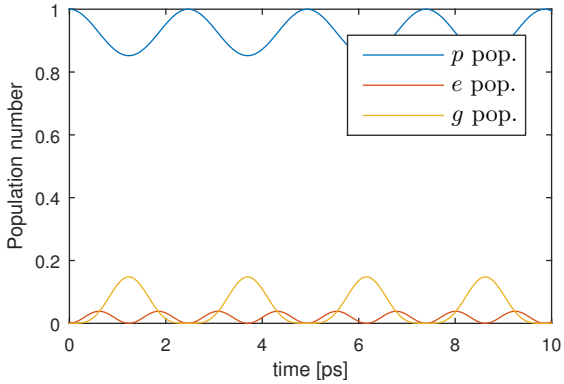

Figure 4.26: Population number for three-level system with continuous coupling where $\Omega_{pe} = 1\,\mathrm{ps}^{-1}, \Omega_{eg} = 5\,\mathrm{ps}^{-1}$ and $\Gamma = \gamma = 0$. Now that Ω_{eg} is significantly larger than Ω_{pe} it becomes clear that the QZE is achieved for $\Omega_{eg} \to \infty$ while Ω_{pe} is finite.

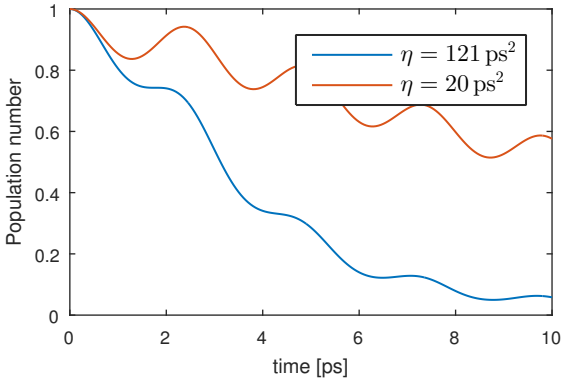

Figure 4.27: Population number of $|p\rangle$ in a three-level system with continuous coupling and dissipation; $\Omega_{pe} = 1\,\mathrm{ps}^{-1}, \Omega_{eg} = 5\,\mathrm{ps}^{-1}$ and dissipation rate given by $\Gamma(t)$ from eq. (4.41) where η is specified on the plot. The non-zero values of Γ causes dissipation, and even for weak dissipation, $\eta = 20\,\mathrm{ps}^2$, the QZE cannot be obtained regardless of how large Ω_{eg} is. If we introduce measurements however, it is still possible, see fig. 4.28.

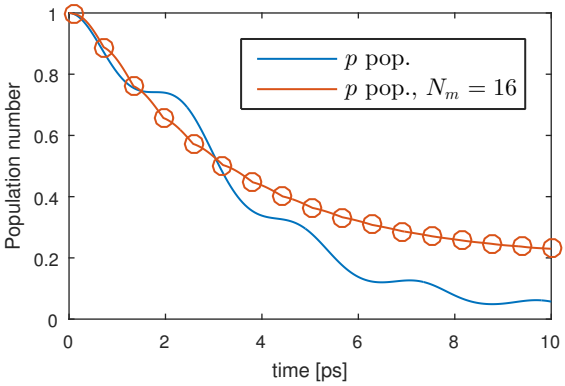

Figure 4.28: Population number of $|p\rangle$ in a three-level system with continuous coupling and dissipation; $\Omega_{pe} = 1\,\mathrm{ps}^{-1}, \Omega_{eg} = 5\,\mathrm{ps}^{-1}$ and $\Gamma = \Gamma(t)$ with $\eta = 121\,\mathrm{ps}^2$, eq. (4.41), with and without measurements being performed. The red curve is based on 16 measurements, while the blue curve is based on no measurements being performed. The higher population number of the red curve indicates that the QZE can be obtained in this system.

Itano's experiment

The experiment done by Itano et al. [1] can be simplified to the three-level system shown in figure 4.22c. In Itano's experiment however, the state is prepared in its ground state, whereas we have almost only (the exception being the Bloch sphere) considered systems prepared in the excited state. The difference between Itano's actual experiment and the system 4.22c is that Itano used laser pulses that rapidly swept the upper subsystem instead of having 'continuous coupling', but by assuming that the laser pulses are frequent enough, the pulses can be described by 'continuous coupling' [28].

We have implemented the simplified version of Itano's experiment. The result can be seen in figure 4.29, where it is clear that the population numbers indicate confined dynamics. This is because of the strong driving in the pe-subsystem, which makes the driving in the eg-subsystem off-resonant – similarly to what was seen on figure 4.26. However, when increasing the dissipation in the pe-subsystem, the population number of $|g\rangle$ decays significantly, see figure 4.30. To counteract this we could increase Ω_{pe} even further, so clearly the confined dynamics depend on the balance between Ω_{pe} and Γ.

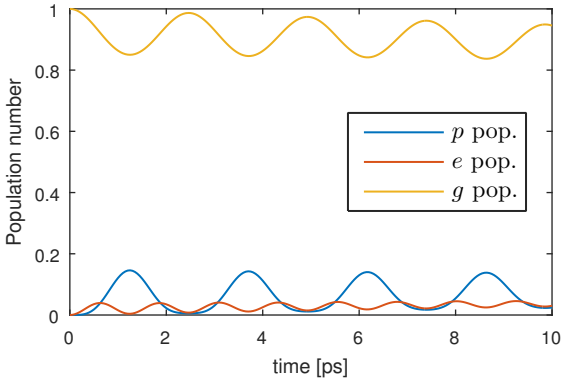

Figure 4.29: Population numbers for three-level system with continuous coupling where $\Omega_{pe} = 5, \Omega_{eg} = 1$ and $\Gamma = 0.1\,\mathrm{ps}^{-1}$. Initial state is $|g\rangle$ and not $|e\rangle$ as usual.

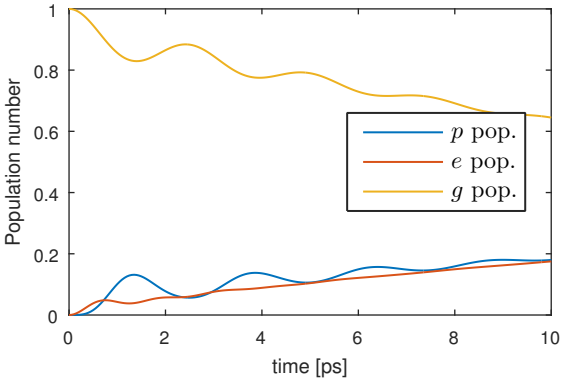

Figure 4.30: Population numbers for three-level system with continuous coupling where $\Omega_{pe} = 5\,\mathrm{ps}^{-1}, \Omega_{eg} = 1\,\mathrm{ps}^{-1}$ and $\Gamma = 1\,\mathrm{ps}^{-1}$. Initial state is $|g\rangle$ and not $|e\rangle$ as usual. The increased value for Γ has a significant effect when compared to figure 4.29.

Chapter 5

Master equation from first principles

The aim of this chapter is to derive a more detailed form of the Born-Markov master equations used throughout the analysis of the QZE in the previous chapter. By virtue of these derivations and with the use of a couple of approximations, we will hereafter justify the general Lindblad form of the master equations. As previously stated, master equations govern the evolution of open systems under the influence of weak environmental interactions. The dynamics generally is not unitary and greatly depends on the system and environmental interaction under consideration. We are therefore going to examine a realistic and practical model, based on a QD.

In our model we are both considering a two-level and a three-level QD interacting with an environment comprising of a denumerably infinite set of independent harmonic oscillators. This model is practical since the environment is a truncated version of a bath of bosons, which, if treated as photons, is dynamically equivalent to a (quantized) electromagnetic field. It can therefore be used to study a wide range of open systems in quantum optics and is also considered being one of the most fundamental models within this field. If the bosons instead are treated as phonons, the same model can be used to for example represent the coupling to lattice vibrations of crystalline solids. We will consider both of these cases, and based on these derive the master equations for a QD undergoing respectively spontaneous emission and pure dephasing.

In section (2.5.1), a general expression for the Born-Markov master equation (2.23) was derived and shown to be restricted to the Born and Markov approximations (2.5.1.1). In the next sections we will make use of this expression and hence also implicitly its approximations. We follow the outline of [29].

5.1 Spontaneous emission with driving

The first case we want to consider, is a two-level QD undergoing spontaneous emission while being driven by a electromagnetic field (a laser). Its corresponding Hamiltonian is given by:

$$\begin{aligned} H &= H_S + H_E + H_I \\ &= \frac{\epsilon}{2}\sigma_z + \Omega\cos(\omega_l t)\,\sigma_x + \sum_k \omega_{\mathbf{k}} b_{\mathbf{k}}^\dagger b_{\mathbf{k}} + \sum_{\mathbf{k}} g_{\mathbf{k}}\left(\sigma^\dagger b_{\mathbf{k}} + \sigma b_{\mathbf{k}}^\dagger\right) \end{aligned} \tag{5.1}$$

The system Hamiltonian – first two terms – represents the two-level QD driven by the laser with frequency ω_l and coupling strength Ω, where the ground state $|g\rangle$ and excited state $|e\rangle$ are split by the energy ϵ. The zero point energy of the system is placed in the middle of the energy gap, and therefore we may represent the system as $\frac{\epsilon}{2}\sigma_z = \frac{\epsilon}{2}\left(|e\rangle\langle e| - |g\rangle\langle g|\right)$. The bath of harmonic oscillators – third term – of frequencies $\omega_{\mathbf{k}}$ is described respectively by the annihilation $b_{\mathbf{k}}^\dagger$ and creation $b_{\mathbf{k}}$ operator and have wavevectors $\mathbf{k}$. The interaction Hamiltonian – fourth term– couples the two-level system with the harmonic oscillators by the coupling constants $g_{\mathbf{k}}$, where $\sigma^\dagger = |e\rangle\langle g|$ and $\sigma = |g\rangle\langle e|$. It is worth noting that the coupling strength Ω is proportional to the amplitude (not the optical intensity) of the light field and to the dipole moment of the level transition.

In order to simplify our calculation, we want to put the Hamiltonian into a frame rotating at the laser frequency ω_l, defined by the transformation $H \to H' = U_R(t)HU_R^\dagger(t) + i\left(\partial_t U_R(t)\right)U_R^\dagger(t)$ with the unitary operator $U_R(t) = e^{i\frac{\omega_l}{2}\sigma_z t}$. The corresponding transformed Hamiltonian is:

$$H' = \frac{\Delta}{2}\sigma_z + \frac{\Omega}{2}\left(\left(1+e^{2i\omega_l t}\right)\sigma^\dagger + \left(1+e^{-2i\omega_l t}\right)\sigma\right) + H_E + \sum_{\mathbf{k}} g_{\mathbf{k}}\left(\sigma^\dagger e^{i\omega_l t}b_{\mathbf{k}} + \sigma e^{-i\omega_l t}b_{\mathbf{k}}^\dagger\right) \tag{5.2}$$

Where H_E is unaffected and $\Delta = \epsilon - \omega_l$ is the detuning of the laser from the atomic transition frequency. In calculating this transformed Hamiltonian we have taken advantage of the transformation of the unitary operator into the form: $U_R(t) = e^{i\frac{\omega_l}{2}\sigma_z t} = e^{i\frac{\omega_l}{2}t}|e\rangle\langle e| + e^{-i\frac{\omega_l}{2}t}|g\rangle\langle g|$.

The exponential terms in Eq. (5.2) can be neglected, since they represent fast oscillating factors that average to unity. The transformed Hamiltonian then simplifies to:

$$H' = \frac{\Delta}{2}\sigma_z + \frac{\Omega}{2}\sigma_x + \sum_{\mathbf{k}}\omega_{\mathbf{k}}b_{\mathbf{k}}^\dagger b_{\mathbf{k}} + \sum_{\mathbf{k}} g_{\mathbf{k}}\left(\sigma^\dagger e^{i\omega_l t}b_{\mathbf{k}} + \sigma e^{-i\omega_l t}b_{\mathbf{k}}^\dagger\right) \tag{5.3}$$

In order to make use of the general expression of the Born-Markov master equation (2.23), we need to move the rotated interaction Hamiltonian into the interaction picture, with respect to the rotation free system and environment Hamiltonians: $\tilde{H_I'} = e^{i(H_S+H_E)t}H_I' e^{-i(H_S+H_E)t}$. We first write it as:

$$\tilde{H_I'}(t) = \sum_{\mathbf{k}} g_{\mathbf{k}}\left(\tilde{\sigma}^\dagger(t)e^{i\omega_l t}b_{\mathbf{k}}e^{-i\omega_{\mathbf{k}}t} + \tilde{\sigma}(t)e^{-i\omega_l t}b_{\mathbf{k}}^\dagger e^{i\omega_{\mathbf{k}}t}\right) \tag{5.4}$$

where $\tilde{\sigma}(t) = U_{S'}^\dagger(t)\sigma U_{S'}(t) = e^{iH_{S'}t}\sigma e^{-iH_{S'}t}$. Comparing this with (2.19) we see that: $A_1(t) = \tilde{\sigma}^\dagger(t)e^{i\omega_l t}$, $A_2(t) = \tilde{\sigma}(t)e^{-i\omega_l t}$, $B_1(t) = \sum_{\mathbf{k}} g_{\mathbf{k}}b_{\mathbf{k}}e^{-i\omega_{\mathbf{k}}t}$ and $B_2(t) = \sum_{\mathbf{k}} g_{\mathbf{k}}b_{\mathbf{k}}^\dagger e^{i\omega_{\mathbf{k}}t}$. In order to proceed, we need to derive $\tilde{\sigma}$ and $\tilde{\sigma}^\dagger$. This can be done by diagonalizing the rotated system Hamiltonian and writing it in its eigenstate basis:

$$H_{S'} = \frac{1}{2}\begin{pmatrix}\Delta & \Omega\\ \Omega & -\Delta\end{pmatrix} = \frac{1}{2}V\begin{pmatrix}\Lambda & 0\\ 0 & -\Lambda\end{pmatrix}V^{-1} = \Lambda\frac{1}{2}\left(|+\Lambda\rangle\langle+\Lambda| - |-\Lambda\rangle\langle-\Lambda|\right) \tag{5.5}$$

Where $\pm\frac{1}{2}\Lambda = \pm\frac{1}{2}\sqrt{\Delta^2+\Omega^2}$ are the eigenvalues of $H_{S'}$, the invertible matrix V is composed of the normalized eigenvectors $|+\Lambda\rangle = V|e\rangle$ and $|-\Lambda\rangle = V|g\rangle$ of $H_{S'}$. We can use this representation to write $U_{S'}(t) = e^{-iH_{S'}t} = |+\Lambda\rangle\langle+\Lambda| e^{-i\frac{1}{2}\Lambda t} + |-\Lambda\rangle\langle-\Lambda| e^{i\frac{1}{2}\Lambda t}$, from which we see that the operators $A_1(t)$ and $A_2(t)$ become:

$$A_1(t) = \tilde{\sigma}^\dagger(t)e^{i\omega_l t} = \sum_i X_i e^{i\omega_i t} \tag{5.6}$$

$$A_2(t) = \tilde{\sigma}(t)e^{-i\omega_l t} = \sum_i Y_i e^{-i\omega_i t} \tag{5.7}$$

where the sums run over i = 1,2,3 with $\omega_1 = \omega_l$, $\omega_2 = \omega_l + \Lambda$, and $\omega_3 = \omega_l - \Lambda$. Which means that the operators $A_1(t)$ and $A_2(t)$ have three Fourier components each, with frequencies ω_l and $\omega_l \pm \Lambda$. The operators X_i are respectively $X_1 = \big(|+\Lambda\rangle\langle+\Lambda|\sigma^\dagger|+\Lambda\rangle\langle+\Lambda| + |-\Lambda\rangle\langle-\Lambda|\sigma^\dagger|-\Lambda\rangle\langle-\Lambda|\big)$, $X_2 = |+\Lambda\rangle\langle+\Lambda|\sigma^\dagger|-\Lambda\rangle\langle-\Lambda|$ and $X_3 = |-\Lambda\rangle\langle-\Lambda|\sigma^\dagger|+\Lambda\rangle\langle+\Lambda|$, and the complex conjugate of these gives the operators of Y_i. Its also worth noting that $\sum_i X_i = \sigma^\dagger$ and $\sum_i Y_i = \sigma$.

In order to solve the Born-Markov master equation (2.23) we need to derive the correlation functions $C_{\alpha\beta}(\tau)$. This can only be done if we know the density operator of the environment ρ_E. We will consider a general case where the environment is assumed to be in thermal equilibrium, then the density operator becomes:

$$\rho_E = \frac{e^{-H_E/k_BT}}{\mathrm{Tr}\left(e^{-H_E/k_BT}\right)} \tag{5.8}$$

where k_B is the Boltzmann constant, and T is the environmental temperature. For this density operator the correlation functions become:

$$\begin{aligned} C_{11}(\tau) &= \langle B_1(\tau)B_1(0)\rangle \qquad (5.9)\\ &= \sum_{\mathbf{kk'}} g_{\mathbf{k}}g_{\mathbf{k'}}, e^{-i\omega_{\mathbf{k}}\tau}\langle b_{\mathbf{k}}b_{\mathbf{k'}},\rangle \\ &= 0 \end{aligned}$$

$$\begin{aligned} C_{12}(\tau) &= \langle B_1(\tau)B_2(0)\rangle \qquad (5.10)\\ &= \sum_{\mathbf{kk'}} g_{\mathbf{k}}g^*_{\mathbf{k'}}, e^{-i\omega_{\mathbf{k}}\tau}\left\langle b_{\mathbf{k}}b^\dagger_{\mathbf{k'}},\right\rangle_E \\ &= \sum_{\mathbf{k}} |g_{\mathbf{k}}|^2 e^{-i\omega_{\mathbf{k}}\tau}(1+N(\omega_{\mathbf{k}})) \end{aligned}$$

$$\begin{aligned} C_{22}(\tau) &= \langle B_2(\tau)B_2(0)\rangle \qquad (5.11)\\ &= \sum_{\mathbf{kk'}} g^*_{\mathbf{k}}g^*_{\mathbf{k'}}, e^{i\omega_{\mathbf{k}}\tau}\left\langle b^\dagger_{\mathbf{k}}b^\dagger_{\mathbf{k'}},\right\rangle_E \\ &= 0 \end{aligned}$$

$$\begin{aligned} C_{21}(\tau) &= \langle B_2(\tau)B_1(0)\rangle \qquad (5.12)\\ &= \sum_{\mathbf{kk'}} g^*_{\mathbf{k}}g_{\mathbf{k'}}, e^{i\omega_{\mathbf{k}}\tau}\left\langle b^\dagger_{\mathbf{k}}b_{\mathbf{k'}},\right\rangle_E \\ &= \sum_{\mathbf{k}} |g_{\mathbf{k}}|^2 e^{i\omega_{\mathbf{k}}\tau}N(\omega_{\mathbf{k}}) \end{aligned}$$

where $N(\omega_{\mathbf{k}}) = \left(e^{\omega_{\mathbf{k}}/k_BT}-1\right)^{-1}$ is the Bose-Einstein occupation number. Here we have used the following: $\langle b_{\mathbf{k}}b_{\mathbf{k'}},\rangle = \left\langle b^\dagger_{\mathbf{k}}b^\dagger_{\mathbf{k'}},\right\rangle = 0$, $\left\langle b^\dagger_{\mathbf{k}}b_{\mathbf{k'}},\right\rangle = \delta_{\mathbf{kk'}}N(\omega_{\mathbf{k}})$ and $\left\langle b_{\mathbf{k}}b^\dagger_{\mathbf{k'}},\right\rangle = \delta_{\mathbf{kk'}}(1+N(\omega_{\mathbf{k}}))$. In substituting these correlation functions into the master equation (2.23) we first need to convert them into an integral instead of a sum. Both $C_{11}(\tau)$ and $C_{22}(\tau)$ of course stay the same, but the other two become:

$$C_{12}(\tau) = \int_0^\infty J(\omega) e^{-i\omega\tau}(1 + N(\omega))d\omega \tag{5.13}$$

$$C_{21}(\tau) = \int_0^\infty J(\omega) e^{i\omega\tau}(N(\omega))d\omega \tag{5.14}$$

where the spectral density $J(\omega)$ is defined as:

$$J(\omega) = \sum_{\mathbf{k}} |g_{\mathbf{k}}|^2 \delta(\omega - \omega_{\mathbf{k}}) = D(\omega)|g(\omega)|^2 \tag{5.15}$$

This spectral density function measures the coupling strength between the system and environment. Substituting everything into the Schrödinger picture Born-Markov master equation (2.23) we find:

$$\begin{aligned}
\frac{d\rho}{dt} =& - i\left[H_S, \rho_S(t)\right] - \int_0^\infty \left(\left[A_1, A_2(-\tau)\rho_S(t)\right] C_{12}(\tau) + \left[\rho_S(t)A_2(-\tau), A_1\right] C_{21}(-\tau)\right) \\
&\qquad + \left(\left[A_2, A_1(-\tau)\rho_S(t)\right] C_{21}(\tau) + \left[\rho_S(t)A_1(-\tau), A_2\right] C_{12}(-\tau)\right) d\tau \\
=& - i\left[H_S, \rho_S(t)\right] - \int_0^\infty \left(\left[A_1, A_2(-\tau)\rho_S(t)\right] C_{12}(\tau) + \left[A_2, A_1(-\tau)\rho_S(t)\right] C_{21}(\tau) + h.c.\right) d\tau \\
=& - i\left[H_{S'}, \rho_S(t)\right] - \sum_i^3 \int_0^\infty \left(\left[\sigma^\dagger, Y_i\rho_S(t)\right] e^{i\omega_i\tau} C_{12}(\tau) + \left[\sigma, X_i\rho_S(t)\right] e^{-i\omega_i\tau} C_{21}(\tau) + h.c.\right) d\tau
\end{aligned} \tag{5.16}$$

The six integrals in the master equation (5.16), representing environment response functions, become:

$$\begin{aligned}
K_{12}(-\omega_i) =& \int_0^\infty e^{i\omega_i\tau} C_{12}(\tau) d\tau = \int_0^\infty \int_0^\infty \left(e^{i(\omega_i - \omega)\tau} J(\omega)(1 + N(\omega))\right) d\tau d\omega \\
=& \frac{1}{2}\Gamma_{12}(-\omega_i) + iS_{12}(-\omega_i)
\end{aligned} \tag{5.17}$$

and

$$\begin{aligned}
K_{21}(\omega_i) =& \int_0^\infty e^{-i\omega_i\tau} C_{21}(\tau) d\tau = \qquad \int_0^\infty \int_0^\infty \left(e^{-i(\omega_i - \omega)\tau} J(\omega) N(\omega)\right) d\tau d\omega \\
=& \frac{1}{2}\Gamma_{21}(\omega_i) + iS_{21}(\omega_i)
\end{aligned} \tag{5.18}$$

It will be shown that the imaginary parts of the solutions will give rise to environment-induced energy shifts for the system, while the real parts will cause dissipation of the system. It is worth noting that both depend on the attained Fourier frequencies ω_i, which respectively depend on ω_l and $\Lambda = \sqrt{\Delta^2 + \Omega^2}$. This means that both the energy shifts and dissipation rates depend on the detuning Δ, the Rabi frequency Ω and also directly on the laser frequency ω_l. The most interesting variable of these three is the Rabi frequency Ω, since it makes it possible to change the dissipation of the system by varying the amplitude of the driving light field. Since the $\Gamma(x)$-function becomes approximately zero in the cases $x \approx 0$ and $x \gg 0$, it is even possible to cut out the dissipation rates $\Gamma\left(\omega_l \pm \sqrt{\Delta^2 + \Omega^2}\right)$ when $\Lambda \sim \omega_l$. The problem is though that there is always going to be a dissipation rate that solely depends on the laser frequency $\Gamma(\omega_l)$, which experimentalists generally can not vary much. This means that even though it is possible to change - and even cut out

- the dissipation rates $\Gamma\left(\omega_l \pm \sqrt{\Delta^2+\Omega^2}\right)$, there will always be a dissipation rate that depends on ω_l. For the two-level system, it is therefore not possible to totally cut out the dissipation.
Generally speaking the energy shifts and dissipation rates are not constant in time, which this solution shows. The time dependence is lost by the Markov approximation, which is inherited in our calculation. The Markov approximation brings the equation into a time local form, such that the dynamics does not depend on the past history.

Let us now consider the response functions in more detail and end up with a more rigorous form of the master equation. The integrals for the response functions can be evaluated by the use of the Sokhotskyi-Plemelj theorem in exponential form (also called a Plemelj formula), given by:

$$\int_0^\infty e^{\pm i\epsilon t}dt = \pi\delta(\epsilon) \pm i\frac{\mathcal{P}}{\epsilon} \tag{5.19}$$

The integral would equal a Dirac-delta function if it had started from negative infinity, but since it does not, the Cauchy principal value $\mathcal{P}$ is introduced to compensate for this.

To make the master equation (5.16) more manageable, we will apply some simplifications. Since the general case is that $\omega_l \gg \Delta, \Omega$ we can approximate $K_{12}(-\omega_i) = K_{12}(-\omega_l)$ and similar $K_{21}(\omega_i) = K_{21}(\omega_l)$ for all i=1,2,3. With this definition we arrive at:

$$\begin{aligned} K_{12}(-\omega_l) &= \int_0^\infty \left(\pi\delta(\omega_l-\omega) + i\frac{\mathcal{P}}{\omega_l-\omega}\right) J(\omega)(1+N(\omega))d\omega \\ &= \pi J(\omega_l)(1+N(\omega_l)) + i\mathcal{P}\int_0^\infty \frac{J(\omega)(1+N(\omega))}{\omega_l-\omega}d\omega \\ &= \frac{1}{2}\Gamma_{12}(-\omega_l) + iS_{12}(-\omega_l) \end{aligned} \tag{5.20}$$

and

$$\begin{aligned} K_{21}(\omega_l) &= \int_0^\infty \left(\pi\delta(\omega_l-\omega) - i\frac{\mathcal{P}}{\omega_l-\omega}\right) J(\omega)N(\omega)d\omega \\ &= \pi J(\omega_l)N(\omega_l) - i\mathcal{P}\int_0^\infty \frac{J(\omega)N(\omega)}{\omega_l-\omega}d\omega \\ &= \frac{1}{2}\Gamma_{21}(\omega_l) - iS_{21}(\omega_l) \end{aligned} \tag{5.21}$$

Substituting the response functions into the master equation (5.16) and expand out the commutators, we arrive at:

$$\begin{aligned} \frac{d\rho_S(t)}{dt} =& -i\left[H_{S'} + H_{LS}(\omega_l), \rho_S(t)\right] + \underbrace{\Gamma_{12}(-\omega_l)(\sigma\rho_S(t)\sigma^\dagger - \frac{1}{2}\left\{\sigma^\dagger\sigma, \rho_S(t)\right\})}_{\textit{spontaneous and stimulated emission}} \\ &+ \underbrace{\Gamma_{21}(\omega_l)(\sigma\rho_S(t)\sigma^\dagger - \frac{1}{2}\left\{\sigma\sigma^\dagger, \rho_S(t)\right\})}_{\textit{Radiation absorption}} \end{aligned} \tag{5.22}$$

where $\{a,b\} = ab+ba$ is the anticommutator. The first term describes the unitary coherent evolution of the system, where $H_{LS}(\omega_l) = S_{12}(-\omega_l)\sigma\sigma^\dagger + S_{21}(\omega_l)\sigma^\dagger\sigma$ represents an energy shift of the ground to excited state energy; generally known as the Lamb shift [1]. The last

[1] This is not the Lamb shift in its full form, since terms get lost by making the rotating-wave approximation.

two terms describe the non-unitary system dynamics that arise due to the environmental influence. The first non-unitary term describes the decay of the system (from the excited state to the ground state) by respectively spontaneous or stimulated emission of radiation into the environment, with rates $\pi J(\omega_l)$ and $\pi J(\omega_l)N(\omega_l)$. Since the rate of the stimulated emission process is $\pi J(\omega_l)N(\omega_l)$, it requires occupation of environmental states at energy matching ω_l. The spontaneous emission however is independent of the occupation number $N(\omega_l)$ and can therefore always occur. The last non-unitary term describes the radiation absorption of the system from the environment, which has the rate $\pi J(\omega_l)N(\omega_l)$ and is therefore also dependent on the occupation number.

5.2 Pure dephasing with driving

We will now briefly derive the master equation for a two-level QD undergoing pure-dephasing, while being driven by a laser with frequency ω_l and coupling strength Ω. The primary difference with this model and the spontaneous emission model, is the environment. Instead of comprising of photons, the environment comprises of a bath of phonons, which is quantized harmonic vibrations of crystalline solids, and can also be treated as harmonic oscillators. The corresponding Hamiltonian is given by:

$$\begin{aligned} H &= H_S + H_E + H_I \\ &= \frac{\epsilon}{2}\sigma_z + \Omega\cos(\omega_l t)\,\sigma_x + \sum_{\mathbf{k}} \omega_{\mathbf{k}} b_{\mathbf{k}}^\dagger b_{\mathbf{k}} + \sum_{\mathbf{k}} \sigma_z g_{\mathbf{k}} \left(b_{\mathbf{k}} + b_{\mathbf{k}}^\dagger\right) \end{aligned} \tag{5.23}$$

As can be seen, the interaction Hamiltonian is different from the spontaneous emission case, since the environment is different. The first step is again to put the Hamiltonian into a frame rotating at the laser frequency ω_l, which becomes:

$$H' = \frac{\Delta}{2}\sigma_z + \frac{\Omega}{2}\sigma_x + \sum_{\mathbf{k}} \omega_{\mathbf{k}} b_{\mathbf{k}}^\dagger b_{\mathbf{k}} + \sum_{\mathbf{k}} \sigma_z g_{\mathbf{k}} \left(b_{\mathbf{k}} + b_{\mathbf{k}}^\dagger\right) \tag{5.24}$$

The crucial point here is that the transformation does not change the interaction Hamiltonian, which now needs to be moved into the interaction, with respect to the rotation free Hamiltonians:

$$\tilde{H_I'} = \tilde{H_I} = \sum_{\mathbf{k}} \tilde{\sigma}_z(t) g_{\mathbf{k}} \left(b_{\mathbf{k}} e^{-i\omega_{\mathbf{k}} t} + b_{\mathbf{k}}^\dagger e^{i\omega_{\mathbf{k}} t}\right) \tag{5.25}$$

where $\tilde{\sigma}_z(t) = e^{iH_{S'}t}\sigma_z e^{-iH_{S'}t}$. Since the detuning Δ generally is very small, so that $\Omega \gg \Delta$, we can approximate $H_{S'} = \frac{\Omega}{2}\sigma_x$. This means that:

$$\begin{aligned} \tilde{\sigma}_z(t) =& e^{i\frac{\Omega}{2}\sigma_x t}\sigma_z e^{-i\frac{\Omega}{2}\sigma_x t} = \left(e^{i\frac{\Omega}{2}t}\left|+\right\rangle\left\langle+\right| + e^{-i\frac{\Omega}{2}t}\left|-\right\rangle\left\langle-\right|\right)\sigma_z\left(e^{-i\frac{\Omega}{2}t}\left|+\right\rangle\left\langle+\right| + e^{i\frac{\Omega}{2}t}\left|-\right\rangle\left\langle-\right|\right) \\ =& e^{-i\Omega\tau}\left|-\right\rangle\left\langle+\right| + e^{i\Omega\tau}\left|+\right\rangle\left\langle-\right| \end{aligned}$$

where $\left|\pm\right\rangle = \frac{1}{\sqrt{2}}\left(\left|e\right\rangle \pm \left|g\right\rangle\right)$. Comparing with (2.19), we can deduce: $A_1(t) = A_2(t) = e^{-i\Omega t}\left|-\right\rangle\left\langle+\right| + e^{i\Omega t}\left|+\right\rangle\left\langle-\right|$, $B_1(t) = \sum_{\mathbf{k}} g_{\mathbf{k}} b_{\mathbf{k}} e^{-i\omega_{\mathbf{k}} t}$ and $B_2(t) = \sum_{\mathbf{k}} g_{\mathbf{k}} b_{\mathbf{k}}^\dagger e^{i\omega_{\mathbf{k}} t}$. Since $B_1(t)$ and $B_2(t)$ are the same as the ones in the previous case with spontaneous emission, the

correlation functions $C_{\alpha\beta}$ become respectively (5.13) and (5.14). Substituting everything into the Schrödinger picture Born-Markov master equation (2.23) we find:

$$\begin{aligned}\frac{d\rho}{dt} =& -i\left[H_S, \rho_S(t)\right] - \int_0^\infty \left(\left[A_1, A_2(-\tau)\rho_S(t)\right] C_{12}(\tau) + \left[A_2, A_1(-\tau)\rho_S(t)\right] C_{21}(\tau) + h.c.\right) d\tau \\ =& -i\left[H_{S'}, \rho_S(t)\right] - \int_0^\infty \Big(\left[\sigma_z, \left(e^{i\Omega\tau}\left|-\right\rangle\left\langle+\right| + e^{-i\Omega\tau}\left|+\right\rangle\left\langle-\right|\right)\rho_S(t)\right] C_{12}(\tau) \\ &+ \left[\sigma_z, \left(e^{i\Omega\tau}\left|-\right\rangle\left\langle+\right| + e^{-i\Omega\tau}\left|+\right\rangle\left\langle-\right|\right)\rho_S(t)\right] C_{21}(\tau) + h.c.\Big) d\tau\end{aligned} \tag{5.26}$$

The response functions in this case become – the derivation is done briefly, since it was done rigorously in the previous section:

$$K_{12}\left(\pm\Omega\right) = \int_0^\infty e^{\mp i\Omega\tau} C_{12}(\tau) d\tau = \begin{cases} -iS_{12}\left(\Omega\right) & \text{for } K_{12}\left(\Omega\right) \\ \frac{1}{2}\gamma_{12}\left(-\Omega\right) + iS_{12}\left(-\Omega\right) & \text{for } K_{12}\left(-\Omega\right) \end{cases} \tag{5.27}$$

and

$$K_{21}\left(\pm\Omega\right) = \int_0^\infty e^{\mp i\Omega\tau} C_{21}(\tau) d\tau = \begin{cases} \frac{1}{2}\gamma_{21}\left(\Omega\right) - iS_{21}\left(\Omega\right) & \text{for } K_{21}\left(\Omega\right) \\ iS_{21}\left(-\Omega\right) & \text{for } K_{21}\left(-\Omega\right) \end{cases} \tag{5.28}$$

where

$$S_{12}\left(\pm\Omega\right) = \mathcal{P}\int_0^\infty \frac{J(\omega)(1+N(\omega))}{\Omega \pm \omega} d\omega, \qquad \gamma_{12}\left(-\Omega\right) = 2\pi J(\Omega)(1+N(\Omega)) \tag{5.29}$$

$$S_{21}\left(\pm\Omega\right) = \mathcal{P}\int_0^\infty \frac{J(\omega)N(\omega)}{\Omega \pm \omega} d\omega, \qquad \gamma_{21}\left(\Omega\right) = 2\pi J(\Omega)N(\Omega) \tag{5.30}$$

Note that the response functions $K_{12}(\Omega)$ and $K_{21}(\Omega)$ do not have any dissipation rates γ, because we impose $J(-\Omega) = 0$, which holds true for any physical model of $J(\omega)$.

5.2.1 QZE: pure dephasing with strong 'continuous coupling'

In contrast to the spontaneous emission case, the dissipation rates only depend of the Rabi frequency $\gamma(\pm\Omega)$. Hence it is possible to change the total dissipation of the system only by varying the amplitude of the driving laser. In this case it is even possible to completely cut out the dissipation of the system by making the Rabi frequency Ω large enough. This can be seen visually by plotting the dissipation as a function of the Rabi frequency, as seen in figure (5.1). This fact alone means that it is possible to obtain the QZE for a QD undergoing pure dephasing, only by influencing the QD by a strong 'continuous coupling'.

Substituting the response functions into (5.26) and expanding out the commutators:

$$\begin{aligned}\frac{d\rho_S}{dt} =& -i\left(\left[H_{S'} + H_{LS}(\Omega), \rho_S(t)\right] - \sigma_z\left[H_d(\Omega), \rho_S(t)\right]\sigma_z^\dagger\right) \\ &+ \frac{1}{2}\gamma_{12}(-\Omega)\left(\sigma_z\left\{\left|+\right\rangle\left\langle+\right|, \rho_S(t)\right\}\sigma_z^\dagger - \left\{\left|+\right\rangle\left\langle+\right|, \rho_S(t)\right\}\right) \\ &+ \frac{1}{2}\gamma_{21}(\Omega)\left(\sigma_z\left\{\left|-\right\rangle\left\langle-\right|, \rho_S(t)\right\}\sigma_z^\dagger - \left\{\left|-\right\rangle\left\langle-\right|, \rho_S(t)\right\}\right)\end{aligned} \tag{5.31}$$

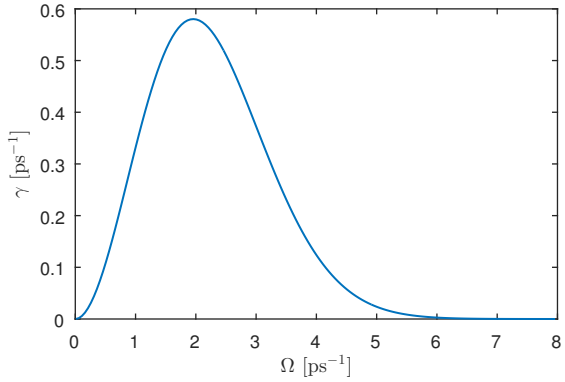

Figure 5.1: Graph showing how the dissipation rate γ depends on the coupling strength Ω. We have used $\alpha = 0.03\,\mathrm{ps}^2$, $\omega_c = 2.2\,\mathrm{ps}^{-1}$ and $T = 20\,\mathrm{K}$.

where $H_{LS}(\Omega) = H_d(\Omega) = (S_{21}(-\Omega) + S_{12}(-\Omega))\,|+\rangle\langle+| - (S_{21}(\Omega) + S_{12}(\Omega))\,|-\rangle\langle-|$ represents a Lamb shift – presented as H_{LS} – but also partly works as a source of decoherence – presented as H_d. In other words, the first term gives rise to coherent unitary dynamics of the system, while the last three give rise to non-unitary system dynamics that arise due to the environmental influence. The non-unitary terms lead to the dephasing of the QD, which ultimately makes the quantum state more mixed (classical). This final expression is not in Lindblad form, but it resembles a more detailed and rigorous form of the Born-Markov master equation. With the help of this expression, we will be able to make a better physical description of how the QD undergoes pure dephasing, which potentially can improve the study of the QZE in the cases of 'pure dephasing' models. The two first terms represent coherent unitary evolution of the system.

5.3 Three level system: spontaneous emission with driving

We are now going one step further and look at specific case of a three level QD, driven by a electromagnetic field in its lower sub-level - see (4.22a). The environment is again modelled as a bath of independent harmonic oscillators, and the total Hamiltonian corresponds to:

$$H = \omega_p\,|p\rangle\langle p| + \omega_e\,|e\rangle\langle e| + \Omega_{eg}\cos(\omega_l t)\left(\sigma_{x_{eg}}\right) + \sum_{\mathbf{k}} \omega_{\mathbf{k}} b_{\mathbf{k}}^\dagger b_{\mathbf{k}} + \sum_{\mathbf{k}} g_{\mathbf{k}}\left(\sigma_{pe}^\dagger b_{\mathbf{k}} + \sigma_{pe} b_{\mathbf{k}}^\dagger\right) \tag{5.32}$$

where the zero point energy is set to be at the ground state. The system Hamiltonian (first three terms) represents the three level system driven by the classical field with frequency ω_l that couples the ground $|g\rangle$ and the excited $|e\rangle$ states with coupling strength Ω_{eg}. The pump state $|p\rangle$ has energy ω_p and the excited state has energy ω_e. The bath of harmonic oscillators (fourth term) is the same as for the previous cases. The interaction Hamiltonian (last term) couples the subspace comprising of the excited and the pump state with the harmonic oscillators by the coupling constants $g_{\mathbf{k}}$, where $\sigma_{pe} = |e\rangle\langle p|$ and $\sigma_{pe}^\dagger = |p\rangle\langle e|$. It should also be noted that $\sigma_{x_{eg}} = |g\rangle\langle e| + |e\rangle\langle g|$ and $\sigma_{x_{pe}} = |e\rangle\langle p| + |p\rangle\langle e|$.
The first step in deriving the master equation for this system, is again to put the Hamiltonian into a frame rotating at the laser frequency, with the unitary operator $U_R(t) = e^{i\omega_l(|p\rangle\langle p| + |e\rangle\langle e|)t} = |e\rangle\langle e|\,e^{i\omega_l t} + |p\rangle\langle p|\,e^{i\omega_l t} + |g\rangle\langle g|$. This transformed Hamiltonian becomes:

$$H' = \Delta_{pl} |p\rangle \langle p| + \Delta_{el} |e\rangle \langle e| + \frac{\Omega_{eg}}{2}\sigma_{x_{eg}} + \sum_{\mathbf{k}} \omega_{\mathbf{k}} b_{\mathbf{k}}^\dagger b_{\mathbf{k}} + \sum_{\mathbf{k}} g_{\mathbf{k}} \left(\sigma_{pe}^\dagger b_{\mathbf{k}} + \sigma_{pe} b_{\mathbf{k}}^\dagger\right) \tag{5.33}$$

where $\Delta_{pl} = \omega_p - \omega_l$ and $\Delta_{el} = \omega_e - \omega_l$. As can be seen, in contrast to the two level case with spontaneous emission, the interaction Hamiltonian is not affected by the rotating frame transformation. As done previously, we now move the interaction Hamiltonian into the interaction picture:

$$\tilde{H}_I = \sum_{\mathbf{k}} g_{\mathbf{k}} \left(\tilde{\sigma}_{+_{pe}}(t) b_{\mathbf{k}} e^{-i\omega_{\mathbf{k}} t} + \tilde{\sigma}_{-_{pe}}(t) b_{\mathbf{k}}^\dagger e^{i\omega_{\mathbf{k}} t}\right) \tag{5.34}$$

where $\tilde{\sigma}_{\pm_{pe}}(t) = U_{S'}^\dagger(t)\sigma_{\pm_{pe}} U_{S'}(t) = e^{iH_{S'}t}\sigma_{\pm_{pe}} e^{-iH_{S'}t}$. Comparing this with (2.19) we see that: $A_1(t) = \tilde{\sigma}_{+_{pe}}$, $A_2(t) = \tilde{\sigma}_{+_{pe}}$, $B_1(t) = \sum_{\mathbf{k}} g_{\mathbf{k}} b_{\mathbf{k}} e^{-i\omega_{\mathbf{k}} t}$ and $B_2(t) = \sum_{\mathbf{k}} g_{\mathbf{k}} b_{\mathbf{k}}^\dagger e^{i\omega_{\mathbf{k}} t}$. Comparing $A_1(t)$ and $A_2(t)$ with the ones we got in the two-level system with spontaneous emission (5.7), we see that the only difference is the lack of rotational exponential factors $e^{\pm i\omega_l t}$.

Before going any further, we simplify the problem by specifying the system even more, making the detuning $\Delta_{el} = 0$. This means that we are driving the system with a laser resonant with the lower subsystem of the three level system, which is often the case experimentally; i.e. $\omega_l = \omega_e$ and $\Delta_{pl} = \omega_p - \omega_e$. The derivation of $\tilde{\sigma}_{\pm_{pe}}$ then becomes much easier, which is done by first diagonalizing the rotated system Hamiltonian:

$$\begin{aligned} H_{s'} &= \begin{pmatrix} \Delta_{pl} & 0 & 0 \\ 0 & 0 & \frac{1}{2}\Omega_{eg} \\ 0 & \frac{1}{2}\Omega_{eg} & 0 \end{pmatrix} = V \begin{pmatrix} \Delta_{pl} & 0 & 0 \\ 0 & \frac{1}{2}\Omega_{eg} & 0 \\ 0 & 0 & -\frac{1}{2}\Omega_{eg} \end{pmatrix} V^{-1} \\ &= \Delta_{pl} |\Delta_{pl}\rangle \langle \Delta_{pl}| + \frac{\Omega_{eg}}{2} \left(|+\Omega_{eg}\rangle \langle +\Omega_{eg}| - |-\Omega_{eg}\rangle \langle -\Omega_{eg}|\right) \end{aligned} \tag{5.35}$$

where $\pm\frac{1}{2}\Omega_{eg}$ and Δ_{pl}, are the eigenvalues of $H_{S'}$, V is composed of the normalized eigenvectors $|\Delta_{pl}\rangle = V|p\rangle$, $|+\Omega_{eg}\rangle = V|e\rangle$ and $|-\Omega_{eg}\rangle = V|g\rangle$ for $H_{S'}$. Using this representation to write $U_{S'}(t) = e^{-iH_{S'}t} = e^{-i\Delta_{pl}t} |\Delta_{pl}\rangle \langle \Delta_{pl}| + e^{-i\frac{\Omega_{eg}}{2}t} |+\Omega_{eg}\rangle \langle +\Omega_{eg}| + e^{i\frac{\Omega_{eg}}{2}t} |-\Omega_{eg}\rangle \langle -\Omega_{eg}|$ the operators $A_1(t)$ and $A_2(t)$ become:

$$A_1(t) = \tilde{\sigma}_{+_{pe}} = \sum_i X_i e^{i\omega_i t} \qquad A_2(t) = \tilde{\sigma}_{-_{pe}} = \sum_i Y_i e^{-i\omega_i t} \tag{5.36}$$

The sums run over the Fourier components i=1, 2 with frequencies $\omega_1 = \left(\Delta_{pl} - \frac{1}{2}\Omega_{eg}\right)$ and $\omega_2 = \left(\Delta_{pl} + \frac{1}{2}\Omega_{eg}\right)$. The operators X_i are respectively: $X_1 = |\Delta_{pl}\rangle \langle \Delta_{pl}| \sigma_{pe}^\dagger |\Omega_{eg}\rangle \langle \Omega_{eg}|$ and $X_2 = |\Delta_{pl}\rangle \langle \Delta_{pl}| \sigma_{pe}^\dagger |-\Omega_{eg}\rangle \langle -\Omega_{eg}|$, and the complex conjugate of these gives the operators of Y_i. As in the two-level case, $\sum_i X_i = \sigma_{pe}^\dagger$ and$\sum_i Y_i = \sigma_{pe}$.

Since the operators $B_1(t)$ and $B_2(t)$ are the same in the two level case with spontaneous emission, the response functions $K_{12}(\omega_i)$ and $K_{21}(-\omega_i)$ end up also being the same: (5.17) and (5.18) - though depending on the Fourier frequencies ω_i that we just found. From this we can therefore already conclude that the dissipation and the energy shifts in the three

level case depend on the Rabi frequency of the system Ω_{eg} and on the detuning Δ_{el}. As will be stated below, the dissipation rates for the system become: $\frac{1}{2}\Gamma\left(\Delta_{pl} \pm \frac{1}{2}\Omega_{eg}\right)$. The situation is therefore almost exactly the same as for the two-level case, the only difference being that there is no dissipation rate that directly depends on the classical driving field frequency $\Gamma(\omega_l)$. The frequency ω_l only appears implicitly in the detuning for the three level case. This ultimately means that the dissipation of the system can be altered just by varying the Rabi frequency Ω_{eg}. The $\Gamma(x)$-function is approximately the same as for the pure dephasing case – seen on figure (5.1) – and becomes approximately zero in the cases $x \approx 0$ and $x \gg 0$. It is therefore possible to turn off the dissipation for the three level system just by making Ω_{eg} large enough.

This result can be explained physically as being a consequence of electromagnetically induced transparency[30]. Driving a system with an alternating electromagnetic field induced shifts in its energy spectrum that increase with the strength of the applied field. This effect is known as the AC Stark effect [31]. In our case, the strong coupling between e and g shifts the states into two so-called dressed states $|\pm\rangle = \frac{1}{\sqrt{2}}(|e\rangle \pm |g\rangle)$ of energy $\pm\Omega_{eg}$. If Ω_{eg} is sufficiently large, the spontaneous transitions between $|p\rangle$ and $|+\rangle$ will not be in resonance. Hence, the *pe*-subsystem becomes transparent so that the transition can not be made. As discussed in [30] the transparency of the *pe*-subsystem also depends on the interference of the two dressed states, but this will not be further explained here since it is outside the scope of this report.

We now want to consider the problem in more detail in order to end up with a usable rigorous form of the master equation. Substituting $A_1(t)$, $A_2(t)$ into the Schrödinger picture Born-Markov master equation (2.23) we find:

$$\begin{aligned}\frac{d\rho}{dt} =& -i\left[H_S, \rho_S(t)\right] - \int_0^\infty \left(\left[\sigma_{pe}^\dagger, \left(e^{i\left(\Delta_{pl}-\frac{\Omega_{eg}}{2}\right)t} Y_1 + e^{i\left(\Delta_{pl}+\frac{\Omega_{eg}}{2}\right)t} Y_2 \right) \rho_S(t) \right] C_{12}(\tau) \right. \\ &\left. + \left[\sigma_{pe}, \left(e^{-i\left(\Delta_{pl}-\frac{\Omega_{eg}}{2}\right)t} X_1 + e^{-i\left(\Delta_{pl}+\frac{\Omega_{eg}}{2}\right)t} X_2 \right) \rho_S(t) \right] C_{21}(\tau) + h.c. \right) d\tau \end{aligned} \tag{5.37}$$

The response functions in this case, where $\xi_\pm = \Delta_{pl} \pm \frac{\Omega_{eg}}{2}$, are given by

$$K_{12}(-\xi_\pm) = \int_0^\infty e^{i\xi_\pm \tau} C_{12}(\tau) d\tau = \begin{cases} \frac{1}{2}\Gamma_{12}(-\xi_+) + iS_{12}(-\xi_+), & \text{for } K_{12}(-\xi_+) \\ \frac{1}{2}\Gamma_{12}(-\xi_-) + iS_{12}(-\xi_-), & \text{for } K_{12}(-\xi_-) \end{cases} \tag{5.38}$$

and

$$K_{21}(\xi_\pm) = \int_0^\infty e^{-i\xi_\pm \tau} C_{21}(\tau) d\tau = \begin{cases} \frac{1}{2}\Gamma_{21}(\xi_+) - iS_{21}(\xi_+), & \text{for } K_{21}(\xi_+) \\ \frac{1}{2}\Gamma_{21}(\xi_-) - iS_{21}(\xi_-), & \text{for } K_{21}(\xi_-) \end{cases} \tag{5.39}$$

where

$$S_{12}(-\xi_\pm) = \mathcal{P}\int_0^\infty \frac{J(\omega)(1+N(\omega))}{\xi_\pm - \omega} d\omega, \qquad \Gamma_{12}(-\xi_\pm) = 2\pi J(\xi_\pm)(1+N(\xi_\pm)) \tag{5.40}$$

$$S_{21}(\xi_\pm) = \mathcal{P}\int_0^\infty \frac{J(\omega)N(\omega)}{\xi_\pm - \omega} d\omega, \qquad \Gamma_{21}(\xi_\pm) = 2\pi J(\xi_\pm)N(\xi_\pm) \tag{5.41}$$

We want to study two cases for the three level system. The first is a general case for physical systems, where it is anticipated that $\Delta_{pl} \gg \Omega_{eg}$. This makes it possible to

approximate $K_{12}(-\xi_\pm) = K_{12}(-\Delta_{pl})$ and $K_{21}(\xi_\pm) = K_{21}(\Delta_{pl})$. Substituting the resulting response functions into the master equation (5.37) and expanding our the commutators, we for this case get:

$$\frac{d\rho_S(t)}{dt} = -i\left[H_{S'} + H_{LS}(\Delta_{pl}), \rho_S(t)\right] + \underbrace{\Gamma_{12}(-\Delta_{pl})(\sigma_{pe}\rho_S(t)\sigma_{pe}^\dagger - \frac{1}{2}\left\{\sigma_{pe}^\dagger\sigma_{pe}, \rho_S(t)\right\})}_{\textit{spontaneous and stimulated emission}}$$
$$+ \underbrace{\Gamma_{21}(\Delta_{pl})(\sigma_{pe}^\dagger\rho_S(t)\sigma_{pe} - \frac{1}{2}\left\{\sigma_{pe}\sigma_{pe}^\dagger, \rho_S(t)\right\})}_{\textit{Radiation absorption}} \tag{5.42}$$

where $H_{LS} = S_{12}(-\Delta_{pl})\sigma_{pe}^\dagger\sigma_{pe}^\dagger + S_{21}(\Delta_{pl})\sigma_{pe}\sigma_{pe}^\dagger$ is the Lamb shift. The similarity with the two-level case undergoing spontaneous emission is evident. The first term describes the unitary coherent evolution of the system, while the last two terms describe the non-unitary system dynamics. The decay of the three-level system from the pump state to the excited state by either spontaneous or stimulated emission processes is represented with the first non-unitary term, with rates proportional to $\pi J(\Delta_{pl})$ and $\pi J(\Delta_{pl})N(\Delta_{pl})$ respectively. The spontaneous emission is independent of the occupation number $N(\Delta_{pl})$ and can therefore always occur. Likewise, the final term describes absorption processes, and is given by the rate proportional to $\pi J(\Delta_{pl})N(\Delta_{pl})$, which on the contrary requires occupation of environmental states matching the energy Δ_{pl}.

The second case is theoretical, since we hypothesize that $\frac{\Omega_{eg}}{2} > \Delta_{pl}$, which may not be true in physical systems. This case is interesting, since it makes it possible to study the above mentioned effects of having a large coupling strength, which can turn off the dissipation for the system. This relationship between Ω_{eg} and Δ_{pl}, annihilates half of the dissipation rates, namely $\gamma_{12}(\pm\xi_-)$. The detuning $\Delta_{pl} = \omega_p - \omega_e$ will typically be large – generally at least $\sim 1\,\text{eV}$ – and if our requirement is that Ω_{eg} has to be twice as big, this means that $N(\xi_+) = \left(e^{\xi_+/k_BT} - 1\right)^{-1} \approx 0$ for any temperature T under about 1000 K. Applying these approximations and substituting the resulting response functions into (5.37) leaves us with:

$$\frac{d\rho_S(t)}{dt} = -i\left[H_{S'}, \rho_S(t)\right] - iS_{12}(-\xi_-)\left[\sigma_{pe}^\dagger, Y_1\rho_S(t)\right]$$
$$-\left(\frac{1}{2}\Gamma_{12}(-\xi_+) + iS_{12}(-\xi_+)\right)\left[\sigma_{pe}^\dagger, Y_2\rho_S(t)\right] + h.c. \tag{5.43}$$

This is not an aesthetic expression, but it makes it possible to study the QZE by strong coupling in three-level systems – see sec. 6.2.2.

5.4 Three level system: multiple Rabi oscillations

The motive of this section is to further discuss the notion that driving a system strongly can substantially reduce its dissipation – even entirely. As stated, the reduced dissipation can be physically explained as being a result of the AC-Stark splitting of states, which is created by the coupling laser. Instead of having a system having spontaneous emission between the pump level $|p\rangle$ and the excited level $|e\rangle$, we will discuss a three level QD driven by two distinct Rabi oscillations in its respective sub-systems - see (4.22b). It will be shown that this system, consisting of only unitary evolution, will also show the same characteristic behaviour when it is being strongly driven in one of its sub-systems.

The Hamiltonian for the considered system driven by two different laser fields ω_1 and ω_2 is given by:

$$H(t) = \omega_p \left|p\right\rangle \left\langle p\right| + \omega_e \left|e\right\rangle \left\langle e\right| + \Omega_{pe} \cos\left(\omega_1 t\right) \sigma_{x_{pe}} + \Omega_{eg} \cos\left(\omega_2 t\right) \sigma_{x_{eg}} \tag{5.44}$$

where the zero point energy is set to be at the ground state. The Hamiltonian describes a closed system, completely described in terms of the time-dependent Hamiltonian (2.6), even though it is not completely isolated from environmental influence. As stated, this Hamiltonian has two Rabi oscillation, with the coupling strengths Ω_{pe} and Ω_{eg} for respectively the upper- and lower sub-system, driven separately by the laser frequencies ω_1 and ω_2.

As always, the first step is to put the Hamiltonian into a rotating frame. For this case, we are using the unitary operator $U_R(t) = e^{i(\omega_1 \left|e\right\rangle \left\langle e\right| + \omega_2 \left|p\right\rangle \left\langle p\right|)t} = \left|e\right\rangle \left\langle e\right| e^{i\omega_1 t} + \left|p\right\rangle \left\langle p\right| e^{i\omega_2 t}$. The corresponding rotated Hamiltonian becomes:

$$H^{'}(t) = \Delta_{p2} \left|p\right\rangle \left\langle p\right| + \Delta_{e1} \left|e\right\rangle \left\langle e\right| + \frac{\Omega_{pe}}{2} \sigma_{x_{pe}} + \frac{\Omega_{eg}}{2} \sigma_{x_{eg}} \tag{5.45}$$

where $\Delta_{p2} = \omega_p - \omega_2$ and $\Delta_{e1} = \omega_e - \omega_1$.

We will now consider the case where the coupling strength for the lower level Ω_{eg} is being increased, while Ω_{pe} is being held constant. For the sake of simplicity, we theorize that the lasers are finely tuned to match the respective energy levels of the system, such that both detunings, Δ_{p2} and Δ_{e1} are set to zero.
It is not easy to see from the general Schrödinger equation (2.6) how the system will react to a stronger drive. In order to explain how the system reacts to the stronger drive of the lower sub-system, it is necessary to write the system Hamiltonian in the basis of the two dressed levels that form the complete orthogonal set $\{\left|p\right\rangle, \left|\pm\right\rangle = \frac{1}{\sqrt{2}} \left(\left|e\right\rangle \pm \left|g\right\rangle\right)\}$. Since $\mathbf{I} = \left|p\right\rangle \left\langle p\right| + \left|e\right\rangle \left\langle e\right| + \left|g\right\rangle \left\langle g\right| = \left|p\right\rangle \left\langle p\right| + \left|+\right\rangle \left\langle +\right| + \left|-\right\rangle \left\langle -\right|$, we can transform the system Hamiltonian into the new basis by the operation:

$$\mathbf{I}H'\mathbf{I} = \left(\left|p\right\rangle \left\langle p\right| + \left|+\right\rangle \left\langle +\right| + \left|-\right\rangle \left\langle -\right|\right) \frac{1}{2} \begin{pmatrix} 0 & \Omega_{pe} & 0 \\ \Omega_{pe} & 0 & \Omega_{eg} \\ 0 & \Omega_{eg} & 0 \end{pmatrix} \left(\left|p\right\rangle \left\langle p\right| + \left|+\right\rangle \left\langle +\right| + \left|-\right\rangle \left\langle -\right|\right) \tag{5.46}$$

$$= \frac{1}{2\sqrt{2}} \begin{pmatrix} 0 & \Omega_{pe} & \Omega_{pe} \\ \Omega_{pe} & \sqrt{2}\Omega_{eg} & 0 \\ \Omega_{pe} & 0 & -\sqrt{2}\Omega_{eg} \end{pmatrix} \tag{5.47}$$

From this we can conclude that an increase in the coupling strength for the lower sub-system Ω_{eg} will step-up the influence of the two states $\left|\pm\right\rangle$. The effect of driving the lower sub-system more strongly is thus a shift of the states $\left|e\right\rangle$ and $\left|g\right\rangle$ to the dressed states $\left|\pm\right\rangle$. As for the case with spontaneous emission, if Ω_{eg} is sufficiently large the transitions between $\left|p\right\rangle$ and $\left|+\right\rangle$ will not be in resonance with the source Ω_{pe} that is causing the driving. Hence, the *pe*-subsystem becomes transparent and no driving occurs. We will analyze this model in respect to the QZE in sec. 4.5.2.

5.5 Justification of Lindblad formalism

This section is meant to justify the Lindbald formalism, which we made use of in chapter (4) to describe QZE in both two- and three-level QD's in open systems. We studied QZE in a two-level QD undergoing both spontaneous emission and pure dephasing. For the three-level QD we briefly discussed a specific case undergoing spontaneous emission, driven by a laser in only its lower level. A rigorous derivation of the Born-Markovs master equation for all these cases was done in the previous sections.

Spontaneous emission for two-level QD

The rigorous form of the master equation for a two-level QD given by (5.22) will yield the Lindblad form, by making some further approximations. Typically the laser frequency ω_l is approximately equal to the ground to excited state energies, which are of the order $\epsilon \sim 1\,\text{eV}$. At room temperature we have $k_BT \sim 25\,\text{meV}$, which leaves us with the fraction $\frac{\omega_l}{k_BT} \gg 1$. In considering the definition of the occupation of states $N(\omega_l) = \left(e^{\omega_l/k_BT} - 1\right)^{-1}$ this means that even at these elevated temperatures thermal occupation of states is low and we can approximate $N(\omega_l) \approx 0$. The shift in energy of the system can often also be neglected since they often are very small, so $H_{LS} \approx 0$. With these approximations get the master equation in Lindblad form:

$$\begin{aligned}\frac{d\rho_S}{dt} &= -i\left[H_{S'}, \rho_S(t)\right] + \underbrace{\Gamma(\sigma\rho_S(t)\sigma^\dagger - \frac{1}{2}\left\{\sigma^\dagger\sigma, \rho_S(t)\right\})}_{spontaneous\ emission} \\ &= -i\left[H_{S'}, \rho_S(t)\right] + \Gamma L(\sigma) \end{aligned} \tag{5.48}$$

where $\Gamma = 2\pi J(\omega_l)$.

Dephasing for two-level QD

For the rigorous pure dephasing form (5.31), it follows that the driving frequency Ω typically is of the order $\Omega = 0.1ps^{-1}$ which corresponds to approximately 1 meV. QDs undergoing pure dephasing are usually considered in the regime of low temperatures, and since $k_BT \sim 200 - 300\,\text{meV}$ in temperatures reaching from 30-50 K, we have $\frac{\Omega}{k_BT} \ll 1$. This means that $N(\Omega) \approx (N(\Omega) + 1)$ or equivalently $\gamma(-\Omega) = \gamma(\Omega)$. If the energy shifts again are considered small $S(\pm\Omega) \approx 0$, these approximations yield the master equation in Lindblad form:

$$\begin{aligned}\frac{d\rho_S}{dt} &= -i\left[H_{S'}, \rho_S(t)\right] + \underbrace{\gamma\left(\sigma_z\rho_S(t)\sigma_z^\dagger - \frac{1}{2}\left\{\sigma_z^\dagger\sigma_z, \rho_S(t)\right\}\right)}_{Dephasing\ term} \\ &= -i\left[H_{S'}, \rho_S(t)\right] + \gamma L(\sigma_z) \end{aligned} \tag{5.49}$$

where $\gamma = 2\pi J(\Omega)$. It should also be remarked that the resulting master equation is presented in its lindblad form, but can be further reduced since $\frac{1}{2}\left\{\sigma_z^\dagger\sigma_z, \rho_S(t)\right\} = \rho_S(t)$.

5.5.1 Spontaneous emission for three-level QD

The Lindblad form for the three level QD undergoing spontaneous emission can be found by making approximations on the derived master equation (5.42). The approximations

are the same as those for the two-level case with spontaneous emission, the only difference being that $\Delta_{pl} \sim 1\,\text{eV}$ instead of ω_l. Ultimately this means that we arrive at the Lindblad form:

$$\begin{aligned}\frac{d\rho_S(t)}{dt} &= -i\left[H_{S'}, \rho_S(t)\right] + \underbrace{\Gamma(\sigma_{pe}\rho_S(t)\sigma_{pe}^\dagger - \frac{1}{2}\left\{\sigma_{pe}^\dagger\sigma_{pe}, \rho_S(t)\right\})}_{spontaneous\ emission} \\ &= -i\left[H_{S'}, \rho_S(t)\right] + \Gamma L(\sigma_{pe}) \end{aligned} \tag{5.50}$$

where $\Gamma = 2\pi J(\Delta_{pl})$.

5.6 Non-Markovian master equation

In the derivation leading to the master equations (5.22) and (5.31), we now want to undo the Markov approximation. This will give a new expression for $\frac{d\rho}{dt}$ from which we can obtain time-dependent models for $\Gamma(t)$ and $\gamma(t)$. These models have already been used in the calculations based on the Lindblad formalism in sec. 4.2.2.

Time-dependent spontaneous emission

The result of removing the Markov approximation is simply that the upper integration limit in 5.16 is not $\tau = \infty$ but $\tau = t$. Thus,

$$\frac{d\rho}{dt} = -i\left[H_S, \rho_S(t)\right] - \sum_i^3 \int_0^t \left([\sigma_+,\, Y_i\rho_S(t)]\, e^{i\omega_i\tau} C_{12}(\tau) + [\sigma_-,\, X_i\rho_S(t)]\, e^{-i\omega_i\tau} C_{21}(\tau) + h.c.\right) d\tau \tag{5.51}$$

Again we use the simplification $\omega_l \gg \Omega, \Delta$, which holds true for spontaneous emission, whereby the Fourier components ω_1, ω_2 and ω_3 become equal to ω_l. This allows us to write (5.51) as

$$\begin{aligned}\frac{d\rho}{dt} &= -i\left[H_S, \rho_S(t)\right] - \int_0^t \left([\sigma_+, \sigma_-\rho_S(t)]\, e^{i\omega_l\tau} C_{12}(\tau) + [\sigma_-, \sigma_+\rho_S(t)]\, e^{-i\omega_l\tau} C_{21}(\tau) + h.c.\right) d\tau \\ &= -i\left[H_S, \rho_S(t)\right] - \Big([\sigma_+, \sigma_-\rho_S(t)]\, K_{12}(-\omega_l) + [\sigma_-, \sigma_+\rho_S(t)]\, K_{21}(\omega_l) + h.c.\Big). \end{aligned} \tag{5.52}$$

using the relations $\sum_i X_i = \sigma_+$ and $\sum_i Y_i = \sigma_-$ and where the response functions can easily be identified as

$$K_{12}(-\omega_l, t) = \int_0^t e^{i\omega_l\tau} C_{12}(\tau)\, d\tau = \frac{1}{2}\Gamma_{12}(-\omega_l, t) + iS_{12}(-\omega_l, t) \tag{5.53}$$

$$K_{21}(\omega_l, t) = \int_0^t e^{-i\omega_l\tau} C_{21}(\tau)\, d\tau = \frac{1}{2}\Gamma_{21}(\omega_l, t) + iS_{21}(\omega_l, t). \tag{5.54}$$

Hence, due to the definitions we have $\Gamma_{ab} = 2 \cdot \mathrm{Re}(K_{ab})$, which can be rewritten by inserting the derived correlation functions (5.13) and (5.14),

$$\begin{aligned}\Gamma_{12}(-\omega_l, t) = 2 \cdot \mathrm{Re}(K_{12}(-\omega_l, t)) &= 2\mathrm{Re}\left(\int_0^t e^{i\omega_l \tau} \int_0^\infty J(\omega) e^{-i\omega\tau}(1 + N(\omega))\, d\omega d\tau\right) \\ &= 2\int_0^t \int_0^\infty \cos\big(\tau(\omega_l - \omega)\big) J(\omega)(1 + N(\omega))\, d\omega d\tau \\ &= 2\int_0^\infty \frac{\sin\big(t(\omega_l - \omega)\big)}{\omega_l - \omega} J(\omega)(1 + N(\omega))\, d\omega, \qquad (5.55)\end{aligned}$$

$$\begin{aligned}\Gamma_{21}(\omega_l, t) = 2 \cdot \mathrm{Re}(K_{21}(\omega_l)) &= 2\int_0^t e^{-i\omega_l \tau} \int_0^\infty J(\omega) e^{i\omega\tau} N(\omega)\, d\omega d\tau \\ &= 2\int_0^\infty \frac{\sin\big(t(\omega_l - \omega)\big)}{\omega_l - \omega} J(\omega) N(\omega)\, d\omega \qquad (5.56)\end{aligned}$$

As used previously the approximation $N(\omega) \approx 0$ is appropriate at low temperatures, which we assume for spontaneous emission, and consequently $\Gamma_{21}(\omega_l, t) \approx 0$. This leaves us with only one dissipation rate for spontaneous emission,

$$\Gamma(\omega_l, t) = \Gamma_{12}(\omega_l, t)|_{N(\omega)\to 0} = \boxed{2\int_0^\infty \frac{\sin\big(t(\omega_l - \omega)\big)}{\omega_l - \omega} J(\omega)\, d\omega,} \qquad (5.57)$$

where $J(\omega)$, for spontaneous emission, is assumed to be (ω_c is the cut-off frequency)

$$J(\omega) = \eta \omega^3 e^{-\omega/\omega_c}. \qquad (5.58)$$

The relation (5.57) is the one that was used in section 4.2.2.

Time-dependent dephasing

As shown in the previous section the result of undoing the Born-Markov approximation is that the response functions change their integration end limit to t. This also applies to the dephasing master equation (5.26). We therefore have the four response functions

$$K_{12}(\pm\Omega, t) = \int_0^t e^{\mp i\Omega\tau} C_{12}(\tau) d\tau = \frac{1}{2}\gamma_{12}(\pm\Omega, t) \mp i S_{12}(\pm\Omega, t), \qquad (5.59)$$

$$K_{21}(\pm\Omega, t) = \int_0^t e^{i\mp\Omega\tau} C_{21}(\tau) d\tau = \frac{1}{2}\gamma_{21}(\pm\Omega, t) + i S_{21}(\pm\Omega, t). \qquad (5.60)$$

In sec. 5.2 we found that γ_{12} was only valid for $-\Omega$ and γ_{21} only valid for $+\Omega$. Even though we do not use the Markov approximation now, one could expect we might have the same tendency. This is indeed the case, which can be confirmed by computing all the rates and noting that two of them always admit negative values for the rates, which is unphysical. Thus, we find the

$$\begin{aligned}\gamma_{12}(-\Omega, t) = 2 \cdot \mathrm{Re}\big(K_{12}(-\Omega, t)\big) &= 2 \cdot \mathrm{Re}\left(\int_0^t e^{i\Omega\tau} \int_0^\infty J(\omega) e^{-i\omega\tau}(1 + N(\omega))\, d\omega d\tau\right) \\ &= 2\int_0^t \int_0^\infty \cos\big(\tau(\Omega - \omega)\big) J(\omega)(1 + N(\omega))\, d\omega d\tau \\ &= 2\int_0^\infty \frac{\sin\big(t(\Omega - \omega)\big)}{\Omega - \omega} J(\omega)(1 + N(\omega))\, d\omega, \qquad (5.61)\end{aligned}$$

$$\begin{aligned}\gamma_{21}(\Omega, t) = 2 \cdot \mathrm{Re}\big(K_{21}(\Omega, t)\big) &= 2\int_0^t e^{-i\Omega\tau} \int_0^\infty J(\omega) e^{i\omega\tau} N(\omega)\, d\omega d\tau \\ &= 2\int_0^\infty \frac{\sin\big(t(\Omega - \omega)\big)}{\Omega - \omega} J(\omega) N(\omega)\, d\omega. \qquad (5.62)\end{aligned}$$

For dephasing we tend to use the high temperature approximation $N(\omega)+1 \to N(\omega)$, and in this case we see that $\gamma_{12}(-\Omega,t) = \gamma_{21}(\Omega,t)$. This leaves us again with a single form of the dissipation rate

$$\gamma(\Omega,t) = \gamma_{12}(-\Omega,t)|_{N(\omega)+1\to N(\omega)} = \gamma_{21}(\Omega,t)|_{N(\omega)+1\to N(\omega)} = \boxed{2\int_0^\infty \frac{\sin\big(t(\Omega-\omega)\big)}{\Omega-\omega} J(\omega)N(\omega)\,d\omega,} \tag{5.63}$$

where $J(\omega)$ for phonon coupling in a quantum dot can be described as [26]

$$J(\omega) = \alpha\omega^3 e^{\omega^2/\omega_c^2}. \tag{5.64}$$

The relation (5.63) is the one that was used in section 4.2.2.

The result (5.63) can be put into a more standardized form by rewriting the Bose-Einstein occupation number $N(\omega) = (e^{\omega\beta}-1)^{-1}$ – where $\beta = \hbar/k_BT$ – and inserting it into (5.63)

$$\gamma(\Omega,t) = 2\int_0^\infty \frac{\sin\big(t(\omega-\Omega)\big)}{\omega-\Omega} J(\omega)\frac{1}{e^{\omega\beta}+1}\coth\left(\frac{1}{2}\omega\beta\right)\,d\omega. \tag{5.65}$$

Chaudry et al. [32] have derived an expression similar to (5.63) for a system governed by pure dephasing. However, they define the dissipation rate as $\rho(t) = \rho(0)e^{-\tilde{\gamma}(t)}$, whereas our definition of the dissipation rate stems from $\partial_t\rho(t) = \gamma(t)\rho(t)$, and so we expect that $-\tilde{\gamma}(t) = \gamma(t)$. Differentiation of their expression indeed results in what corresponds to an integral over $J(\omega)$ with a factor of $\coth(\beta\omega/2)\sin(\omega t)/\omega$. Note that Ω does not appear here, because they have not implemented driving in their model, which corresponds to setting $\Omega = 0$ in our expression.

Chapter 6

Further analysis of QZE

6.1 Numerical solutions for dephasing master equation

We consider the solution to the dephasing master equation, (5.31), and compare it to the previously used Lindblad master equation.

The solution to the Lindblad master equation is plotted on figure 6.1, and the solution to the complete master equation is plotted on figure 6.2. For the Lindblad equation we have adjusted the value of γ such that the two solutions are as similar as possible for comparison purposes.

The spectral density function used in the computations of the complete master equation is given by

$$J(\omega) = \alpha\omega^3 e^{-(\omega/\omega_c)^2}. \tag{6.1}$$

This function corresponds to phonon coupling and is often used to model pure dephasing [26].

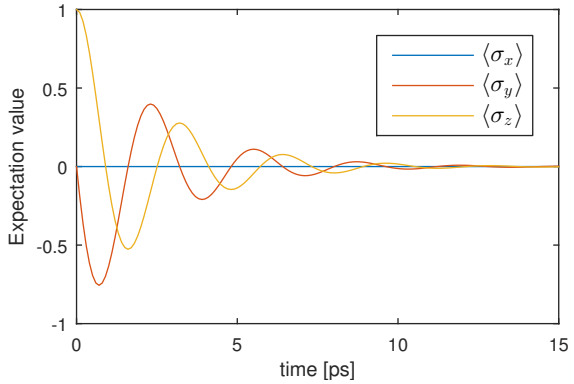

Figure 6.1: Numerical solution to the Lindblad master equation with dephasing and driving, where $\gamma = 0.4\,\mathrm{ps}^{-1}$ and $\Omega = 2\,\mathrm{ps}^{-1}$.

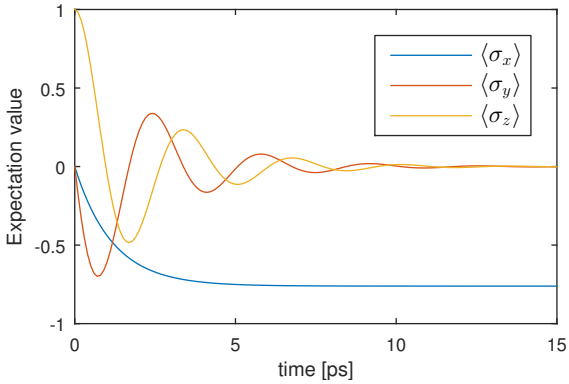

Figure 6.2: Numerical solution to the complete dephasing master equation (5.31). Parameters used are $\Omega = 2\,\mathrm{ps}^{-1}$, $\omega_c = 2.2\,\mathrm{ps}^{-1}$, $\alpha = 0.03\,\mathrm{ps}^2$ and $T = 40\,K$.

First of all the two solutions seem very similar, and thus, to some extent, the previously used Lindblad master equations are numerically confirmed.

One difference that we immediately notice, however, is that the solution to the Lindblad master equation does not have a non-zero evolution of $\langle\sigma_x\rangle$. This is due to the system Hamiltonian being $H_{S'} = \Omega/2\sigma_x$. In the high-temperature limit, $\Omega/k_BT \ll 1$, the steady state value for $\langle\sigma_x\rangle$ becomes 0.

The lack of this behaviour in figure 6.1 is a shortcoming of the Lindblad master equation.

Taking a closer look at the evolution of $\langle\sigma_z\rangle$ with slightly different values for T, Ω and γ, we find that the Rabi oscillations are different due to Lamb shift – see figure 6.3.

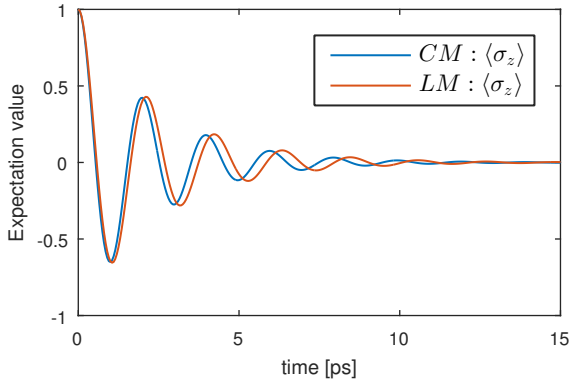

Figure 6.3: Numerical solution to the complete dephasing master equation (5.31) denoted CM and the dephasing Lindblad master equation denoted LM. Parameters used are $\Omega = 3\,\mathrm{ps}^{-1}$, $\omega_c = 2.2\,\mathrm{ps}^{-1}$, $\alpha = 0.03\,\mathrm{ps}^2$, $T = 15\,K$ and $\gamma = 0.4\,\mathrm{ps}^{-1}$. Even though the value for Ω is the same for CM and LM the Rabi frequencies differ. This is due to the Lamb shift described by the complete master equation.

6.2 Numerical solutions for spontaneous emission master equation

6.2.1 Two-level system

We now consider numerical solutions to the complete master equation for spontaneous emission, (5.22), and compare them to the corresponding solutions to the Lindblad master equations. This has been done for a set of parameters, see figure 6.6. The solution to the spontaneous emission Lindblad master equation is based on a chosen constant value for Γ, while the value for η has been adjusted accordingly for best agreement between the solutions.

In figure 4.50 and 4.50 we see that there is again a good overall agreement between the solutions, but with a deviation in the steady state value of $\langle\sigma_x\rangle$.

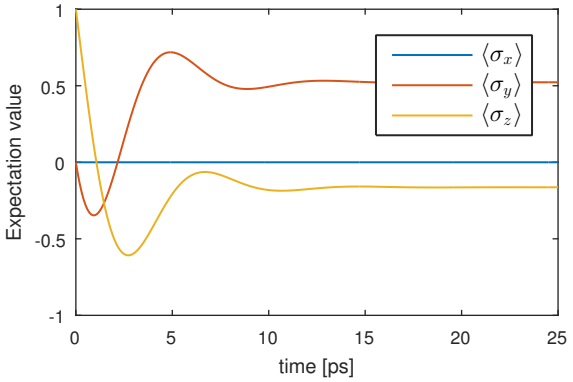

Figure 6.4: Numerical solution to the Lindblad master equation with spontaneous emission and driving, where $\Gamma = 0.5\,\mathrm{ps}^{-1}$ and $\Omega = 0.8\,\mathrm{ps}^{-1}$.

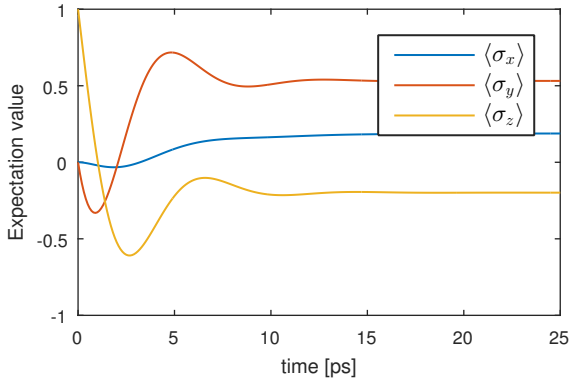

Figure 6.5: Numerical solution to the complete spontaneous emission master equation (5.22). Parameters used are $\Omega = 0.8\,\mathrm{ps}^{-1}$, $\omega_c = 2.2\,\mathrm{ps}^{-1}$, $\eta = 0.008\,\mathrm{ps}^2$ and $T = 5\,K$.

In figure 6.6 we have compared the z-component, $\langle\sigma_z\rangle$, of the two solutions and we once again see a difference in the frequency of the Rabi oscillations due to Lamb shift. Addi-

tionally, we also notice a shift in the steady state value of $\langle\sigma_z\rangle$. The Lindblad solution also shows this behaviour for higher values of Γ, as we saw in figure 4.2.

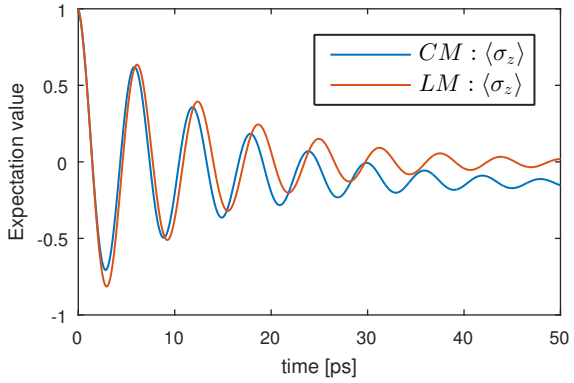

Figure 6.6: Numerical solution to the complete spontaneous emission master equation (5.22) denoted CM and the spontaneous emission Lindblad master equation denoted LM. Parameters used are $\Omega = 1\,\mathrm{ps}^{-1}$, $\omega_c = 1\,\mathrm{ps}^{-1}$, $\eta = 0.35\,\mathrm{ps}^2$, $\omega_l = 10\,\mathrm{ps}^{-1}$ and $T = 20\,K$ and $\Gamma = 0.1\,\mathrm{ps}^{-1}$. The change in frequency shows Lamb shift described by the complete master equation.

6.2.2 Three-level system

From equation (5.43) describing the system 4.22a (dissipation in upper subsystem and driving in lower subsystem), we learned that the dissipation rate depends on the quantity $\xi = \Delta_{pl} + \Omega_{eg}/2$, where Δ_{pl} was set to $\omega_p - \omega_e$.

Since $\Gamma_{12}(\xi)$ is proportional to the spectral density $J(\xi)$, and we know that the spectral density tends to 0 at high values, we infer that $\Gamma_{12}(\xi) \to 0$ for $\xi \to \infty$. Thus we can either increase the driving frequency or the detuning to obtain the QZE as seen on figure 6.7 and 6.8.

In the master equation (5.43) it was assumed that $\frac{\Omega_{eg}}{2} > \Delta_{pl}$, so in order to not violate this, we have set Δ_{pl} to a constant low value on figure 6.7, and Ω_{eg} to a constant high value on figure 6.8.

Note that varying Δ_{pl} simply means that we consider either higher or lower energy differences between the $|p\rangle$ and $|e\rangle$ state (due to our choice $\Delta_{pl} = \omega_p - \omega_e$). In a physical system Δ_{pl} may be a constant rather than a variable.

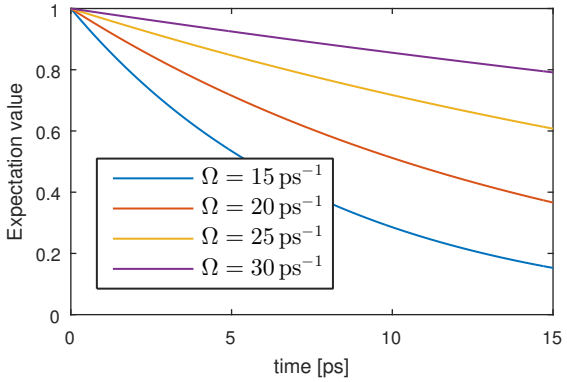

Figure 6.7: Numerical solution to the three-level spontaneous emission master equation with driving. The detuning is kept fixed, $\Delta_{pl} = 6\,\mathrm{ps}^{-1}$, and the driving frequency $\Omega = \Omega_{eg}$ is varied.

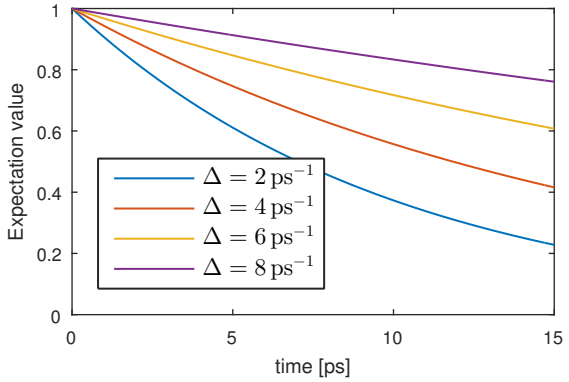

Figure 6.8: Numerical solution to the three-level spontaneous emission master equation with driving. The driving frequency is kept fixed, $\Omega_{eg} = 25\,\mathrm{ps}^{-1}$, and the detuning $\Delta = \Delta_{pl}$ is varied.

Chapter 7

Overview and discussion

Throughout the analysis of the QZE we have made a clear distinction between the two manifestations of QZE, in order to clear out the confusion around the QZE. We want to make an overview over the results we have gathered and discuss certain aspects regarding this matter.

7.1 QZE: projective measurements

In total we have considered three cases that reveal QZE with projective measurements. The first two of the cases are related to the two-level QD undergoing spontaneous emission and pure dephasing, respectively. These reveal the QZE only if the dissipation rates γ and Γ are time-dependent, which can be derived by neglecting the Markov approximation in the derivation of the master equations. We derived the expressions (5.63), (5.57) and performed projective measurements on the systems, which eventually led to the QZE in both cases.
In the last case a two-level QD was influenced by 'continuous coupling' explicitly, and frequent projective measurements were performed. The same system was used to theoretically derive the genuine QZE with projective measurements in section (3.2). The simulation (4.14) also revealed that the QZE was obtained as theorized.

7.2 QZE: strong 'continuous coupling'

Pascazio states in [15] that the QZE can be provoked by practically any external interaction that greatly disturbs the system. This statement is consistent with our findings in the cases we have studied throughout the thesis.

Regarding this matter, the relevant cases for the two-level QD are those for which the QD undergoes pure dephasing. Our simulations and calculations revealed that it is possible to obtain the QZE if the QD is influenced by a large dephasing rate γ (4.3) or by strong 'continuous coupling' (5.2.1), which requires that the dissipation rate γ is dependent on Ω. However, it has to be emphasized that the first of these cases may be violating the Born approximation (2.5.1.1). The Born approximation restricts our master equations to only consider weak dissipative effects of the environment. Since the dephasing rate in this case is increased immensely, it might violate the approximation. Every other case considered in the thesis should be consistent with our approximations; namely all cases with strong 'continuous coupling', since driving does not represent a dissipation effect, hence the Born

approximation is not violated.

For the three-level QD the considered cases have all had a lower subsystem influenced by 'continuous coupling', while respectively having spontaneous emission (4.22a), 'continuous coupling' (4.22b) or a combination of these (4.22c) in its upper subsystem. In the first two of these cases, the QZE was obtained by influencing the lower subsystem with strong 'continuous coupling'. It should however be noted that the case with spontaneous emission in its upper level, requires a dissipation rate Γ dependent on Ω in order to obtain QZE.

The third three-level QD case (4.22c) was special. It was the only system of those we studied that was prepared in its ground state, which by many may seem redundant since the state can be 'frozen' by simply not driving the system. It represents however a simplified version of Itano et al. experiment [1] in 1989, which frequently is reckoned as being evidence for the genuine QZE. This case therefore gave us the opportunity to simulate their results and argue the origin of the appearance of the QZE.

Similar to Itano's experiment our simulations revealed the QZE by strongly driving the upper subsystem. As with all our cases obtaining QZE with strong driving, the appearance of QZE in Itano's experiment is a not a result of wave function collapse – projective measurements – but appears as a consequence of great disturbance from the environment that dominates the evolution of the system. The strong environmental influence on Itano's system may be though of as creating what generally is know as electromagnetically induced transparency [30] which originates from strong 'continuous coupling' – a statement supported by Pascazio and Ballentine [28], [14].

Chapter 8

Conclusion

In this thesis we have investigated different manifestations of the QZE and considered analytical and numerical differences in addition to interpretational consequences. With the use of the Lindblad formalism we were able to study two- and three-level QDs undergoing spontaneous emission and dephasing with or without driving. Firstly, we showed the QZE by projective measurements for QDs with spontaneous emission, pure dephasing as well as for QDs exclusively influenced by 'continuous coupling'. Secondly, we encountered a case for a two-level QD showing QZE provoked by strong dephasing effects. Finally, we showed that it was possible to obtain QZE by strong 'continuous coupling'. For this case we studied a three-level QD only influenced by 'continuous coupling', and then also two- and three-level QDs with spontaneous emission rates shown to be dependent on coupling strength Ω.

Our investigation has included simulating the experiment by Itano [1], which is often cited regarding experimental evidence of the QZE formulated by Sudarshan several decades ago. We have found that this experiment does not require the notion of wave function collapse to be explained, and as such the QZE in this experiment is different in nature to the QZE proposed by Sudarshan [2]. The QZE by projective measurements have been shown to be theoretically possible, but has never been experimentally confirmed.

Hence, in the light of our results and analysis we conclude that the 'physical appearance' of the QZE should be regarded as a more general phenomenon caused by strong disturbances [14][28]. Because of the fundamental differences of the manifestations, one must be careful to distinguish between them. Failing to do so, experiments might be interpreted in misleading ways [14].

References

[1] W M Itano, D J Heizen, J J Bollinger, and D J Wineland. Quantum zeno effect. *Phys. Rev. A 41, 2295*, 1989.

[2] E. C. G. Sudarshan and B. Misra. The zeno's paradox in quantum theory. *Journal of Mathematical Physics*, 18:756, 1977.

[3] B. E. A. Saleh and M.C. Teich. *Fundamentals of Photonics*. John Wiley & Sons, 2007.

[4] K. Jacobi. Atomic structure of inas quantum dots on gaas. *Progress in Surface Science*, 71:196, 2003.

[5] Tim Harper Paul Holister, Cristina Román Vas. Quantum dots. *Technology White Papers*, 13:5, 2003.

[6] Wikipedia. Quantum dots # fabrication. `http://en.wikipedia.org/wiki/Quantum_dot#Fabrication`. [accessed 1-May-2015].

[7] Wikipedia. Stranski–krastanov growth. `http://en.wikipedia.org/wiki/Stranski%E2%80%93Krastanov_growth`. [accessed 1-May-2015].

[8] Goong Chen, Zijian Diao, Jong U. Kim, Arup Neogi, Kerim Urtekin, and Zhigang Zhang. Quantum dot computing gates. *International Journal of Quantum Information*, 4, 2006.

[9] Noson S. Yanofsky and Mirco A. Mannucci. *Quantum Computing for Computer Scientists*. Cambridge University Press, 2008.

[10] J. von Neumann. Die mathematische grundlagen der quantenmechanik. 1932.

[11] A. Beskow and J Nilsson. Arkiv für fysik. *Journal 34 561*, 1967.

[12] C. N. Friedman. Indiana univ. *Math journal 21 1001*, 1972.

[13] R. J. Cook. *Phys. Scr. T 21 49*, 1988.

[14] L.E. Ballentne. Comment on "quantum zeno effect". *Phys. Rev. A 41, 2295*, 1990.

[15] S. Pascazio and Paolo Facchi. Three different manifestations of the quantum zeno effect. *phys. Rev. A 70126*, 2003.

[16] Wikipedia. Interpretations of quantum mechanics #tabularcomparison. `http://en.wikipedia.org/wiki/Interpretations_of_quantum_mechanics#Tabular_comparison`. [accessed 1-May-2015].

[17] W.M. de Muynck. *Foundations of quantum mechanics, an empiricist approach*. Kluwer Academic Publishers, 2002.

[18] Wikipedia. Quantum decoherence. `http://en.wikipedia.org/wiki/Quantum_decoherence`. [accessed 1-May-2015].

[19] Wikipedia. Thought experiments in quantum mechanics. `http://en.wikipedia.org/wiki/Category:Thought_experiments_in_quantum_mechanics`. [accessed 1-May-2015].

[20] Hiromichi Nakazato, Mikio Namiki, Saverio Pascazio, and Helmut Rauch. Understanding the quantum zeno effect. *Physics Letters A*, 1996.

[21] S. Pascazio, M. Namiki, H. Nakazato, and H. Rauch. On the quantum zeno effect. 1995.

[22] L.E. Ballentine. *Advanced Quantum Mechanics - A Modern Development*. World Scientific, 1998.

[23] S. Pascazio and P. Facchi. Quantum zeno subspaces. *Phys. Rev. Lett. 89 080401*, 2002.

[24] S. Pascazio, P. Facchi, and D. A. Lidar. Unification of dynamical decoupling and the quantum zeno effect. *Phys. Rev. A 69, 032314*, 2004.

[25] Ole Christensen. *Differentialligninger og uendelige rækker*. Institut for matematik, Danmarks Tekniske Universitet, 2006.

[26] Dara P. S. McCutcheon. *Open quantum systems in spatially correlated regimes*. PhD thesis, University College London, 2010.

[27] Sandeep K. Goyal, B. Neethi Simon, Rajeev Singh, , and Sudhavathani Simon. Geometry of the generalized bloch sphere for qutrit. *arXiv*, page 1, 2011.

[28] Paolo Facchi, Giuseppe Marmo, and Saverio Pascazio. Quantum zeno dynamics and quantum zeno subspaces. *Journal of Physics: Conference Series*, 196:1, 2009.

[29] Ahsan Nazir. Lecture notes on open quantum systems.

[30] Imamoglu A. Boller K. J. and Harris S. E. Observation of elctromagnetically induced transparency. *Phys. Rev. Lett. 66 2593*, 1991.

[31] Kyle Beloy. Theory of the ac stark effect on the atomic hyperfine structure and applications to microwave atomic clocks. 2009.

[32] Adam Zaman Chaudhry and Jiangbin Gong. Zeno and anti-zeno effects on dephasing. *Physical Review A*, 90:1, 2014.

Appendix A

Appendix

A.1 Analytical solutions to Lindblad master equations

Here we present computed values of referenced quantities. We use the computer algebra software Wolfram Mathematica 10.

A.1.1 Spontaneous emission

The eigenvalues to the coefficient matrix are

$$\lambda = \left\{ -\frac{\Gamma}{2}, \frac{1}{4}(-3\Gamma - \epsilon), \frac{1}{4}(\epsilon - 3\Gamma) \right\}, \tag{A.1}$$

where we have defined $\epsilon = \sqrt{\Gamma^2 - 16\Omega^2}$. The normalized eigenvectors are

$$\mathbf{v}_1 = (1, 0, 0)^{\mathbf{T}} \tag{A.2}$$

$$\mathbf{v}_2 = \left(0, \frac{\Gamma - \epsilon}{\Omega\sqrt{\frac{(\Gamma-\epsilon)^2}{\Omega^2} + 16}}, \frac{4}{\sqrt{\frac{(\Gamma-\epsilon)^2}{\Omega^2} + 16}} \right)^{\mathbf{T}} \tag{A.3}$$

$$\mathbf{v}_3 = \left(0, \frac{\Gamma + \epsilon}{\Omega\sqrt{\frac{(\Gamma+\epsilon)^2}{\Omega^2} + 16}}, \frac{4}{\sqrt{\frac{(\Gamma+\epsilon)^2}{\Omega^2} + 16}} \right)^{\mathbf{T}}. \tag{A.4}$$

The constants c_i in the complete solution

$$\alpha(t) = \sum_{i=1}^{3} c_i e^{\lambda_i t} \mathbf{v}_i, \tag{A.5}$$

are found from the initial values. Using $(\alpha_1(0), \alpha_2(0), \alpha_3(0)) = (0, 0, 1)$ as the initial value, corresponding to the system being in the excited state, we find

$$c_1 = 0 \tag{A.6}$$

$$c_2 = \frac{\sqrt{\frac{(\Gamma-\epsilon)^2}{\Omega^2} + 16}\left(\Gamma^3 + \Gamma^2\epsilon + 5\Gamma\Omega^2 + \Omega^2\epsilon\right)}{4\epsilon\left(\Gamma^2 + 2\Omega^2\right)} \tag{A.7}$$

$$c_3 = \frac{\sqrt{\frac{\Gamma^2+2\Gamma\epsilon+16\Omega^2+\epsilon^2}{\Omega^2}}\left(-\Gamma^3 + \Gamma^2\epsilon - 5\Gamma\Omega^2 + \Omega^2\epsilon\right)}{4\epsilon\left(\Gamma^2 + 2\Omega^2\right)}. \tag{A.8}$$

A.1.2 Pure dephasing

The eigenvalues to the coefficient matrix are

$$\lambda = \{-2\gamma, -\gamma - \epsilon, \epsilon - \gamma\}, \tag{A.9}$$

where we have defined $\epsilon \equiv \sqrt{\gamma^2 - \Omega^2}$. The normalized eigenvectors are

$$\mathbf{v}_1 = (1, 0, 0)^{\mathbf{T}} \tag{A.10}$$

$$\mathbf{v}_2 = \left(0, -\frac{\gamma+\epsilon}{\Omega\sqrt{\frac{(\gamma+\epsilon)^2}{\Omega^2}+1}}, \frac{1}{\sqrt{\frac{(\gamma+\epsilon)^2}{\Omega^2}+1}}\right)^{\mathbf{T}} \tag{A.11}$$

$$\mathbf{v}_3 = \left(0, \frac{\epsilon-\gamma}{\Omega\sqrt{\frac{(\gamma-\epsilon)^2}{\Omega^2}+1}}, \frac{1}{\sqrt{\frac{(\gamma-\epsilon)^2}{\Omega^2}+1}}\right)^{\mathbf{T}}. \tag{A.12}$$

Using $(\alpha_1(0), \alpha_2(0), \alpha_3(0)) = (0, 0, 1)$ as the initial value, corresponding to the system being in the excited state, we find the constants c_i to be

$$c_1 = 0 \tag{A.13}$$

$$c_2 = \frac{(\epsilon-\gamma)\sqrt{\frac{(\gamma+\epsilon)^2}{\Omega^2}+1}}{2\epsilon} \tag{A.14}$$

$$c_3 = \frac{(\gamma+\epsilon)\sqrt{\frac{\gamma^2-2\gamma\epsilon+\Omega^2+\epsilon^2}{\Omega^2}}}{2\epsilon}. \tag{A.15}$$

A.2 Numerical solution to two-level systems with time-dependent dissipation

asd

```
function [t, B] = TwoLS_averagedOutcomes( nMeasurements, ...
    measurementTimes, spon, deph, gamma0, omega, varargin )

%% Preprocessing

% data structures
startTimes = linspace(measurementTimes(1),measurementTimes(2), ...
    nMeasurements);
timeBetweenMeasurements = startTimes(2) - startTimes(1);

B = [];
t = [];
measurementOutcomes = zeros(1,nMeasurements);

% measurement basis
b1 = [1;0];
b2 = [0;1];

bOp1 = b1 * b1';
bOp2 = b2 * b2';

%% Solution

% before first measurement
t0 = 0;
```

```
24 initial_state_vector = [1; 0];
25 initial_state = initial_state_vector * initial_state_vector';
26
27 % solving
28 [IC1, IC2, IC3] = TwoLS_ICs( initial_state );
29 odefun = @(t,B) TwoLS_grad(t, B, t0, gamma, omega, spon, deph);
30 [tnew, Bnew] = ode45( odefun , [t0, t0 + startTimes(1)], [IC1 IC2 IC3]);
31
32 B = [ B ; Bnew];
33 t = [t; tnew];
34
35
36 % after first measurement
37
38 for i = 1:nMeasurements
39    state = DensityOpFromBlochVector( B(end,:) );
40    probabilities(1) = trace( bOp1 * state);
41    probabilities(2) = trace( bOp2 * state);
42
43    initial_state = probabilities(1) * bOp1 + probabilities(2) * bOp2;
44
45    % solving
46    [IC1, IC2, IC3] = TwoLS_ICs( initial_state );
47    t0 = startTimes(i);
48    odefun = @(t,B) TwoLS_grad(t, B, t0, gamma, omega, spon, deph);
49    [tnew, Bnew] = ode45( odefun , [t0, t0 + timeBetweenMeasurements], ...
          [IC1 IC2 IC3]);
50
51    B = [ B ; Bnew];
52    t = [t; tnew];
53
54 end
55
56 end
```

where the functions `TwoLS_ICs` are given by `TwoLS_grad` 1

```
1  function [ IC1, IC2, IC3 ] = TwoLS_ICs( initial_state )
2
3  sigmax = [0 1; 1 0];
4  sigmay = [0 -1i; 1i 0];
5  sigmaz = [1 0; 0 -1];
6
7  IC1 = trace(initial_state * sigmax);
8  IC2 = trace(initial_state * sigmay);
9  IC3 = trace(initial_state * sigmaz);
10
11 end
12
13
14
15
16
17 function [ grad ] = TwoLS_grad( t, B, t0, gamma, omega, spon, deph)
18 %Returns gradient of bloch vector
19 % t: time,  B: bloch vector
20
21
22 sigmax = [0 1; 1 0];
23 sigmay = [0 -1i; 1i 0];
24 sigmaz = [1 0; 0 -1];
25
```

```
26 A = spon * [0 0; 1 0] + deph * sigmaz;
27
28 p =1/2 * [  1 + B(3)          B(1) - 1i*B(2) ; ...
29              B(1) + 1i*B(2)    1 - B(3)       ];
30
31 cA = ctranspose(A);
32 Lindblad = A*p*cA - 1/2*( cA*A*p + p*cA*A);
33
34 H = omega/2 * [ 0 1 ; 1 0 ];
35
36 dpdt = -1i*(H * p - p * H) + gamma(t-t0) * Lindblad;
37
38 grad = zeros(3,1);
39
40 grad(1) = trace( dpdt * sigmax );
41 grad(2) = trace( dpdt * sigmay );
42 grad(3) = trace( dpdt * sigmaz );
43
44
45 end
```

A.3 Time dependent spontaneous emission rate

```
1  function gamma = sponGamma(t)
2
3  gamma0 = 0.28;
4  omega_c = 2.2;
5  omega_l = 2.2;
6
7  eta =  100;
8
9  %% Preprocessing
10 Jtilde = @(omega) eta .* omega.^3 .* exp(-(omega./omega_c));
11
12 %% Calculating gamma
13 f = @(omega) sin(t.* (omega_l - omega) ) ./ (omega_l - omega) .* ...
       Jtilde(omega);
14 gamma = 2 * integral( f, 0.01, 1e2);
```

A.4 Time dependent dephasing rate

```
1  function gamma = dephGamma(t)
2
3  T = 300;
4  beta = 7.6 / T;
5  gamma0 = 0.28;
6  omega_c = 2.2;
7  Omega = 3;
8
9  alpha = 0.03;
10
11 %% Preprocessing
12 Jtilde = @(omega) alpha .* omega.^3 .* exp(-(omega./omega_c).^2);
13 nfunc = @(omega) 1./(  exp(omega .* beta) - 1 );
14
15 %% Calculating gamma
```

```
f = @(omega) sin(t.* (Omega - omega) ) ./ (Omega - omega) .* ...
    Jtilde(omega) .* nfunc(omega);
gamma = 2 * integral( f, 0.01, 1e3);
```

A.5 Complete master equation solved in Mathematica

```
Solution

kom[a_, b_] := a.b - b.a;
x := 1/2 ( {
    {1, 1},
    {-1, -1}
   } )
n := 1/2 ( {
    {1, -1},
    {1, -1}
   } )
\[Sigma]z := ( {
   {1, 0},
   {0, -1}
  } )
\[Sigma]x := ( {
   {0, 1},
   {1, 0}
  } )
\[Sigma]y = ( {
    {0, -I},
    {I, 0}
   } );
a1[t_] = Exp[-I \[CapitalOmega] t] x + Exp[I \[CapitalOmega] t] n;
ps[t_] := 1/2 ( {
     {(1 + az@t), ax@t - I ay@t},
     {ax@t + I ay@t, (1 - az@t)}
    } );
(* dephasing *)
P = -\[CapitalOmega]/2 I kom[\[Sigma]x,
     ps[t]] - (kom[a1[0],
       x.ps[t]] (\[Gamma][-\[CapitalOmega]] + \[CapitalDelta]B[-\
\[CapitalOmega]]) +
     kom[a1[0], n.ps[t]] (-\[CapitalDelta]A[-\[CapitalOmega]])) - (kom[
       ps[t].x, a1[0]] (\[CapitalDelta]A[-\[CapitalOmega]]) +
     kom[ps[t].n,
       a1[0]] (\[Gamma][-\[CapitalOmega]] - \
\[CapitalDelta]B[-\[CapitalOmega]])) - (kom[a1[0],
       x.ps[t]] (\[CapitalDelta]A[\[CapitalOmega]]) +
     kom[a1[0],
       n.ps[t]] (\[Gamma][\[CapitalOmega]] - \
\[CapitalDelta]B[\[CapitalOmega]])) - (kom[ps[t].x,
       a1[0]] (\[Gamma][\[CapitalOmega]] + ...
           \[CapitalDelta]B[\[CapitalOmega]]) \
+ kom[ps[t].n, a1[0]] (-\[CapitalDelta]A[\[CapitalOmega]])) ;

Correlation functions

timestep = 0.01;
\[Alpha] = 0.03;
\[Omega]c = 2.2;
Omega = 1; (*  Driving omega *)
tmax = 10;
J[\[Omega]_] := \[Alpha] \[Omega]^3 Exp[-(\[Omega]/\[Omega]c)^2];
```

```
54 \[CapitalGamma] = beta = 7.6/20;  (*  *)
55 nfunc[\[Omega]_] := (Exp[\[Omega] beta] - 1)^-1;
56
57 c12[t_] :=
58   NIntegrate[
59    J[\[Omega]] Exp[-I \[Omega] t] (1 + nfunc[\[Omega]]), {\[Omega], ...
       0.01, 7},
60    Method -> {Automatic, "SymbolicProcessing" -> False}, MaxRecursion ...
       -> 20,
61    AccuracyGoal -> 7];
62 c12Interp =
63   ListInterpolation[Table[c12[t], {t, 0, tmax, timestep}], {0, tmax}];
64 c12intfunc[\[CapitalOmega]_] :=
65  NIntegrate[Exp[I \[CapitalOmega] t] c12Interp[t], {t, 0.01, tmax},
66   Method -> {Automatic, "SymbolicProcessing" -> 0}, MaxRecursion -> 20]
67 c21[t_] :=
68   NIntegrate[
69    J[\[Omega]] Exp[I \[Omega] t] nfunc[\[Omega]], {\[Omega], 0.01, 7},
70    Method -> {Automatic, "SymbolicProcessing" -> False}, MaxRecursion ...
       -> 20,
71    AccuracyGoal -> 7];
72 c21Interp =
73   ListInterpolation[Table[c21[t], {t, 0, tmax, timestep}], {0, tmax}];
74 c21intfunc[\[CapitalOmega]_] :=
75  NIntegrate[Exp[I \[CapitalOmega] t] c21Interp[t], {t, 0.01, tmax},
76   Method -> {Automatic, "SymbolicProcessing" -> 0}, MaxRecursion -> 20]
77
78 \[CapitalDelta]Bn = I*Im@c12intfunc[Omega];
79 \[CapitalDelta]An = -I Im@c12intfunc[-Omega];
80 \[CapitalDelta]Ap = I Im@c21intfunc[Omega];
81 \[CapitalDelta]Bp = -I*Im@c21intfunc[-Omega];
82 \[Gamma]p = Re@c21intfunc[-Omega];
83 \[Gamma]n = Re@c12intfunc[Omega];
84
85 Solving the master eq.
86
87 dpdt = P /. {\[CapitalDelta]A[\[CapitalOmega]] -> \[CapitalDelta]Ap, \
88 \[CapitalDelta]A[-\[CapitalOmega]] -> \[CapitalDelta]An, \[CapitalDelta]B[\
89 \[CapitalOmega]] -> \[CapitalDelta]Bp, ...
       \[CapitalDelta]B[-\[CapitalOmega]] -> \
90 \[CapitalDelta]Bn, \[Gamma][-\[CapitalOmega]] -> \[Gamma]n, \[Gamma][\
91 \[CapitalOmega]] -> \[Gamma]p} // Simplify;
92 motionEq[\[Sigma]_] := Simplify[Tr[dpdt.\[Sigma]]];
93 eq1 = ax'[t] == motionEq@\[Sigma]x;
94 eq2 = ay'[t] == motionEq@\[Sigma]y;
95 eq3 = az'[t] == motionEq@\[Sigma]z;
96
97 nsolComplete =
98   NDSolve[{eq1, eq2, eq3, ax[0] == 0, ay[0] == 0,
99      az[0] == 1} /. \[CapitalOmega] -> Omega, {ax[t], ay[t], az[t]}, ...
          {t, 0,
100    tmax}];
```